PHYSICAL AND GEOCHEMICAL CHARACTERIZATION OF TWO WETLANDS IN THE EXPERIMENTAL LAKES AREA, NORTH-WESTERN ONTARIO, CANADA

by

Miles Anderson

A thesis
presented to the University of Waterloo
in fulfillment of the
thesis requirement for the degree of
Master of Science
in
Earth Sciences

Waterloo, Ontario, Canada, 2012

© Miles Anderson 2012

AUTHOR'S DECLARATION

I hereby declare that I am the sole author of this thesis. This is a true copy of the thesis, including any required final revisions, as accepted by my examiners. I understand that my thesis may be made electronically available to the public.

ABSTRACT

Anthropogenic disruptions in the form of hydrological alterations, such as dam construction and the associated water diversions are a cause of much upheaval to local and regional ecosystems. Lake 626 within the Experimental Lakes Area of north-west Ontario, along with its downstream wetlands, 626A and 626B are one such system. Construction of a dam at the L626 inflow has completely restricted water flow, reducing and reshaping the watershed, increasing water retention time, and decreasing outflow into the wetlands. This study investigates the state of each wetland through physical and geochemical characterization during the first year following the diversion.

Previous studies have found that hydrological diversions in wetlands can lower water table levels, altering soil chemistry and producing a shift in floral and faunal communities. Ultimate consequences involve significant loss of wetland area through conversion to upland habitat. This provides a model for climatic warming scenarios, wherein sustained drought conditions can produce the same result. Boreal wetlands are surprising fragile ecosystems that store massive quantities of carbon and are at risk of releasing it in such situations. One study showed that an extended summer drought in an otherwise average year with above average precipitation produced losses of 90 g C/m^2 over the course of the year. Maintenance of reduced-flow in wetlands 626A and 626B is expected to convert the system into a carbon source and reduce overall wetland area.

Radiocarbon dating has revealed that following deglaciation, both 626A and 626B basins were open water wetlands, depositing limnic peat for about 3200 and 1300 years respectively. Each site then transitioned into open sedge dominated fen – 626B to the present and 626A until about 2.5 ka BP when *Sphagnum* began to develop. Wetland 626B is decidedly an open

shrub/sedge fen, supporting *Myrica gale, Chamaedaphne calyculata* and *Carex rostrata / lasiocarpa* communities. Wetland 626A is a bog/fen complex, sharing similar communities in the fen areas, but housing a large, centrally located bog of shrub species overlying *Sphagnum* hummocks. Tritium values in 626A were similar to cosmic background levels, indicating that recharge of basal pore water has not occurred in at least 60 years. Tritium in 626B was much higher, suggesting a substantial difference in hydrology or peat hydraulic conductivity between the basins. Measurement of DOC profiles showed high concentrations in near-surface water, reaching over 80 mg/L, and dropping to about 20 mg/L at maximum depths. An opposite trend was seen for DIC and CH_4 profiles which increased concentration with depth (25 – 70 mg/L DIC; 75 – 700 μmol/L CH_4). Isotopically however, ^{13}C signatures from basal DIC were more positive while signatures from CH_4 were typically more negative (-6 ‰ to +4 ‰ DIC; -57 ‰ to -73 ‰ CH_4). Breakdown of DOC by LC-OCD showed high concentrations of humic substances and low molecular weight neutrals. The origin of humic substances in surface water became more pedogenic with increasing distance from the L626 outflow, indicating the influence of decaying wetland vegetation on the DOC of adjacent water.

A comparison between contemporary and future characterization of boreal peatlands under drought-like conditions will provide a better understanding of the impacts suffered by wetlands during hydrological alterations. The high sensitivity of wetlands to changing hydrology should also provide a measure for gauging the effects of long term climate warming. This will assist in the development of environmental policies to better govern both the establishment of water diversions and the multitude of other practices leading to climate change.

ACKNOWLEDGEMENTS

First and foremost, I would like to thank my supervisor, Dr. Barry Warner, for taking me on as a graduate student and providing both guidance and helpful insight over the past two years. I would also like to thank my committee members, Dr. Sherry Schiff and Dr. Ramon Aravena for working with me and providing assistance when needed. Richard Elgood deserves a big thank you for helping to coordinate sampling supplies and guide me during much of the water analyses. You essentially saved the day on more than one occasion. Janessa Zheng helped run many of these samples and deserves a thank you as well. I would also like to thank the ELA staff for feeding and housing me during my stay.

I would also like to thank some of my fellow graduate students who provided help in a variety of ways. Thanks to Pieter Aukes and Nick Flynn for the helpful conversations on various sampling and interpretation. Thanks to Fraser Cummings for enduring the long trip up to the ELA to help with sample collection and for unveiling my hidden talent for tossing washers at wooden boxes. I would also like to thank my predecessor in the Wetlands Laboratory, Stacey MacDonald, for introducing me to graduate life and preparing me for a similarly long term as the lone student. Thank you to Dr. Paul Jasinski for providing an abundance of comic relief and engaging conversation on the many days we crossed paths.

Lastly, I would like to acknowledge all my friends and family for their support during my time at Waterloo. Thank you to Max Julian for being my computer literate accomplice during countless instances of the past several years, including the formatting of this thesis. Thank you to Stephanie Dobson for being a compassionate, understanding companion through thick and thin. I was always in awe of, and appreciated your willingness to spend a weekend doing homework just to motivate me to do the same. A sincere thank you to my parents for their patience while keeping me optimistic and pointed in the right direction, and to my sister for her expert editing. While I may have been slow to accept and put any familial advice into practice, it was invariably correct and almost always worthwhile.

Finally, a thank you to anyone not mentioned here who helped me over the course of this journey. Your support was an integral part of my progress and success.

TABLE OF CONTENTS

LIST OF TABLES

LIST OF FIGURES

CHAPTER 1

INTRODUCTION

1.1 General Introduction & Objectives

The Experimental Lakes Area Water Diversion Project was initiated in 2008 to investigate the impact of water diversions on boreal lakes and wetlands. This study is directed at addressing water level changes brought about by human activities such as water diversions, a widespread practice in industry, road and pipeline construction, and energy production, as well as providing a model of potential climate warming consequences. The growing demand for these practices is brought on by a combination of several natural resource and energy-based industries. Oil and gas companies, along with mining corporations, use large quantities of water in the exploration and extraction process (CAPP, 2010). Hydropower is another problem, often causing extensive disruption upstream and downstream of dam sites (Graf, 2006). Water management in all of these cases can result in diversions or withdrawals that cause flooding in some areas (Experimental Lakes Area Reservoir Project – ELARP) (Kelly *et al.*, 1997) and significant drying in others. Loss of water and reduced flow in the affected areas will also present a direct simulation of climate warming on boreal lake and wetland systems. While all of these factors influence the quantity of water in a given space, fluctuations can also affect water quality, such as the production of mercury in flooded areas (Schindler, 2009).

The oil and gas industry in Canada has grown over the past several decades, a trend that is expected to continue, doubling total production by the year 2030 (CAPP, 2012). Currently, water is used in a variety of processes, including drilling, hydraulic fracturing, and enhanced oil recovery (EOR). Water is so significant that roughly 75% of all bitumen production in Alberta is water-assisted, and on average, between three to six barrels of water are required to produce one

barrel of oil (CAPP, 2010; Schindler and Donahue, 2006). This extensive reliance on water for oil extraction has been noted in several studies that question the sustainability of this practice, and its impact on downstream wetlands, such as the Peace-Athabasca Delta at the confluence of the two rivers (Vitt *et al*., 2000; Turetsky *et al*., 2002; Schindler *et al*., 2007).

The metal and mineral mining sector uses large quantities of water for cooling drills, separating ore from rock, and dust containment (Environment Canada, 2007). Yet it is water flow manipulation that has the greatest impact on the surrounding environment. A large withdrawal of water from one watershed can render it unable to sustain other uses, while inundating its new location. This was seen during the Kemano Diversion in British Columbia (Quinn *et al*., 2004). Most locations require extensive pumping to dewater the site, and in many cases, diversions or adits are used to keep water away from mine operations, so as to avoid interference or contamination (Ptacek *et al*., 2004). Collectively, these processes have swift and severe impacts upon local ecosystems.

Construction of dams may be initiated for many reasons, among which hydroelectric power is at the forefront, with over 70% of large Canadian dams built solely for this purpose (Prowse *et al*. 2004). While dams are important for minimizing flood risks, providing energy, and supplying reliable sources of water for municipalities and agriculture, they can also have a multitude of negative effects. These include alterations to water temperature and chemistry, and barriers to nutrient, sediment and fish transport (Prowse *et al*. 2004). From a hydrologic perspective, dams flood swathes of upstream habitat, while regulating flow downstream, reducing maximum flow rates, the range of flow rates, and daily mean flow (Graf, 2006). For downstream wetlands, a dam can suspend delivery of nutrients, reduce water levels, and alter the duration and frequency of flooding. These aberrations to local hydrology will ultimately

influence the biochemistry of wetland soils, causing sweeping changes to vegetation, microbial communities and the waterfowl population (Mitsch and Gosselink, 2007).

Current predictions indicate that air temperatures over Canada will continue to increase in the near future; as much as 3-4 ºC by 2020 and 5-10 ºC by 2050 (IPCC, 2007). Climate warming is expected to have the most significant effects on Canadian peatlands in the southern arctic, subarctic, and boreal regions (Tarnocai, 2009). The more northern perennially frozen peatlands will thaw, creating warmer, saturated conditions that favor anaerobic decomposition and lead to methane production. Boreal wetlands will experience drought conditions due to high rates of evapotranspiration and altered precipitation patterns. This loss of water will expose previously saturated, anaerobic peat to oxygen, leading to widespread decomposition and release of carbon dioxide. In addition to the heightened levels of greenhouse gas (GHG) production, dry conditions in southern boreal peatlands will make them prone to burning (Tarnocai, 2006). This would lead to an increase in the frequency and severity of wildfires, releasing even more CO_2 gas into the atmosphere. Aside from the feedback loop caused by increased GHG production, the drought-like conditions brought on by climate warming will also have detrimental effects on wetlands in the form of reduced biodiversity and losses in general function (Mitsch and Gosselink, 2007). In one climate change study by Johnson et al. (2005), waterfowl habitat loss was investigated. In any scenario with coupled temperature increase and precipitation decrease, the birds would immediately relocate to more favourable habitat.

While it is evident that hydrological alterations place stress on the environment due to fluctuation in water quantity, there are also major impacts derived from changes in water quality. In the mining industry, acid mine drainage (AMD) is a process that oxidizes exposed rock containing sulphide minerals into sulphuric acid. This reduces water pH, and can degrade it so

far as to make it unsuitable for aquatic life. Many heavy metals are more mobile in acidic conditions, meaning that as AMD progresses, other more harmful metals will begin to leach out of excavated rock. Certain chemicals, often toxic to humans and animals, are also used in separating target minerals from ore. Companies use impermeable barriers and create treatable tailings ponds to prevent contamination beyond the mining site and comply with environmental regulations. However, these techniques are not one hundred percent efficient and inevitably lead to some downstream issues. Additionally, extensive disturbances to soil and rock during construction and maintenance of the mine site will encourage erosion (Ptacek *et al*., 2004). If this is left uncontrolled, higher sediment loads will congest streams and deposit in river and lake beds. Construction of hydroelectric reservoirs also influences water quality in varying degrees. In the reservoir itself, inorganic mercury found in flooded materials is converted to methylmercury by bacteria. This leads to bioaccumulation of the neurotoxin in fish and eventually humans (Rosenberg *et al*., 1997; 2000). Some dams draw water from the bottom of reservoirs, which contain little to no dissolved oxygen. This adversely affects water quality, leading to an oxygen starved zone downstream. Forestry also impacts water quality in many ways. Soils in recently forested areas contain an abundance of nutrients that are no longer being taken up by trees. Decomposition of stumps and brash adds to this nutrient pool, while also making soils more prone to erosion. This leads to elevated levels of sediment, as well as organic carbon, potassium and sometimes nitrate in nearby streams (Neal *et al*., 1992; Thormann *et al*., 2004).

The ELA Water Diversion Project is situated in a large catchment area of about 370 ha (Fig. 4) located in the Experimental Lakes Area, near the southern edge of the boreal forest. It includes a chain of interconnected and isolated small lakes, marshes, fens, and bogs with mixed

forest on the uplands. The study site houses a 4th order lake that was artificially isolated to stimulate drying by damming and cutting off inflow from an adjacent lake. A diversion channel was constructed to connect the upstream and downstream lakes to simulate watering up. Such changes are expected to have a significant impact on the wetlands downstream of the diversion. The research undertaken as part of this thesis aims to characterize the status of these wetlands during the early stage of the diversion.

Both study sites are small peatlands that can be classified as bog and fen with low shrubs, sedges and *Sphagnum* which occupy small bedrock basins (2.2 and 1.2 ha in area). Such peatlands are widespread throughout the Boreal Region of Canada and as such are representative examples for assessing environmental impacts of water diversions. Canadian peatlands contain large quantities of organic carbon, storing 147 Pg (1015 g) of soil carbon and 56% of all soil carbon nationwide (Tarnocai, 2006). Under dry conditions, aerobic decomposition of formerly anaerobic water-logged peat could contribute large volumes of greenhouse gases (i.e. CO_2 and CH_4) to the atmosphere. Understanding the impacts of water diversions on soil carbon processes in Canada's peatlands will likely be important as many provinces, including Ontario, develop policies for meeting future greenhouse gas reduction goals (ECO, 2011).

Therefore, the main objective of this study is to provide an initial assessment of an artificial water diversion on two Canadian Shield peatlands aimed to mimic future impacts imposed by natural (i.e. climate change, fire, permafrost melting) and human-induced (i.e. damming, water withdrawals, industry) factors. Vegetation, sediments and peat, and geochemistry will be characterized. This study will form an important baseline for future follow-up work that will gauge the extent of physical and geochemical transformations over several years. This will provide a better understanding of the threat that water diversions pose to

peatlands in Canada's Boreal landscape. It should also be noted that this study anticipates water level shifts on a decimetre scale, while many of the hydrological alterations discussed here are capable of causing much larger changes, measured in meters to tens of meters. This indicates that the conclusions drawn from this study will provide a good model for small to medium scale diversions, but could actual underestimate the true harm that large scale hydrological alterations have on the environment.

1.2 Formation and Classification of Peatlands

Canadian peatlands cover roughly 12 % (1.136×10^6 km^2) of the country's land surface, with 97% falling within boreal or subarctic regions (Tarnocai, 2009). As a dominant feature of Canada's landscape and an ecosystem under threat from climate change and land use practices, their maintenance and well-being should be of interest to all Canadians. Wetlands are defined as: "land that is saturated with water long enough to promote wetlands or aquatic processes as indicated by poorly drained soils, hydrophytic vegetation and various kinds of biological activity which are adapted to a wet environment" (National Wetlands Working Group, 1997; Mitsch and Gosselink, 2007). In Canada, an organic wetland, also known as peatland, develops organic soils of at least 40 cm of peat accumulation, in accordance with established soil classification standards (National Wetlands Working Group, 1997; Canada Soil Survey Committee, 1978). Peat itself is loosely defined as a light brown to black soil formed under waterlogged conditions, consisting of partially decomposed vegetation, but can also refer to any soil with organic material as a significant component (Berglund, 1986; Shotyk, 1988; Warner, 2003).

Organic soils can be distinguished from mineral soils quite readily through differences in bulk density, porosity, hydraulic conductivity, nutrient availability, cation exchange capacity, and organic content (Mitsch and Gosselink, 2007). However, not all organic soils are equal.

Botanical origin of the organic material, be it mosses, herbaceous compounds, or wood and leafy litter, can allow for further differentiation, along with the extent of humification. Typically, boreal peatlands form in depressional formations where moisture is more easily retained, resulting in palludification (Zoltai and Pollett, 1983; Rydin and Jeglum, 2006; Vitt, 2006). Terrestrialization may also occur as encroaching *Sphagnum* moss covers over and fills in lakes or ponds. In general, cool climates favour the formation of peatlands, where input from groundwater, surface water, and precipitation exceeds outputs from groundwater, surface water, and evapotranspiration (Boelter and Verry, 1977). These landscapes and conditions are commonly found in the Canadian Shield and contain an average accumulation of 5-7 m of peat (Zoltai and Pollett, 1983; Vitt, 2006).

Under the Canadian Wetland Classification System, wetlands are divided into five primary classes (marshes, swamps, bogs, fens, and open water) based on the overall genetic origin of the ecosystem. Further subdivision by 'form' uses surface morphology, surface patterns, water type, and morphology of underlying mineral soil as criteria. The final level, referred to as 'type,' is based upon the physiognomic characteristics of the vegetation communities within the wetland (National Wetlands Working Group, 1997). Peatlands fall under three of the primary classes (bogs, fens, and swamps), depending on the descriptions above. A peatland swamp is dominated by trees, shrubs and forbs, with waters that are rich in dissolved minerals. Peatlands dominated by bryophytes and graminoid species can be classified as bogs or fens, with most locations being some combination of the two, termed a bog-fen complex (National Wetlands Working Group, 1997).

Bogs are characterized by a variety of geochemical and morphological features. They come in many shapes and sizes, but are consistently level with, if not raised above surrounding

terrain. Consequently, bogs are ombrogenous and rarely affected by runoff or groundwater flows (National Wetlands Working Group, 1997). These requirements encourage bog formation in regions with cool climates that receive high precipitation (Foster et al., 1988). Organic acids released during decomposition of peat creates a low pH environment, usually between 4.0 and 4.8 (Gorham and Janssens, 1992). Bog hydrology also produces low nutrient conditions for surface vegetation, which is chiefly dominated by varying species of *Sphagnum*. The growth of these mosses tend to form dry raised hummocks on which ericaceous shrubs, such as *Vaccinium oxycoccos*, *Andromeda glaucophylla*, *Kalmia polifolia*, *chamaedaphne calyculata*, and *Rhododendrum groenlandicum* are commonly found (Newmaster et al., 1997; Schwintzer, 1981). The intercises between hummocks, termed hollows, tend to be more wet and depressed in relation to the surroundings. Trees are also found in bogs, such as black spruce, though they are often stunted due to the lack of nutrients (Newmaster et al., 1997). As such, the underlying peat is typically a mixture of moderately decomposed *Sphagnum*, with a wood based contingent from trees and shrubs (National Wetlands Working Group, 1997).

Like bogs, fens are characterized by the accumulation of layers of peat and a wide variety of forms based partially on surface morphology. However, all fens have a surface that is level with the water table and feature water flow through both the surface and subsurface. This often takes the form of channels or pools and can shift up or down a few centimetres depending on seasonal or local fluctuations in water level (National Wetlands Working Group, 1997). Exposure to surface and/or groundwater means that fens are minerotrophic and range from 'poor' low nutrient systems with an acidic pH of around 5, to 'extremely 'rich' systems with abundant nutrients and an alkaline pH as high as 8 (Hebert and McGinley, 2010). The elevated nutrient status of fens allows for greater diversity of plant species, but these will vary extensively

depending on water table levels and where, on the minerotrophic gradient, that particular wetland exists. Wetter fens tend to be dominated by graminoid and bryophyte species, whereas in dry sites shrubs are much more prominent (National Wetlands Working Group, 1997). Meanwhile, nutrient-poor fens are similar to bogs, featuring *Sphagnum* species and ericaceous shrubs, with black spruce in treed variations. On the other end of the scale, extremely rich fens are dominated by a combination of sedges and brown mosses, with shrubs from the *Salix* and *Betula* genera, as well as *Larix* species in the drier areas. The underlying peat in fens consists of decomposed sedge and brown moss, with appropriate sites containing the woody remains of shrubs and trees (National Wetlands Working Group, 1997). Despite the fact that low oxygen content and a high water table both inhibit aerobic decomposition, fens generally accumulate less peat than bogs. This is due to the minerotrophic nature of the source water, which acts as a stimulant, enhancing both productivity and anaerobic decomposition within the wetland (Boelter and Verry, 1977).

Although bogs develop through a combination of autogenic processes (peat build-up) and allogenic forcings, (climate or physical disturbance) (Robichaud and Bégin, 2009), some theories suggest that they ultimately lie further along the same evolutionary path as fens (Boelter and Verry, 1977). When the Wisconsin ice sheet began to retreat between 9000 and 14000 ^{14}C yr BP, large chunks of ice were broken from the main glacier, creating depressions in the landscape. The depressions were characterized by poor drainage and eventually filled with water from the melting ice to become lakes (Boelter and Verry, 1977). Climate at the time was conducive to the formation of aquatic peats, which were eventually covered by sedge peats derived from cattails, reeds, and sedges. These peats impeded drainage, allowing the water table to rise and more peat to accumulate until fens were formed. Around 3000 years ago, *Sphagnum* peats began to form in raised areas where precipitation was the primary source of water (Boelter and Verry, 1977). So

long as conditions remained consistent - with higher levels of precipitation than evapotranspiration - the peat surface continued to grow and expand, becoming further isolated from the water table. With time, these fens evolved into bogs, though in many situations the basin shapes and hydrology dynamics of peatlands facilitated formation of complex hybrids of both bog and fen classes (Boelter and Verry, 1977).

1.3 Carbon Cycling in Peatlands

The concentration of greenhouse gases (GHGs) in the atmosphere has become a steadily growing topic of concern over the past half century. Carbon dioxide and methane comprise the bulk of global GHG emissions at 82.9% and 9.5% respectively (Lal, 2008). However, the global warming potential of these GHGs is also important, indicating the warming contribution of the gas (vs. CO_2) and the timeline during which it affects the atmosphere. Before the onset of the industrial era, atmospheric CO_2 levels had been maintained for thousands of years at approximately 280 ppm (Lal, 2008, NOAA, 2012). The global annual average for 2011 was in excess of 390 ppm, the highest level in recorded history (NOAA, 2011) and is expected to grow at a rate of roughly 2 ppm per year (NOAA, 2011; Lal, 2008). Current predictions expect mean levels to surpass 400 ppm by 2016, levels that have already been exceeded in the arctic this year (NOAA, 2012).

Historically, undisturbed peatlands have been a small sink for CO_2 and a moderate to large source of CH_4; however, this balance is eternally in flux depending on local factors, including climate and hydrology. While this often results in peatlands being a net overall sink for atmospheric carbon, unfavourable conditions can lead to carbon neutral, or carbon source scenarios (Bridgham et al., 2006; Roulet, 2000; Kelly and Rudd, 1993). Peatlands contain a massively disproportionate amount of carbon relative to their surface area. Globally, peatlands

contain 16-33% of the soil carbon pool, while only covering 3% of the surface (Gorham, 1991). In Canada, these numbers are 56% and 12% respectively, representing an enormous carbon pool accumulated over thousands of years (Tarnocai, 2006). According to Tarnocai (2009), climate warming will have a severe to extremely severe effect on 60% of Canada's peatlands, releasing as much as 50% of all stored carbon. Silvola et al. (1996) have predicted that a 2° C rise in global temperatures could increase CO_2 output from wetlands by 30%. Likewise, a 15-20 cm drop in water table depth, brought on by drought or diversion, is thought to be sufficient to increase CO_2 output by as much as 50-100%. It has been suggested that expelling such a massive amount of carbon could trigger strong feedback mechanisms, causing even further warming (Oechel et al., 1993). Thus, understanding peatland carbon dynamics is of significant concern.

The actual cycling of carbon within peatlands is a complex system involving transformations within and between aerobic and anaerobic layers within the sediments. A simplification of these processes is shown in Fig. 1. Net primary production (NPP) is the primary means by which a wetland takes in carbon from the atmosphere. As vegetation dies, it forms litter in the acrotelm, an oxic layer of peat, and begins to decompose, returning as much as 90% of carbon, via CO_2, to the air (Rydin and Jeglum, 2006). However, as the vegetation becomes water logged and compressed by new layers above, it enters the catotelm where anoxic conditions are prevalent and decay is slowed significantly. Any further production of CO_2 (usually initiated through micro-organisms) eventually diffuses or ebulliates to the surface. Inevitably, some carbon is leached from the peat into groundwater and exits the wetland in the form of dissolved inorganic carbon (DIC), dissolved organic carbon (DOC), or particulate organic matter (Rydin and Jeglum, 2006). In addition, under the anaerobic conditions within the

catotelm, methanogenic archaea can reduce CO_2 using H_2 to form CH_4 (Mitsch and Gosselink, 2007). Methane can also be produced through other pathways, such as acetate fermentation of organic matter (Rydin and Jeglum, 2006). Laine and Vasander (1996) showed that a decrease in water levels within a wetland created a thicker aerobic zone, leading to more decomposition, heightened CO_2 emissions and substantially reduced CH_4 efflux. Alm et al. (1997) attempted to determine the carbon budget of a Finnish boreal fen.

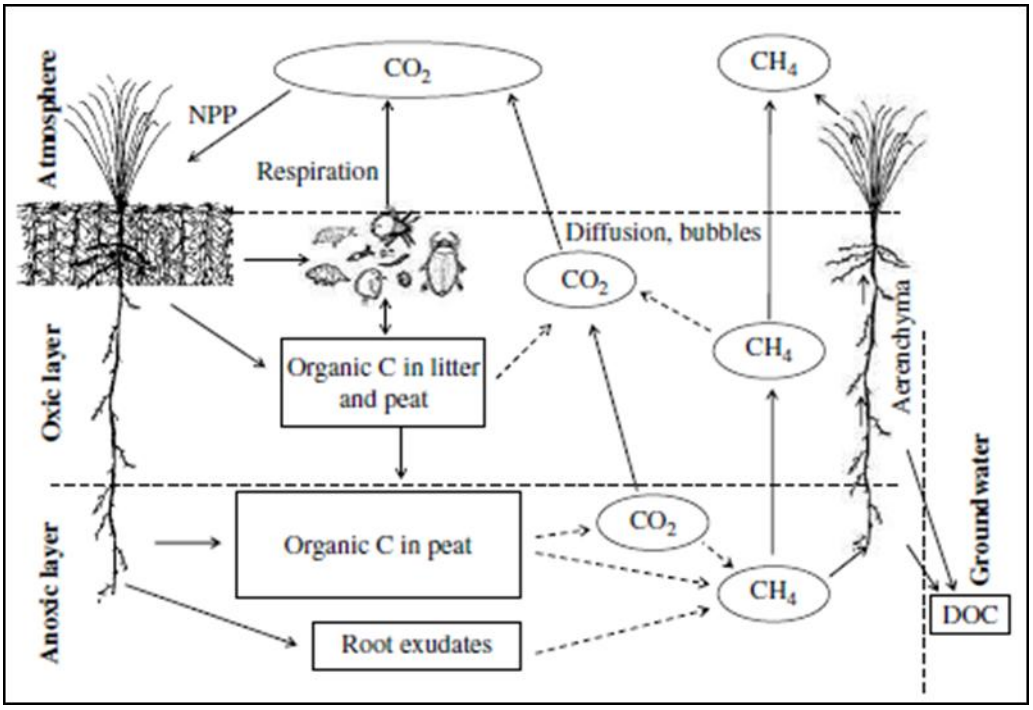

Figure 1. Schematic of the carbon cycle within peatlands. Dashed lines represent microbial processes. Adapted from (Rydin and Jeglum, 2006).

They found both Carex lawns and Sphagnum hummocks to be net sinks for carbon, of 34.0 and 31.9 g m-2 yr-1. However, with gross photosynthesis totaling 317.3 and 314.3 g m-2 yr-1 respectively, this indicates that a total of 89-90% of all accumulated carbon was lost through various means (CO_2 – 75.4-83.1%, CH_4 – 4.2-11.4%, and DOC leeching into groundwater – 2.5%). A similar study by Alm et al. (1999) done during the unusually dry summer of 1994 on a Sphagnum bog highlighted the impact of drought like conditions on peatland carbon balance.

The bog accumulated 205 g C/m2 over the entire year, but lost 255 and 30 g C/m2 over summer and winter respectively through respiration. Methane losses totaled 2 g C/m2 in the summer and 1 g C/m2 in the winter, while leaching removed 7 g C m-2 yr-1. This led to a total net carbon balance of -90 g C m-2 yr-1, effectively converting the bog from a carbon sink to a carbon source.

While methane releases from peatlands have been shown to be far lower than carbon dioxide emissions (Alm et al., 1997; Alm et al., 1999; Lal, 2008), peatlands are the largest natural contributor to the global CH_4 budget, responsible for 25% of the world's methane production annually (Keppler et al., 2006). In addition, each CH_4 molecule is a more potent threat to climate change than an equivalent CO_2 molecule. Methane has a radiative forcing that gives a global warming potential (GWP) of 25 times that of carbon dioxide over 100 years (IPCC, 2007). Bridgham et al. (2006) also calculated a GWP for CH_4 of 17 time that of CO_2. Consequently, much of the research on carbon emissions from peatlands has focused on methane.

Methane can be released from peatland sediments via three different pathways: (1) bubble ebullition, (2) molecular diffusion, and (3) gas transport through the aerenchyma of emergent plants (Rydin and Jeglum, 2006; Chanton, 2005). Bubble ebullition occurs when dissolved gases, including methane, which has a low solubility in water, equilibrate with the bubble reservoir (Yamamoto et al., 1976). When gases are stripped from the solution a bubble forms and is transported directly to the atmosphere, bypassing the oxidative effects of the acrotelm (Chanton, 2005). Levels of ebullition tend to fluctuate with pressure changes, occurring in episodes due to external factors such as wind events (Keller and Stallard, 1994), tidal variations (Chanton et al., 1989), or changes in atmospheric pressure (Glasser, et al., 2004).

Molecular diffusion is a passive system that moves molecules down a concentration gradient. In wetlands, the rate of diffusion is regulated by the diffusion coefficient, the sediment porosity and the strength of the concentration gradient (Chanton, 2005). Methane has a smaller diffusion co-efficient relative to CO_2, indicating that it moves more slowly, and less preferentially through the peatland (Domenico and Schwartz, 1990). As methane diffuses into oxygenated sediments, methanotrophic bacteria consume the gas, converting it to CO_2 before release. Despite the presence of this proverbial oxidative gauntlet, large amounts of methane still reach the surface untouched and enter the atmosphere (Crill, 1991). The final method of methane transport occurs within the lacunae or aerenchyma of aquatic macrophytes, a gas transport system responsible for bringing oxygen to roots and rhizomes to support respiration. The organic-rich sediments and soils surrounding the roots and rhizomes are often anoxic, and thus the methane produced in this layer can escape directly through the plant stem to the atmosphere (Chanton and Dacey, 1994). Ventilation of CH_4 via this method reduces methane partial pressures within the saturated soils, causing a subsequent decrease in diffusive flux and ebullition (Chanton et al., 1989). Therefore, vegetated wetlands, especially those with vascular emergent macrophytes, will emit methane almost exclusively through plants. Non-vegetated surfaces will use a combination of diffusion and ebullition as the primary means of CH_4 transport (Tyler et al., 1997). A study by Lansdown et al. (1992) on a temperate bog in Washington State found that ebullition was responsible for 89% of annual methane flux. However, only 6% of anoxic CO_2 release was attributed to ebullition, with the remaining 94% accounted for by diffusion and transport through plant tissue. Although diffusion, ebullition and aerenchymous transport are the primary means by which gases are removed from a wetland, advection also enables CH_4, DIC (both CO_2, HCO_3^-) and DOC to move through shallow peats in the groundwater (Waddington et al., 1995).

1.4 Isotopic Indicators of Carbon Cycling in Peatlands

Both stable and radioactive isotopes are commonly used in ecology to study the transport or interactions of molecules in a system (Fry, 2006). Isotopes play a role in all chemical reactions that involve a redistribution of atoms, and are usually divided into equilibrium or kinetic processes (USGS, 2004). Differences in the masses of atoms can cause slight differences in how those atoms react, resulting in fractionation of heavy and light isotopes in different phases. A fractionation factor (α) measures the extent of this fractionation by dividing the ratio (Ra) of the heavy to light isotopes in the first compound by the corresponding ratio in the second compound (Rb) (Kendall and Caldwell, 1998).

$$\propto_{(a-b)} = \frac{R_a}{R_b} \qquad \textbf{Eq.1}$$

During evaporation, an equilibrium reaction, heavier water molecules containing ^{2}H and/or ^{18}O accumulate in the higher energy state liquid phase. The lighter molecules, containing ^{1}H and ^{16}O, remain in the vapour phase. In biological reactions, which are typically one-way kinetic reactions, the lighter isotopes, such as ^{12}C, form weaker chemical bonds while the heavy isotopes, like ^{13}C, form stronger ones. Consequently, during a reaction, the lighter isotope is selectively used due to the lower energy cost of breaking its initial bonds. The extent of isotopic fractionation depends on several variables, including the ratio of isotopes masses, the comparative energy of the bonds being severed, the temperature, and the speed at which the reaction takes place – with slower reactions allowing the organism to be more selective. Stable isotope measurements are usually reported as a delta (δ) value in parts per thousand (‰):

$$\delta = \left(\frac{R_{sample}}{R_{standard}} - 1\right) \cdot 1000 \qquad \textbf{Eq.2}$$

Here, (R) represents the ratio of heavy to light isotopes in both the sample and the accepted standard, such as VPDB for carbon isotopes, and VSMOW for hydrogen and oxygen isotopes. Although there are several methods to compare delta values, in general, a higher delta corresponds to a sample with a higher proportion of the heavier isotope (USGS, 2004).

Stable isotopes are a valuable geochemical tool in the characterization of wetlands, and have seen widespread use. Schiff *et al*. (1996) reported a $\delta^{13}C$ values between -25.5 and -28.5 ‰ in the dissolved organic carbon and peat carbon of a forested catchment on the Canadian Shield. Hornibrook *et al*. (2000) found similar values in the freshwater wetlands of Sifton Bog and Point Pelee Marsh in southwestern Ontario. An average of isotopic signatures from all plant species within the study area showed $\delta^{13}C$ values of approximately -27.6 ‰ and -28.2 ‰ respectively. Another article, by Chasar *et al*. (2000) investigated DIC in pore water of a Minnesota peatland. Measurements were taken in both fen and bog regions of the wetland, showing profiles that became more enriched with depth. The fen had a minimum $\delta^{13}C$ of -3.1 ‰ near the surface, and a maximum of about +6.5 ‰ near the bottom of the basin, while the bog demonstrated less variation with a surface value of +6.7 ‰ and a basal signature just under +10 ‰. Both of these scenarios indicate more aerobic, oxidative surfaces (depleted signals) and the occurrence of methanogenesis in deeper peat layers (enriched signal). Measurements by Mewhinney (1996) at the ELA on a small boreal peatland located in the L632 basin found comparable ^{13}C-DIC signatures. Although the speciation of DIC is dependent on local pH, in most fen or bog systems, the pH of pore water is between 4 and 6, meaning that the CO_2:HCO_3^- equilibrium is dominated by CO_2 (Mewhinney, 1996).

Methane can be generated by a variety of pathways, making the $\delta^{13}C$-DIC pool more positive, and thus making ^{13}C an excellent tracer for differentiating its method of formation.

Quay *et al*. (1988) were able to separate biotic and abiotic processes by showing that biogenically produced methane from wetlands has a $\delta^{13}C$ signature in the range of -50 to -70 ‰, while thermogenically produced methane is typically around -30 ‰. In purely biogenic methane pools, acetate fermentation and CO_2 reduction pathways can be distinguished by $\delta^{13}C$ signatures, typically falling within ranges of -50 to -65 ‰ and -55 to -80 ‰ respectively (Whiticar *et al*., 1986). Based on work by Lazerte (1981), CO_2 is formed during methanogenesis by two processes. The first, during acetate fermentation (eq. 3), is a direct production method that hydrolytically cleaves the acetate molecule to produce CO_2 and CH_4 as shown below (Lansdown *et al*., 1992:

$$CH_3COO^- + H^+ \rightarrow CO_2 + CH_4 \qquad \textbf{Eq.3}$$

The second is a two-step, enzymatically mediated reaction, initially producing H_2 gas alongside CO_2 (eq. 4),

$$CH_3COOH + 2H_2O \rightarrow 4H_2 + 2CO_2 \qquad \textbf{Eq.4}$$

before continuing to CO_2 reduction (eq. 5).

$$CO_2 + 4H_2 \rightarrow CH_4 + 2H_2O \qquad \textbf{Eq.5}$$

Both Steinmann *et al*. (2008) and Mewhinney (1996) reported $\delta^{13}C$-CH_4 signatures in the latter range, -58 to -71 ‰ and -64 to -75 ‰ respectively, indicating that methane was produced almost exclusively by CO_2 reduction in both peatlands (eq. 4 & 5). Lansdown et al. (1992) showed similar findings with a measured $\delta^{13}C$ of -74 ± 5 ‰ from CH_4 flux in a temperate bog. Soil incubation experiments using ^{14}C labeled acetate and CO_2 confirmed that CO_2 reduction is the

primary method of methane production, with acetate fermentation only responsible for <1% of methane release.

Tritium, a radioactive isotope of hydrogen (^3H) is formed naturally by cosmic radiation in the upper atmosphere, and anthropogenically through the detonation of nuclear warheads in the atmosphere (Gat *et al.*, 2001). Naturally produced concentrations existed prior to the 1950s at around 5 TU. With the advent of nuclear weapons testing in the 1950s and 60s, tritium concentrations spiked to over 5000 TU in the northern hemisphere. Precipitation is the primary method for transporting tritium over the continents and into surface, and eventually ground waters. The isotope has a relatively short half-life of 12.32 years, making it a useful tracer of natural water in many hydrological studies (Lucas and Unterweger, 2000). In boreal wetlands, Mewhinney (1996) found tritium concentrations between 10 – 30 TU in the top 3 m of an 8 m peatland, indicating exposure of near surface water to the atmosphere within the past 50 years. A look at water in the deep peat below 4 m showed a tritium concentration between about 1 – 6 TU, suggesting that this water had not recharged since before the 1950s. In the 1970s, Gorham and Hofstetter (1971) looked at the penetration of tritium from atmospheric fallout in bog peats, finding values of over 300 TU near the surface, and concentrations around 3 TU in deep sedge peat below 4 m depth. This suggested a last recharge predating nuclear testing, and indicated that the tritium of the main water body could actually be older if any exposure to downward diffusion of recent tritium had occurred.

1.5 Application of SEC-OCD Techniques in Wetland Ecology

The combination of size-exclusion chromatography and organic carbon detection (SEC-OCD) is an analytical technique that divides natural organic matter (NOM) into individual fractions, each representing different sizes or chemical functions (Huber *et al.*, 2011). Although

the size-exclusion component of this method has been in place for over forty years, improvements and alterations to organic carbon detection have led to the development of the more recent LC-OCD-OND (Liquid Chromatography – Organic Carbon Detection – Organic Nitrogen Detection) system. Based on the Grantzel thin-film reactor, this approach has improved the detection limit well into the low-ppb range, allowing for detailed analyses of a variety of natural waters, as well as quality control on NOM-free technical waters (Huber *et al*., 2011).

The left boundary of each LC-OCD chromatogram is defined by the column exclusion limit, which elutes quickly over the first ten minutes. The first fraction of note, termed "Biopolymers" is typically eluted between 30 - 40 minutes, indicating that it is composed of non ionic, high weight (>10 kDa), hydrophilic compounds that are unaffected by both cation and anion exchange resins. Comparing OCD, UVD (Ultraviolet Detection), and OND responses suggests that the biopolymer fraction consists primarily of polysaccharides, with some proteins and amino sugars also present.

The second fraction, named "Humic Substances" (HS) elutes at roughly 45 minutes and agrees with the retention times for both fulvic acid (46.7 min) and humic acid (43.3 min) (Huber *et al*., 2011). Huber and Frimmel (1996) used the differences between the aromaticity and molecular weight of humic acid and fulvic acid, along with standards from the International Humic Substances Society (IHSS) to create the humic substances diagram (HS-diagram). Plotting individual data on this diagram can help divulge the origins, be they pedogenic or aquagenic, of the humic substance fraction. In the context of analyzing natural waters, this can be useful for approximating the origin of DOC, improving both hydrological and geochemical understanding of a site.

Breakdown products from the humic substances form the third fraction, termed "Building Blocks". Consequently, these molecules share similar characteristics to the humic substances, but are of lower molecular weight. They elute from the column immediately after humic substances, at about 50 minutes, often overlapping with the former signal (Huber *et al*., 2011).

Low molecular-weight acids (LMW acids) are the fourth fraction, eluting in a typically small peak following the building blocks at 55 minutes. These acids are anions at the neutral pH of the mobile buffer phase and are pushed out of the column by repulsive forces between the sample and the weak cation exchange resin of stationary phase. Their quantification can often be overestimated, as LMW-humic substances sometimes co-elute with them, but an empirical formula can be used to correct the calculation (Huber *et al*., 2011).

Low molecular-weight neutrals (LMW neutrals) compose the remaining elution volume, from the right boundary of the LMW-acid peak to the end of the analysis (60 – 120 minutes). This fraction consists of wide variety of molecules, including LMW alcohols, aldehydes, ketones, sugars and amino acids, meaning that in some waters, it will be a highly complex mixture (reading as an asymptotic line), while in others it will show distinct peaks (Huber *et al*., 2011).

The final fraction is termed "Hydrophobic organic carbon" (HOC) and does not appear on the chromatogram. Instead, it represents the organic material that remains on the column, retained by hydrophobic interactions (Huber *et al.*, 2011). In addition, because the HOC fraction is calculated as a direct difference between total DOC and the sum of eluted carbon, it should also include any cationic low molecular-weight particles that were affected by the cation

exchange resin. For a visual representation of the different fractions discussed above, see the chromatogram below (Fig. 2).

The focus of the LC-OCD technique for the past 15 year has been as a highly sensitive method for analyzing drinking water. It is used in water treatment plants to test raw sewage, ensuring that appropriate treatment measures are applied to deal with each of the different DOC fractions. Further tests are performed after each stage of treatment (ie. flocculation, chlorination, sedimentation, and sand filtration) to assess progress. With respect to wetlands, the technology improves the understanding of how DOC changes within the sediment and along the surface. It also demonstrates why two equal measures of total DOC could be completely different in their individual composition. This is useful in hydrology for estimating both the origin of a particular water source and what it has come in contact with. Application of LC-OCD analysis to the effluent from specific treatment wetlands could also be beneficial in gauging their efficiency.

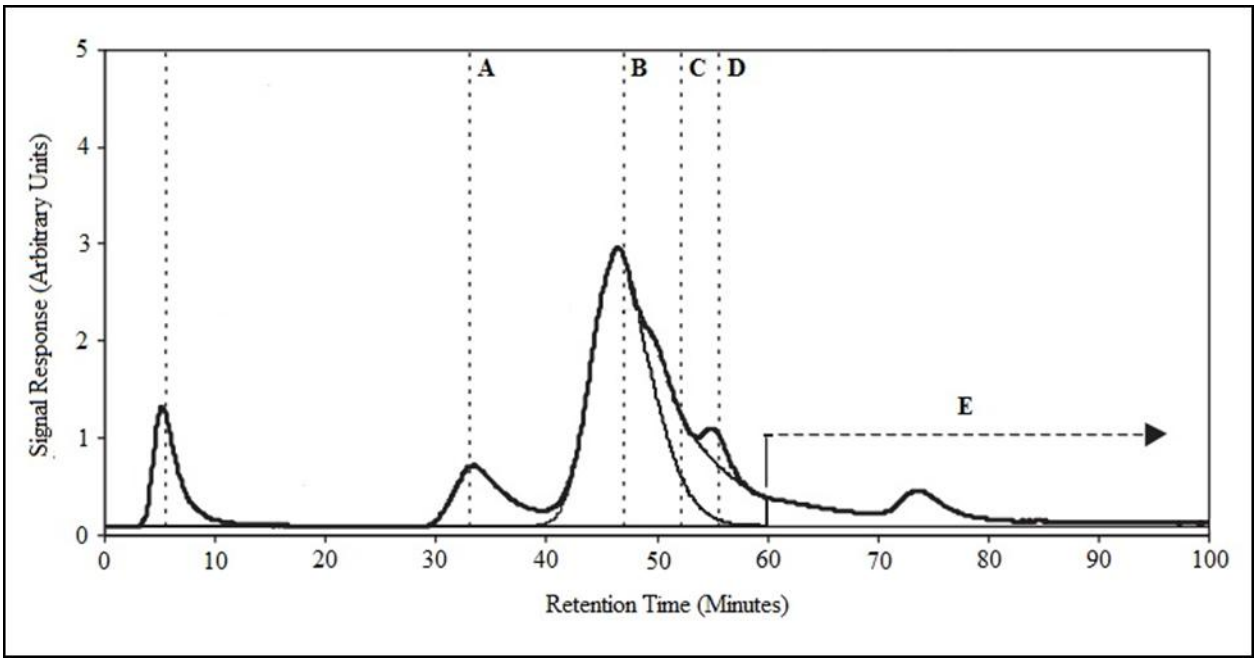

Figure 2. Example of an LC-OCD chromatogram showing the different column fractions, with boundaries between the fitted HS peak and non-humic matter. A = Biopolymers; B = Humic

substances; C = Building blocks; D = Low molecular weight acids; E = Low molecular weight neutrals. Adapted from a figure in Huber et al. (2011).

1.6 Summary

Individual knowledge of specialized fields, such as vegetation, stratigraphy, nutrient cycling and isotopes with respect to wetlands is always valuable and will allow characterization of the ecosystem to a certain extent. However, it is the understanding of interconnectivity between all of these parameters that will allow the researcher to paint the most vivid picture, capturing ideas, patterns and interactions that no one method could elucidate alone. Within the following pages, I have endeavoured to pull information from several such methodologies to better characterize and understand the implications of a water source diversion on two boreal wetlands in the Experimental Lakes Area (ELA).

CHAPTER 2

STUDY SITE

2.1 Location

The Experimental Lakes Area (ELA) is in north-western Ontario, located approximately 60 km south-east of Kenora, Ontario (Fig. 3). This area is home to hundreds of Canadian Shield lakes, with over 50 designated as research sites by the Canadian government. The specific study site lies at the outflow of a small lake (L626), which is situated on the western side of Pine Rd., the primary access route, and about 16km south of the Trans-Canada highway (49°45'26" N, 93°48'10" W) (Fig. 3).

The ELA has been the focus of decades of research on several processes that affect lake systems. Early studies linked phosphates from detergents with the growing eutrophication problems in the Great Lakes region. Additional research looked at the impacts of acid rain and radionuclides on the chemistry of lakes and the food webs they support. In the 1990's, work was done on the production of greenhouse gases and methyl mercury from flooding of wetlands. This was followed up with a second reservoir simulation by flooding of a forested upland area. Both studies revealed the environmental footprint for hydroelectric energy generation at boreal latitudes, a process that was thought to be much less harmful to the environment than it actually has been shown to be (Stokstad, 2009; Schindler, 2009).

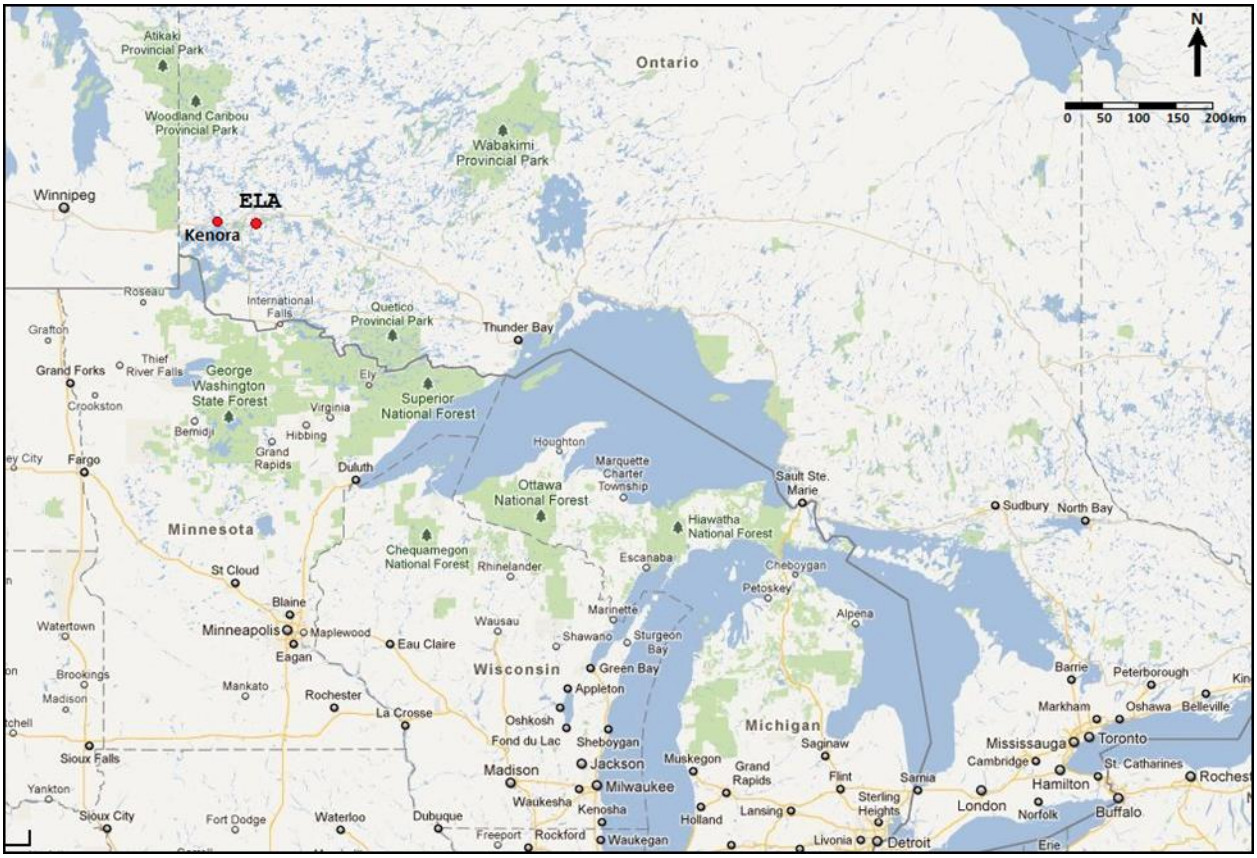

Figure 3. Map of the province of Ontario indicating the location of Kenora and the ELA (Google Maps, 2012).

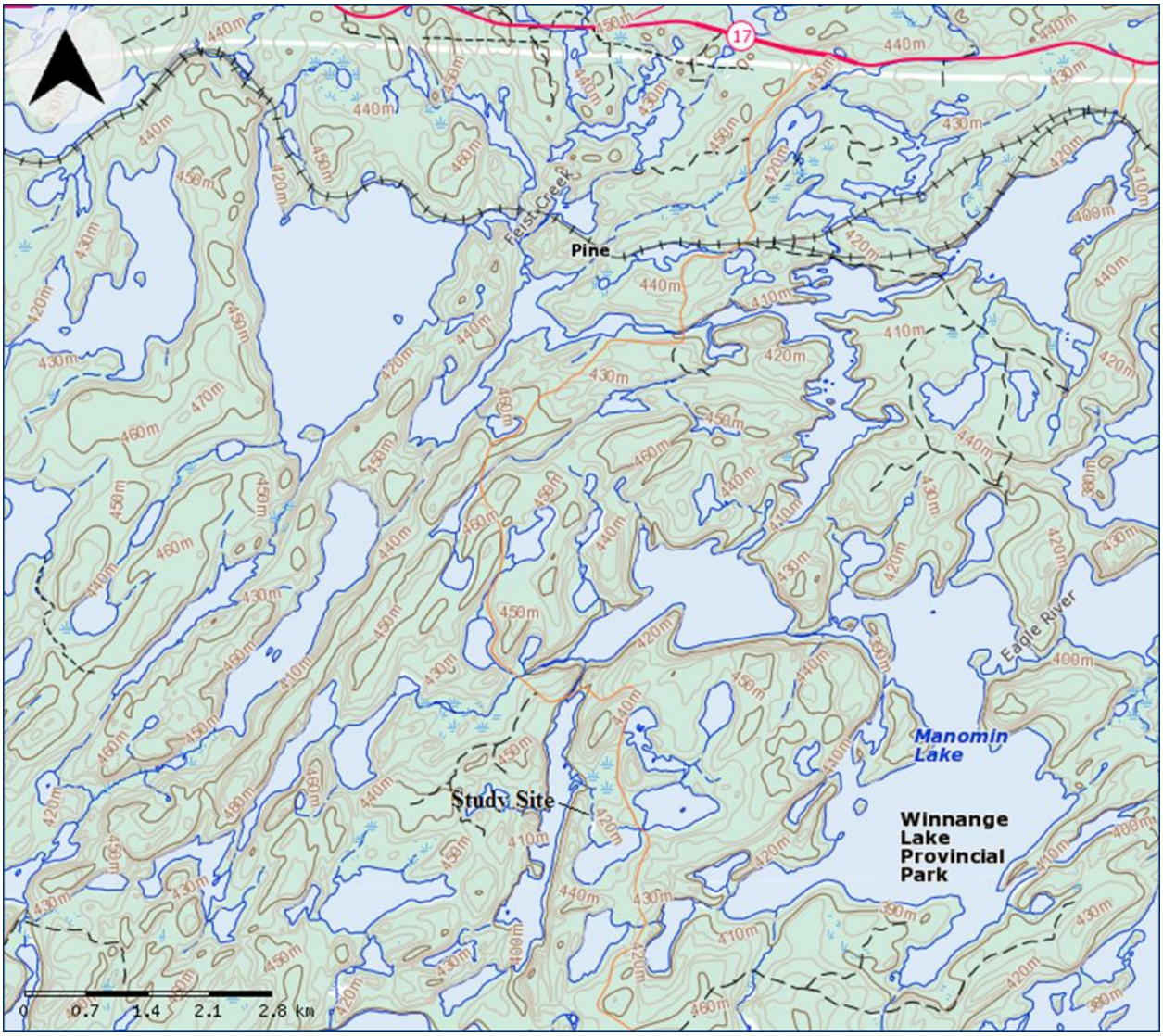

Figure 4. Map showing part of the ELA region including the study site, in relation to the Trans-Canada Highway (top) (Atlas of Canada, 2012).

2.2 Physical Setting

The two study wetlands, designated 626A and 626B, lie in small depressions just north of the larger basin that houses Lake 626, approximately 420 m above sea level (Fig. 4). Both basins are composed of granitic bedrock, with steep western faces and more gradually sloping, oft exposed eastern edges. Wetland 626A is both larger and deeper than wetland 626B, with an area of 2.2 ha vs. 1.2 ha, and a maximum organic material depth of about 4 m versus 2.5 m

respectively. The sediments composing and underlying each wetland are detailed in chapter 4.

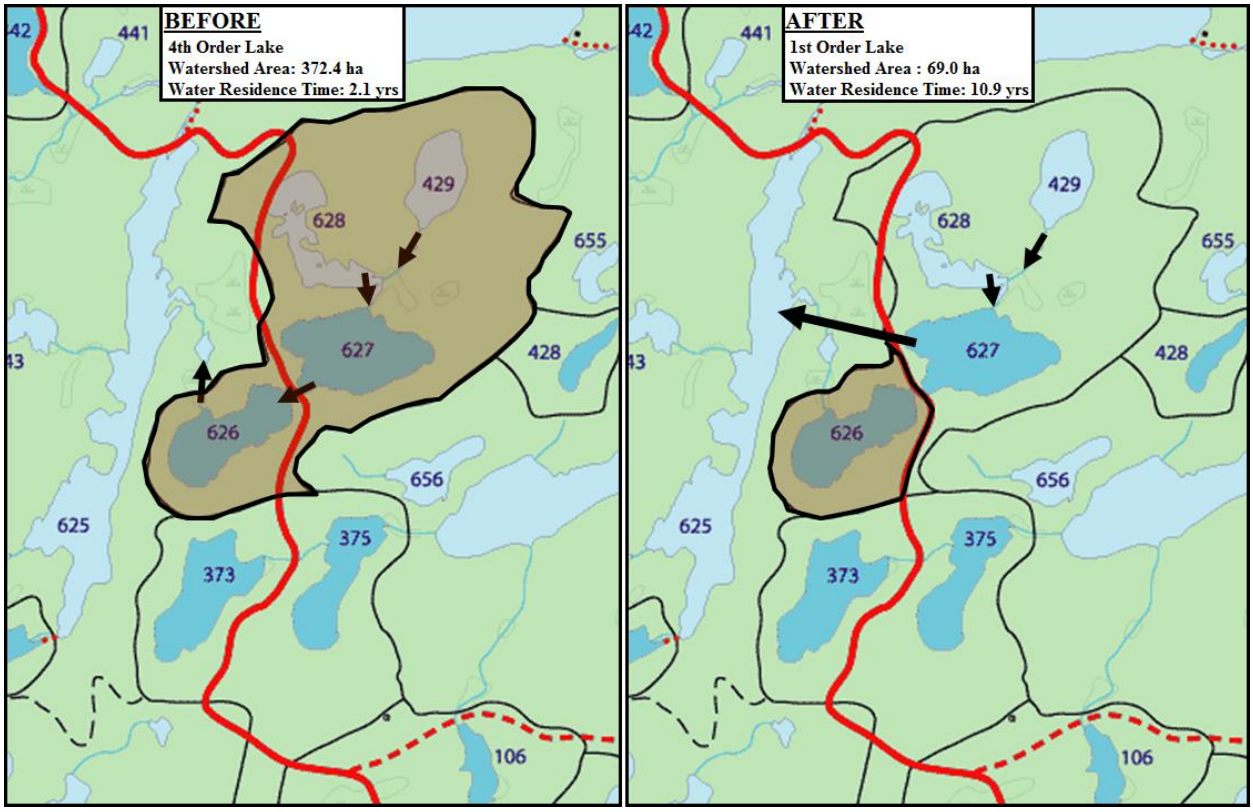

Figure 5. The watershed (outlined in black) for the impacted lake system, both before and after construction of the diversion. Primary access road shown in red. Taken from Beaty (2007).

Local climate studies have shown a mean annual air temperature of 2.4 ˚C, ranging from -17.6 ˚C in January to 19.2 ˚C in July (Beaty and Lyng, 1989). Climate metrics were downloaded from on-site meteorological data loggers for the year of sampling; 2011. Mean annual, January and July temperatures were 3.7 ˚C, -17.3 ˚C, and 20.1 ˚C respectively while total annual rainfall was 475 mm. The primary water input originates in Lake 626, a fourth-order, oligotrophic lake, typical of the region, with an area of 26.2 ha and a maximum depth of about 12 m (Wall and Blanchfield, 2012). The diversion project converted Lake 626 to a first-order lake and effectively reduced the watershed area of Lake 626 from 372.4 ha to 69.0 ha, while

increasing the water residence time from 2.1 years to 10.9 years (Fig. 5) (Beaty, 2010). This water enters the first wetland, designated 626A, via channelized flow, and passes directly through to a small pond at the outflow. This water then enters the second wetland, 626B, and once again, traverses the wetland via a channel to another small pond at the outlet (Fig. 6). Each wetland also receives water input from the surrounding uplands as runoff.

Figure 6. Aerial photograph of the study region. The wetland basins are defined by the black outlines. Wetland A is located on the right and Wetland B is located on the left. Yellow lines represent water flow paths, black lines represent transects, and red dots indicate sampling points.

2.3 Vegetation

The mixed coniferous and deciduous forests of the Boreal Shield Ecozone dominate the area surrounding the ELA (Rowe, 1972; National Atlas Information Service, 1993). The local upland vegetation is covered by mixed coniferous and deciduous trees: *Picea mariana, Pinus banksiana, Abies balsamea, Picea glauca, Populus tremuloides, Larix laricina* and *Betula papyrifera* (Asada *et al*., 2005). The soils are thin, which contributes to many unvegetated patches scattered throughout denser forest. Lower wetland areas typically contain *L. laricina* and *P. mariana*, with drier, upland sites supporting the remaining species, plus *P. mariana*, in various successional stages (National Wetlands Working Group, 1988).

According to the Canadian Wetland Classification System, (National Wetlands Working Group, 1997) wetland 626A is a bog-fen complex and wetland 626B is a fen. In each peatland, typical fen vegetation exists in the basin centre, dominated by *Carex rostrata, C. lasiocarpa*, and *Myrica gale*, while the periphery of the basin is slightly drier and the vegetation is characterized by low shrubs, with *M. gale* and *Chamaedaphne calyculata*.

Wetland 626A contains a raised bog of *Sphagnum fuscum* and *S. magellanicum* along the western edge of the basin. The hollows contain primarily *Sphagnum* species, while the hummocks are dominated by *C. calyculata, M. gale* and *Rhododendrum groenlandicum* in the upper layer, and *Andromeda glaucophylla* and *Vaccinium oxycoccos* in the understory. Wetland 626B also shows the species more common to bogs, with small patches of *Sphagnum* in the north-west area of the basin (Fig. 6 and 7). A small intermittent stream flows through the centre of each basin. Small open water areas are located at the outlets of each basin, where there are submerged aquatic species including *Potamogeton natans, Nuphar variegatum* and *Brasenia schreberi*. The upland areas immediately along the upland edges of each peatland basin support

L. laricina, P. banksiana, B. papyrifera and *Picea mariana* among other species. There are patches of bare bedrock and lichens. The vegetation in these study sites is similar to that described for nearby wetlands, L632 and L979 (Dyck and Shay, 1999; Asada *et al*., 2005).

2.4 Age of the Wetlands

This region of the Canadian Shield became glaciated most recently during the Wisconsin period, which reached a maximum glacial advance approximately 26500 to 19000 years BP. Around 20000 to 19000 years BP, northern regions faced increased insolation during summers, causing sea levels to rise and precipitating the eventual retreat of the ice sheets (Clark et al., 2009). Work by Clayton and Moran (1982) and Björck (1985) suggests that deglaciation of the ELA area likely occurred around 11500 BP. Lake Agassiz initially began draining into Lake Superior around 10900 BP, but the outlet was briefly blocked around 9900 BP by a glacial re-advance before opening permanently. Radiocarbon dating on basal sediments from nearby L979 showed the wetland began to accumulate organic sediments roughly 9600 years ago (Mewhinney, 1996), indicating that the basin became isolated from Lake Agassiz between 12000 and 9000 years ago (Teller and Clayton, 1983). Approximately 5000 years ago, terrestrialization of the lake basin through encroaching vegetation led to the formation of peat, which has accumulated since (Yazvenko *et al*., 1995). The two wetlands at the outflow of Lake 626 were expected to fit the same general parameters, though terrestrialization was expected to have begun earlier due to their smaller size and depth of the basins.

CHAPTER 3

METHODS

3.1 Instrumentation & Field Sampling

Access to both wetland sites was accomplished either on foot via a short (~1 km) trail or by boat. Generally, it is most convenient to access the south end of wetland 626A via the L626 outflow. Most of the 626A and 626B wetlands could be traversed on foot. Initially, transects were set up using flagging tape in a west to east direction , perpendicular to the stream flow, near the middle, or widest part of each wetland. An auger was used to probe peat depths at 20 m intervals along both transects. A number of other probes were taken to assess maximum depth of organic sediments.

Subsurface geochemistry was investigated through installation of piezometer nests along both transects (Fig. 6). In wetland 626A, nests were set up at 20 m, 80 m, 100 m, and 120 m and in wetland 626B, nests were placed at 20 m and 60 m. The number of piezometers at each nest was proportional to the site depth, with the deepest installations at 3.85 m in wetland 626A and 2.50 m in wetland 626B. Individual piezometers were constructed from ½" PVC pipe, fitted onto custom made PVC tips via cemented couplers. Each tip consisted of a 1 ¼" piece of solid PVC, 2" in length, lathed to a point on one end. This was coupled to a 30 cm section of ½" PVC pipe, slotted over a 10 to 15 cm interval and screened with 0.0073 cm nytex mesh. Piezometers were easily driven into pre-augured holes by hand so that the center of the nytex screen lined up with the desired depth. During each installation, attempts to minimize peat disturbance were taken.

3.1.1 Sub-surface water sampling

Piezometers were installed and pumped dry during the first of two ELA field trips, between May 30th and June 3rd, 2011. Sampling was done during the second trip, between June 30th and July 6th, 2011. All pumping was done with a hand-held pump, fitted with ¼" polyethylene tubing, sections of surgical tubing and 3-way valves. Samples were collected in duplicate for DOC, DIC, CH_4, tritium, isotope, and anion analysis. DOC and anion samples were passed through a 0.45 μm filter and collected in 20 mL glass scintillation vials. DIC, CH_4 and isotope samples were collected in 58 mL serum vials, with headspace kept to an absolute minimum, and then preserved through acidification with H_2SO_4. Tritium samples were left untouched. All samples were refrigerated on site, and then shipped back to the laboratory at the University of Waterloo for analysis.

3.1.2 Surface water sampling

Surface water samples were taken at six locations, corresponding to the inflows and outflows of each wetland, as well as the inflow to the downstream lake (L625), and the inflow/outflow of the diversion channel. Surface samples were taken for the same analyses as piezometer samples, except for tritium.

3.1.3 Vegetation Cover

During the second field trip (July, 2011), the percentage cover of tree, tall shrub, low shrub, herb and bryophyte species was estimated. Species cover analysis was performed by randomly selecting a total of twenty five 1 m x 0.5 m plots per wetland, each consisting of two adjacent 0.5 m x 0.5 m quadrats (Dyck, 1998). Percentages were approximated to the nearest 10%, with non-abundant species given values of 5%, 1% or <1%. Underlying species such as sphagnum, which may not have been counted (due to overlying shrubs), were listed as being

present. Individual species of *Sphagnum* were difficult to distinguish by eye in the field, particularly *S. magellanicum* and *S. fuscum*, and were thus consolidated into one general *Sphagnum* category. It should be noted however, that these species occupy different habitat niches within the wetland (Dyck, 1998; Vitt and Bayley, 1984).

3.1.4 Peat & Sediment Core sampling

Coring was performed along the central transect in each wetland. The 626A peatland was cored at 20 m, 80 m, 100 m, and 120 m along the transect, to a maximum depth of 4.0 m, while 626B was cored at 20 m, 60 m, and 80 m, to a maximum depth of 2.75m. Deep coring in both wetlands followed the methods of Jowsey (1966), using a Russian sidewall coring apparatus to remove peat in 50 cm increments. Each segment was wrapped in plastic wrap and aluminum foil before being secured with tape and labeled. Surface cores were taken at select sites from 0-50 cm depth using a stovepipe corer, though these sections were often difficult to sample. In wet sedge dominated areas, there was often too much water in the sample and the core fell apart or shifted during travel and storage. In sphagnum dominated areas, the moss was often compressed during sampling, resulting in a shorter core. These segments were double wrapped in large plastic bags, secured with tape and labeled for future identification. All cores were refrigerated on site before being shipped back to Waterloo for analysis.

3.2 Laboratory Analysis

3.2.1 Sediment description and sub sampling

Upon arrival in Waterloo, all cores were stored in a refrigerator to await analysis. Each segment of core was unwrapped and underwent visual examination to identify sediment composition and stratigraphy. Sub-samples of 1 cm^3 were taken in triplicate at 5 cm intervals and then stored in glass vials, labeled for depth, location and purpose. It should be noted that the

surface of the core was scraped away at sub-sampling sites to prevent contamination due to smearing during the original coring process.

3.2.2 Stratigraphy

Each core was examined in the field promptly after extraction, with significant sediment characteristics being noted. In the laboratory, a more thorough visual inspection was completed to characterize sediment composition within each layer. Classification was roughly based on both apparent density and remnant vegetation. Unfortunately, stratigraphic boundaries between 0 – 50 cm depth could only be approximated due to difficult sampling.

3.2.3 Radiocarbon Dating

One set of peat sub-samples were labeled for ^{14}C radiocarbon dating. Only the deepest core from each wetland was selected for analysis (626A – 80 cm and 626B – 20 cm). Basal samples, as well as samples representing different peat phases and key stratigraphic transitions were prepared accordingly. Each sample was dried overnight in an oven, weighed, and packed into a new labeled vial for shipment. The prepared samples were then sent to L'Université Laval to undergo accelerator-mass-spectrometer (AMS) radiocarbon dating in their lab. The results, when received, were corrected to calendar years using an equation based on the 'Fairbanks0107' calibration curve (Fairbanks et al., 2005).

3.2.4 Organic Matter Content

Loss on ignition (L.O.I.) analysis was performed on subsamples from all cores to estimate moisture and organic matter content. Technique followed standard procedures, which commenced with dried samples that are weighed, and then heated to specific temperatures, allowing for determination of organic and inorganic content (Dean, 1974). The first stage,

performed for one hour at 500-550 °C, produces a measure of organic carbon within the sample, while stage two, performed for the same amount of time at 1000 °C produces a measure of carbonate content. Bulk density was also calculated during the L.O.I. procedure by comparing the sample mass before and after the initial drying was done. Scale precision allowed all weight measurements to be reported to three decimal places.

3.2.5 Tritium Analysis

Tritium (^{3}H) analysis was performed on a total of seven water samples from the deepest core in each wetland. Unfortunately, there was insufficient water in the uppermost sample point in both wetlands to perform enriched analysis and direct analysis was used instead. The remaining samples from three depths in wetland A, and two depths in wetland B were suitable for enriched analysis. No pre-analysis sample preparation was required before submission to the University of Waterloo Environmental Isotope Laboratory. Samples underwent electrolytic enrichment before final analysis on a liquid scintillation counter. Direct tritium counting procedures have high analytical error associated with them and are reported to ±8 T.U., where as enriched results are more precise with an error of ±0.8 T.U.

3.2.6 Dissolved Organic Carbon

Dissolved organic carbon (DOC) analysis was performed on all surface waters, as well as all piezometer samples from both wetlands. Samples were passed through a 0.45 μm filter in the field, and left unacidified. In Waterloo, samples were kept refrigerated until they could be submitted to the University of Waterloo Environmental Geochemistry Laboratory for analysis. Here they were run on a Dohrmann DC190 High Temp carbon analyzer, with results reported in mg/L to two decimal places.

3.2.6 Dissolved Inorganic Carbon & Methane

Dissolved inorganic carbon (DIC) and methane analyses were performed on all surface waters, as well as all piezometer samples from both wetlands. Samples were collected via syringe into evacuated serum vials and preserved with H_2SO_4 before being refrigerated. In the laboratory, samples were weighed, and then injected with 10 mL of inert He gas (used as a carrier). Displacement of 5 mL of water was allowed, so as to maintain pressure in the vial. Each sample was then placed on a shaker for 120 minutes of mixing. Actual analysis was performed in the University of Waterloo Environmental Geochemistry Laboratory, on a Varian CP-3800 GHG analyzer with CombiPal (ECD/TCD/FID). Concentration of CH_4 samples were reported in μmol/L to one decimal place, while DIC was given in mg/L to one decimal place.

3.2.8 LC-OCD Analysis

Liquid Chromatography Organic Carbon Detection (LC-OCD) was performed on all surface waters, as well as all piezometer samples from both wetlands, to determine the abundance of individual organic compounds within the overall DOC pool. During collection, samples were passed through a 0.45 μm filter in the field, and left unacidified. In Waterloo, samples were kept refrigerated until they could be submitted to the NSERC Chair in Water Treatment, a laboratory in the Department of Civil and Environmental Engineering at the University of Waterloo, where they were analyzed. Results for each fraction were reported in ppb of carbon.

3.2.9 Carbon Isotopes

Stable isotope analysis ($\delta^{13}C$) was performed on the DIC and CH_4 of all surface waters, as well as all piezometer samples from both wetlands. Collection and preparation of samples used the same method as DIC/CH_4 analysis (described in 3.2.7 above). Samples were submitted

to the University of Waterloo Environmental Isotope Laboratory and analyzed on an Isochrom GC-C-IRMS. Results were reported as $\delta^{13}C$ in per mil units up to two decimal places.

CHAPTER 4

Results and interpretation

4.1 Vegetation Composition

Percent cover plots in each study site were used to delineate a total of four different plant communities in 626A and three in 626B. All community physiognomy was classified as open, with no treed areas aside from some scattered dwarf *Picea mariana* in A1, an area dominated by low shrub (mean 71% cover) bog (A1 – *Chamaedaphne calyculata, Myrica gale, Rhododendron groenlandicum*). The remaining communities were described as open fen varying in ericaceous shrub or sedge dominance (A2 – *Carex lasiocarpa, M. gale*; A3 – *M. gale, C. calyculata, C. lasiocarpa*; B1 – *C. lasiocarpa, C. rostrata, M. gale*; B2 – *M. gale, C. calyculata*) and open water wetland (A4 – *C. lasiocarpa, Nuphar variegatum*; B3 – *Brasenia schreberi, C. canescens*). The sedge dominated fen communities (37 - 44 % cover) also contained some shrub species (10 - 20 % cover), while the shrub dominated fen (52 - 61 % cover) was also composed of some sedge species (6 - 17 % cover). Herb cover was relatively low (2 - 7 % cover) in bog and fen communities, while the ground layer was typically *Sphagnum* spp. (*S. magellanicum, S. angustifolium* and *S. fuscum*) or covered by dead sedge remains. A map of vegetation communities and a list of average percent cover for plant species in each community can be found below (Fig. 7, Table 1).

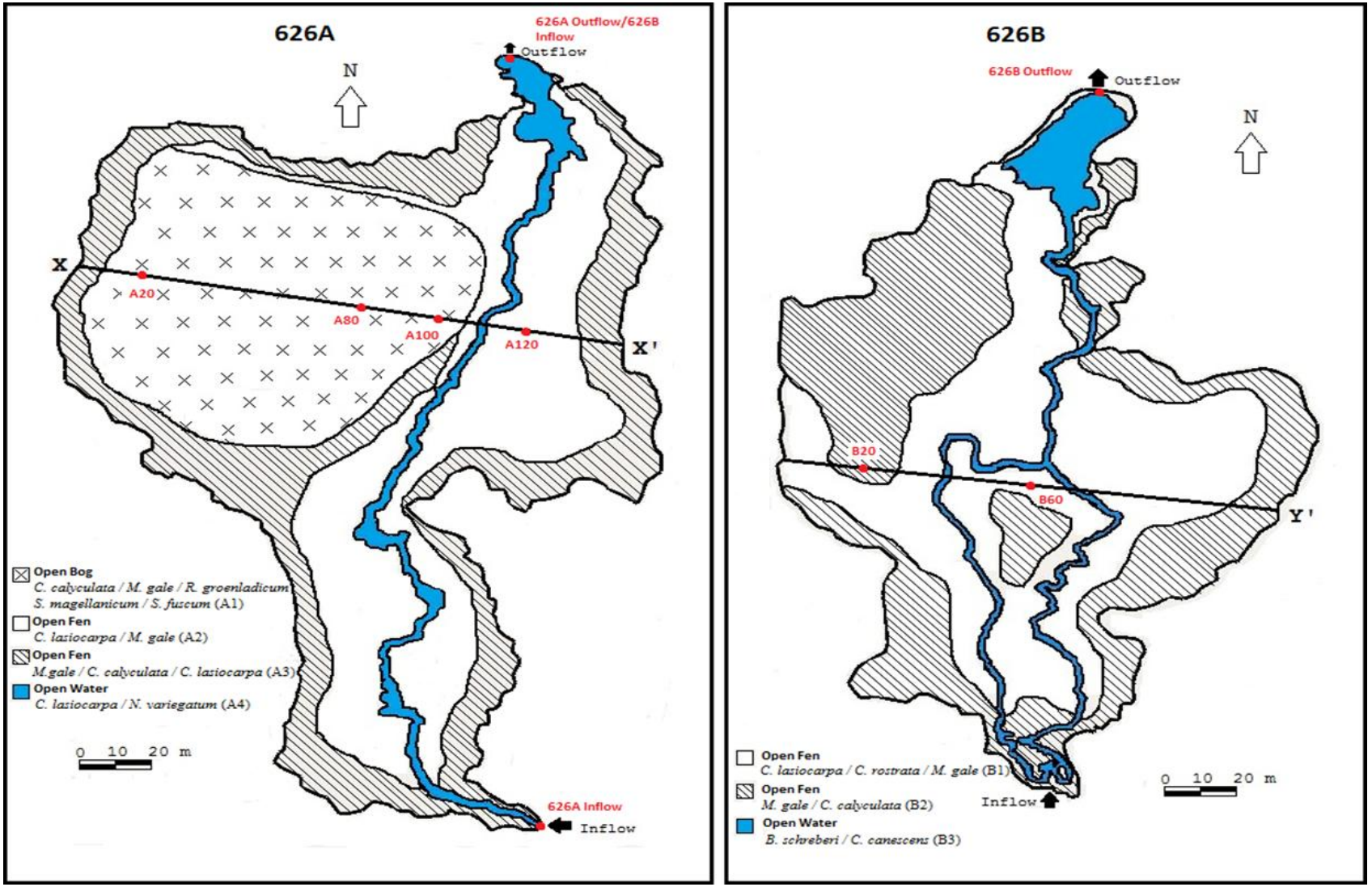

Figure 7. Vegetation maps of the two study wetlands showing different community types. Water from L626 flows into Wetland A (left), then proceeds to Wetland B (right), and upon exiting, eventually makes its way to L625. The black lines (X – X' & Y – Y') represent transects, while red dots indicated sampling stations.

4.2 Basin Stratigraphy and Sediment Composition

Of the two wetlands studied, Wetland 626A was the larger and deeper of the two. It is approximately 225 m in length along a north-south axis, and reaches a maximum width near its centre, along an east-west axis, of about 160 m (fig. 7). An east-west transect was used to characterize the stratigraphy, which consists of a deep basin on the west side of the wetland (0 – 110 m on the transect), and a shallow shelf on the east side (110 – 150 m on the transect).

Table 1. Mean percent cover of plant species in each community. Only species whose mean cover is equal to or greater than 0.5 % are listed. Anything less is described as trace (t). See Figure 5 for the abbreviated community names.

Wetland		626A				626B		
Community		A1	A2	A3	A4	B1	B2	B3
Number of plots		20	12	8	10	24	20	6
Open water (%)		-	1	-	50	1	-	48
	Species							
Trees	*Picea mariana*	t	-	-	-	-	-	-
Shrubs	*Rhododendron groenlandicum*	6	-	-	-	-	-	3
	Alnus rugosa	-	-	-	-	-	t	-
	Vaccinium oxycoccus	4	-	-	-	-	-	-
	Andromeda glaucophylla	3	-	-	-	-	-	-
	Chamaedaphne calyculata	39	2	21	2	3	11	-
	Myrica gale	19	18	31	0.5	7	50	-
	Amelanchier alnifolia	-	-	0.5	-	-	-	-
Herbs	*Smilacina trifolia*	2	-	-	-	-	-	-
	Drosera rotundifolia	t	-	t	-	-	t	-
	Viola nephrophylla	-	-	-	-	t	-	-
	Glyceria canadensis	0.5	t	1	-	-	-	-
	Carex chordorrhiza	-	-	-	-	t	2	-
	Carex canescens	t	-	-	-	-	-	15
	Carex lasiocarpa	0.5	32	10	25	24	1	-
	Carex rostrata	3	4	3	-	16	3	-
	Dulichium arundinaceum	-	0.5	3	4	4	t	1
	Iris versicolor	0.5	-	-	-	-	-	-
	Scirpus cyperinus	-	t	-	-	-	-	-

		Eriophorum angustifolium	1	-	0.5	-	-	t	-
		Hypericum virginicum	t	0.5	t	-	3	4	t
		Potentilla palustris	-	-	-	0.5	3	0.5	-
		Lysimachia terrestris	-	t	-	-	t	t	-
		Decodon verticillatus	-	-	-	-	t	t	-
Aquatic		*Potamogeton natans*	-	-	-	3	-	-	3
		Brasenia schreberi	-	-	-	-	t	-	28
		Utricularia vulgaris	-	t	-	t	-	-	1
		Calla palustris	-	-	-	-	t	-	t
		Sagittaria latifolia	-	-	-	-	-	-	1
		Nuphar variegatum	-	-	-	12	-	-	-
		Typha latifolia	-	2	1	3	4	2	1
		Equisetum fluviatile	-	0.5	t	-	-	-	-
Bryophytes	[a,b]	*Sphagnum* spp.	5	8	10	-	4	10	t
	[a]	*Polytrichum* spp.	-	-	3	-	-	-	-
Lichens	[a]	*Cladonia* spp.	t	-	1	-	-	-	-

[a] Species level separation was not performed on byrophytes or lichens, although a mixture of *P. strictum S. magellanicum, S. fuscum,* and *S. angustifolium* was observed

[b] Sphagnum was estimated as a percentage of overall cover. In many cases it covered 100% of the ground layer, paticularly in A1, but was covered by a layer of herb and shrub species

The deepest point is in the centre of the basin (50 – 60 m on the transect) and around 4 m depth. Cores taken at 20 m and 80 m along the transect contained organic material to depths of 370 cm and 385 cm respectively, with inorganic sediments beneath. Overlain on this layer of silty clay that lines the floor of the basin is a thick layer of dark, dense limnic peat and gyttja. Above this, starting at about 250 cm depth, are several layers of sedge peat, varying in density and texture. A thin layer of fine fibrous sedge peat is overlain by a unit of coarse fibrous sedge peat, which is under yet another layer of fine sedge peat. At about 50 cm depth a segment of moderately decomposed, extremely coarse sedge peat commences, and reaches the surface on the edges of the basin, as well as along the shallow eastern shelf. In the centre of the basin however, a mat of *Sphagnum* peat extends from about 25 cm depth to the surface, and then above that are hummocks of living *Sphagnum* (fig. 8).

Wetland 626B is slightly smaller in area, measuring approximately 200 m in length along a north-south axis, and reaching a maximum width of about 135 m along its east-west axis (fig. 6). A transect was set up along its width, and like Wetland 626A, its stratigraphy shows a deep basin on the west side of the wetland (0 – 75 m) and a gradually sloping shallow shelf on the east (75 – 127 m). Organic material in the deepest core, taken 20 m from the west edge, extended to a depth of 232 cm. The deepest point in the basin is probably around 2.5 m, located in the centre of the basin, between 30 and 40 m along the transect. Sediment composition is also similar to Wetland 626A, with a silty clay base overlain by a thick layer of dense limnic peat and gyttja. From 170 cm to 50 cm depth, a thin layer of coarse fibrous sedge peat transitions to a thick layer that is more fine and fibrous. Once again, at 50 cm depth a unit of moderately decomposed, extremely dense peat extends to the surface. This is true across the majority of the transect, save the first 40 m, where a thin layer of *Sphagnum* peat is forming in the top 5-10 cm of the sediment. This is a fine, inconsistent segment, unlike the extensive mat of hummocked *Sphagnum* peat over the basin of the upstream wetland (Fig. 8)

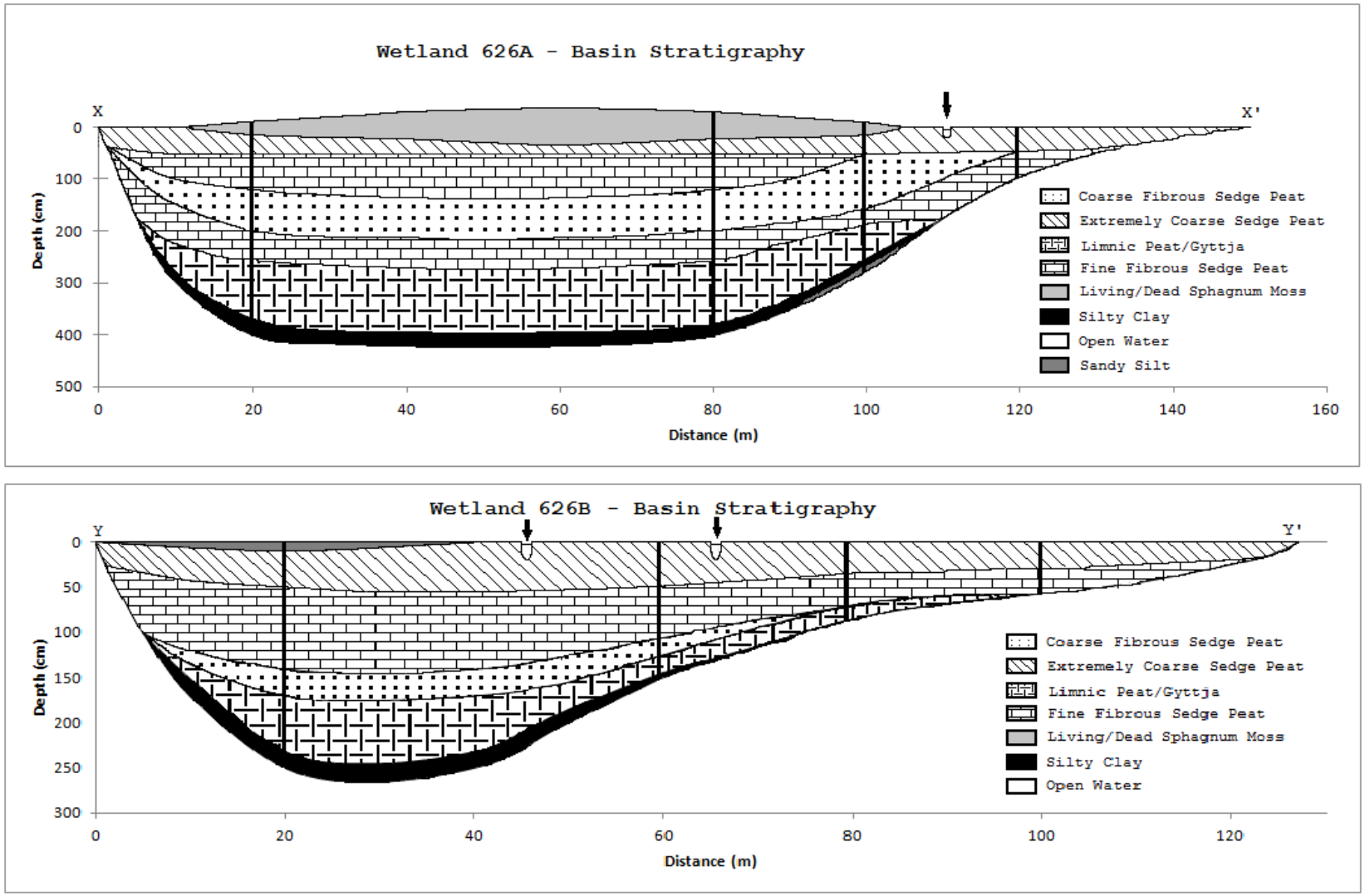

Figure 8. Basin stratigraphy diagrams of the two study wetlands along their respective transects, proceeding from west (left side of the diagram) to east. Arrows at the top of each transect represent locations of present-day water channels or streams. Dark vertical lines indicate coring locations.

4.3 Radiocarbon Dating

Sediment ages revealed that organic accumulation began in both basins around the same time between 11050 and 11200 calendar years BP. Organic sediment continued for about 3200 years in 626A and 1300 years in 626B while limnic peat and gyttja was being deposited. By about 9800 years ago in 626B, limnic peat transitioned to sedge, which existed since. In 626A, the transition to sedge peat occurred about 8000 years ago and existed for approximately 5500 years before shifting to *Sphagnum* peat for the last 2500 years.

Approximations of peat accumulation and deposition rates were determined for the longest core in each basin by taking the slope between their respective depths and ages. Variations in rates of peat accumulation are obvious in each basin (Fig. 9). In Wetland 626A, basin infilling began around 11200 calendar years BP and proceeded at a modest rate, depositing 1.10 m of sediment by 8050 years BP. Over the next 2500 years, the rate of accumulation increased to almost double its former pace. However, around 5600 years BP, net accumulation slowed by over three-fold, a significant decline. This rate seems to have been maintained up to the present day. In Wetland 626B, basin infilling began just over 11000 years BP, around the same time as 626A. Accumulation was slightly faster in 626B, proceeding at roughly 0.044 cm/year and depositing 1 m of organic material by 8780 years BP. Over the past 8700 years however, the average net accumulation rate was stifled to a mere 0.014 cm/year. Thus, the fastest rates of accumulation were seen between 8050 and 5600 years BP in Wetland 626A, and between 11060 and 8780 years BP in Wetland 626B.

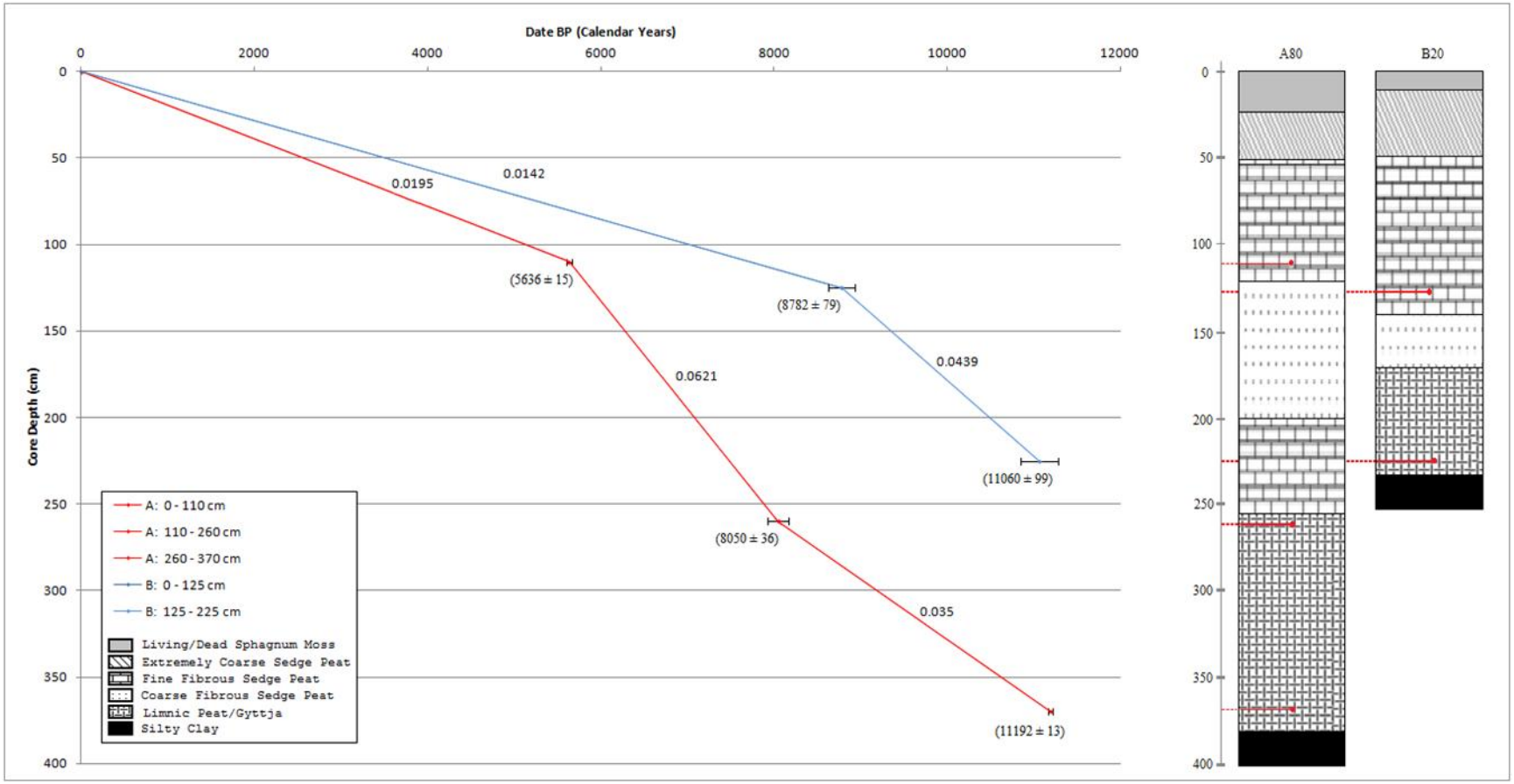

Figure 9. Sediment accumulation rates (cm/year) in both wetlands, indicated by the value above each line. Calibrated radiocarbon dates are listed below each data point. An age of zero years at the surface has been used as an approximation.

Table 2. Radiocarbon data from peat cores from Wetlands 626A & 626B.

Core	Depth (cm)	Fraction Modern	Corrected Radiocarbon Age (B.P) [a]	Calibrated Age (cal B.P. ± 1σ)	Dated Material	Laboratory Designation [b]
626B - 20 m	124.5 - 125.5	0.3719 ± 0.0009	7945 ± 20	8782 ± 79	Humic	ULA-3031
	224.5 - 225.5	0.3011 ± 0.0009	9640 ± 25	11060 ± 99	Limnic	ULA-3032
626A - 80 m	44.5 - 45.5	0.9928 ± 0.0020	Modern	Modern	Humic	ULA-3231
	109.5 - 110.5	0.5419 ± 0.0010	4920 ± 15	5636 ± 15	Humic	ULA-3033
	259.5 - 260.5	0.4056 ± 0.0010	7250 ± 20	8050 ± 36	Limnic	ULA-3034
	369.5 - 370.5	0.2971 ± 0.0009	9750 ± 25	11192 ± 13	Limnic	ULA-3035

Footnotes:

a - Ages are corrected for isotopic fractionation and are reported with 1 standard deviation

b - Laboratory designation: Université Laval

4.4 Organic Matter Content

In each core, bulk density remained between 0 and 0.2 g/cm^3 for the majority of the core, showing little difference among the varying sedge peat layers. In the lower regions of the limnic peat unit, bulk density showed sudden increases, which continued into the silty clay layer, reaching values between 0.6 and 1.0 g/cm^3(Fig. 10, 11 & 12).

The percentage of organic carbon in a sample showed a roughly inverse relationship to bulk density. For any full length core that was analyzed, organic content was at a consistent low of < 5% in the basal silt/clay layer. At the interface between the silt/clay and the overlying limnic peat/gyttja, organic carbon steadily increased above 5% of dry weight. Throughout the limnic peat/gyttja layer, organic carbon content continued to increase, and within the finer sedge peats in the middle of the core, this value reached between 50 – 80 %. For the remaining peat in the middle to upper layers, composed of mostly coarse, semi-degraded sedge species, organic carbon hovered between 80 and 100% of dry weight.

The carbonate content of all cores was extremely low, typically < 5% for the entire length of the profile. There were a few instances of higher carbonate concentrations (5 – 14%), though mostly as localized regions in specific cores. The area between 165 and 175 cm depth in the A100 core (626A – 100 m along the transect), as well as the bottom segment of the B60 core, 100 – 140 cm depth, showed above average levels of carbonate in the peat.

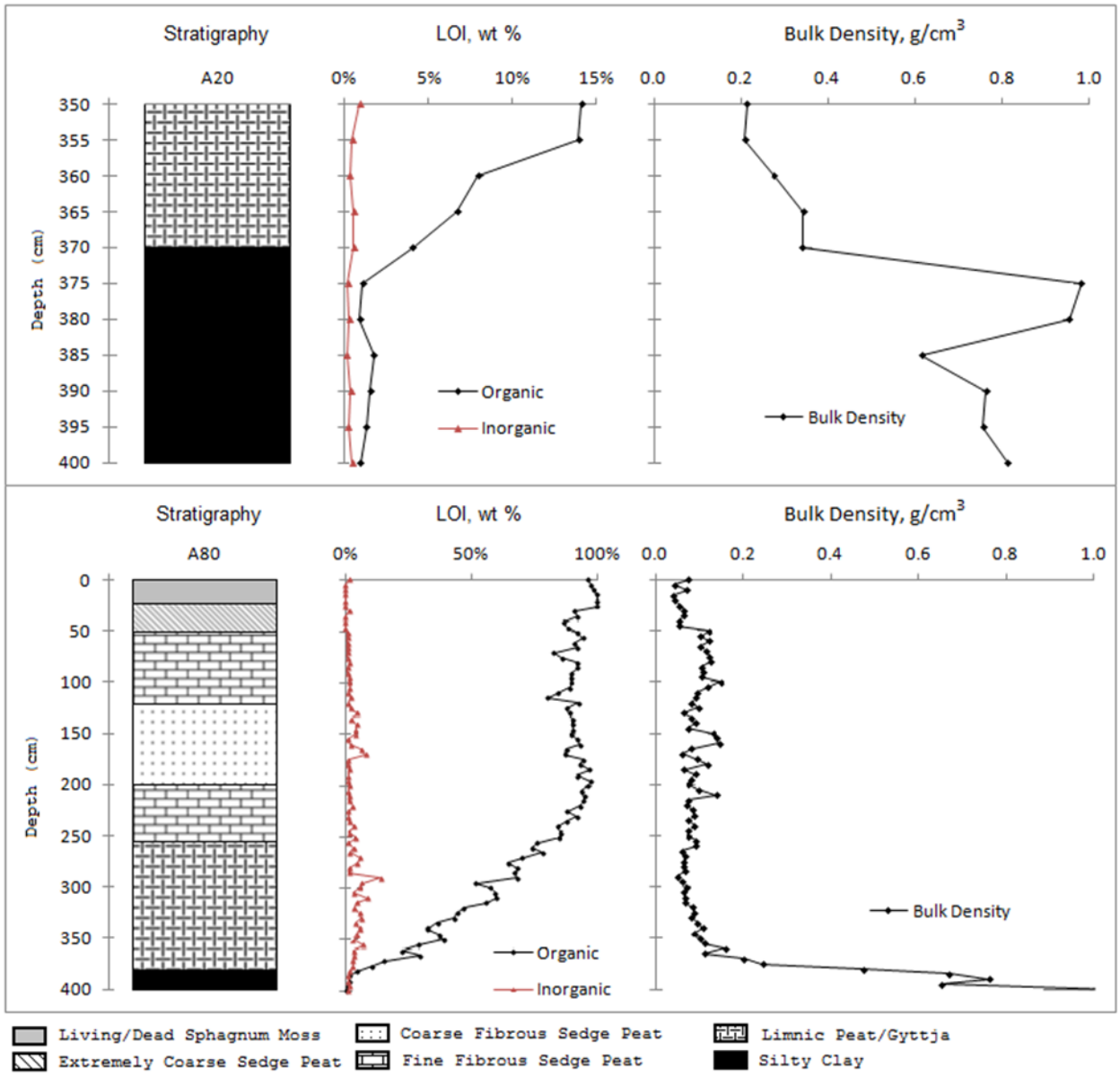

Figure 10. Stratigraphy, loss-on-ignition, and bulk density profiles for two cores in Wetland 626A, at 20 m (top) and 80 m (bottom) along the transect.

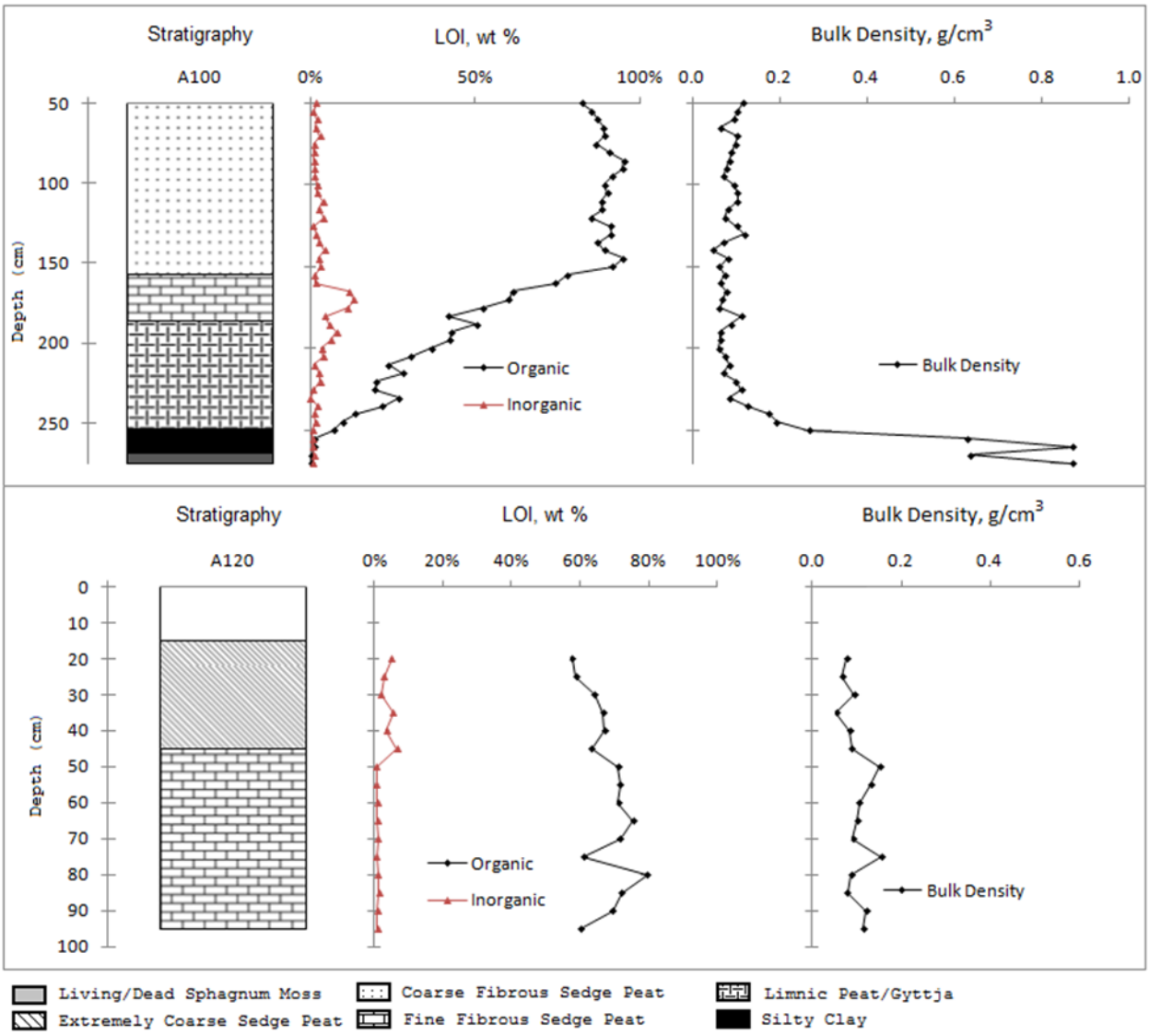

Figure 11. Stratigraphy, loss-on-ignition, and bulk density profiles for two cores in Wetland 626A, at 100 m (top) and 120 m (bottom) along the transect.

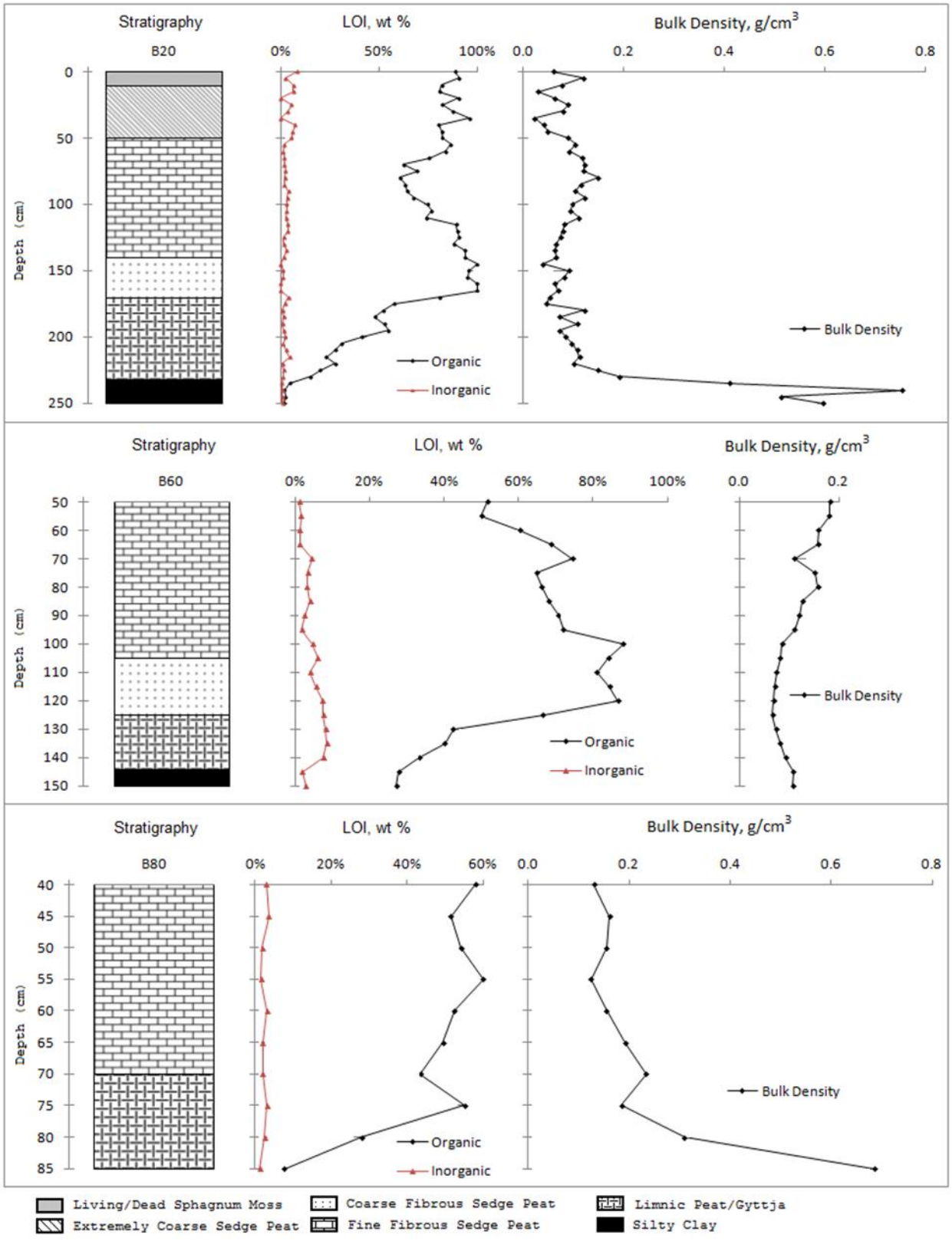

Figure 12. Sediment Stratigraphy, loss-on-ignition, and bulk density profiles for three cores in Wetland 626B, at 20 m (top), 60 m (middle) and 80 m (bottom) along the transect.

4.5 Tritium

A total of seven water samples were analyzed for tritium to create a profile at the location of the deep core in each wetland. The two samples submitted for direct analysis proved inconclusive (7.4 ± 8.0 TU – 626A, 80m on transect, 50 cm depth & < 6.0 ± 8.0 TU – 626B, 20m on transect, 60 cm depth) and were not included in figures, tables, or discussion. The remaining five samples underwent enrichment for ^{3}H (Fig. 13).

Tritium concentrations in 626A decreased with increasing depth from a high of 8.9 ± 0.8 TU at 150 cm depth (middle) to a low of 1.9 ± 0.4 TU at 385 cm depth (basal). With higher concentrations above, the low basal value indicates a good seal between the peat and the piezometer shaft, allowing minimal contamination from overlying sediment layers. Concentration in 626B however, showed vary little variance, with a high of 10.0 ± 0.9 TU at 120 cm depth (middle) and a low of 8.1 ± 0.8 TU at 241 cm depth (basal).

4.6 Dissolved Organic Carbon

The general trend at each site showed a decrease in DOC concentration with increasing depth. Near surface samples in the bog of 626A all showed DOC values in excess of 80 mg C/L, while the deepest samples, in both bog and fen (626A - 120 m not shown graphically) were between 20 and 35 mg C/L (Fig. 14). In 626B, there was less differentiation with depth, with near surface DOC values between 37 and 55 mg C/L and basal values between 18 and 48 mg C/L (Fig. 15). DOC content of channelized surface water showed relatively low and consistent concentrations. Inflow from Lake 626 had a DOC of 5.7 mg C/L, while the three remaining sites were all slightly higher, ranging from 7.23 – 7.33 mg C/L (Fig. 15).

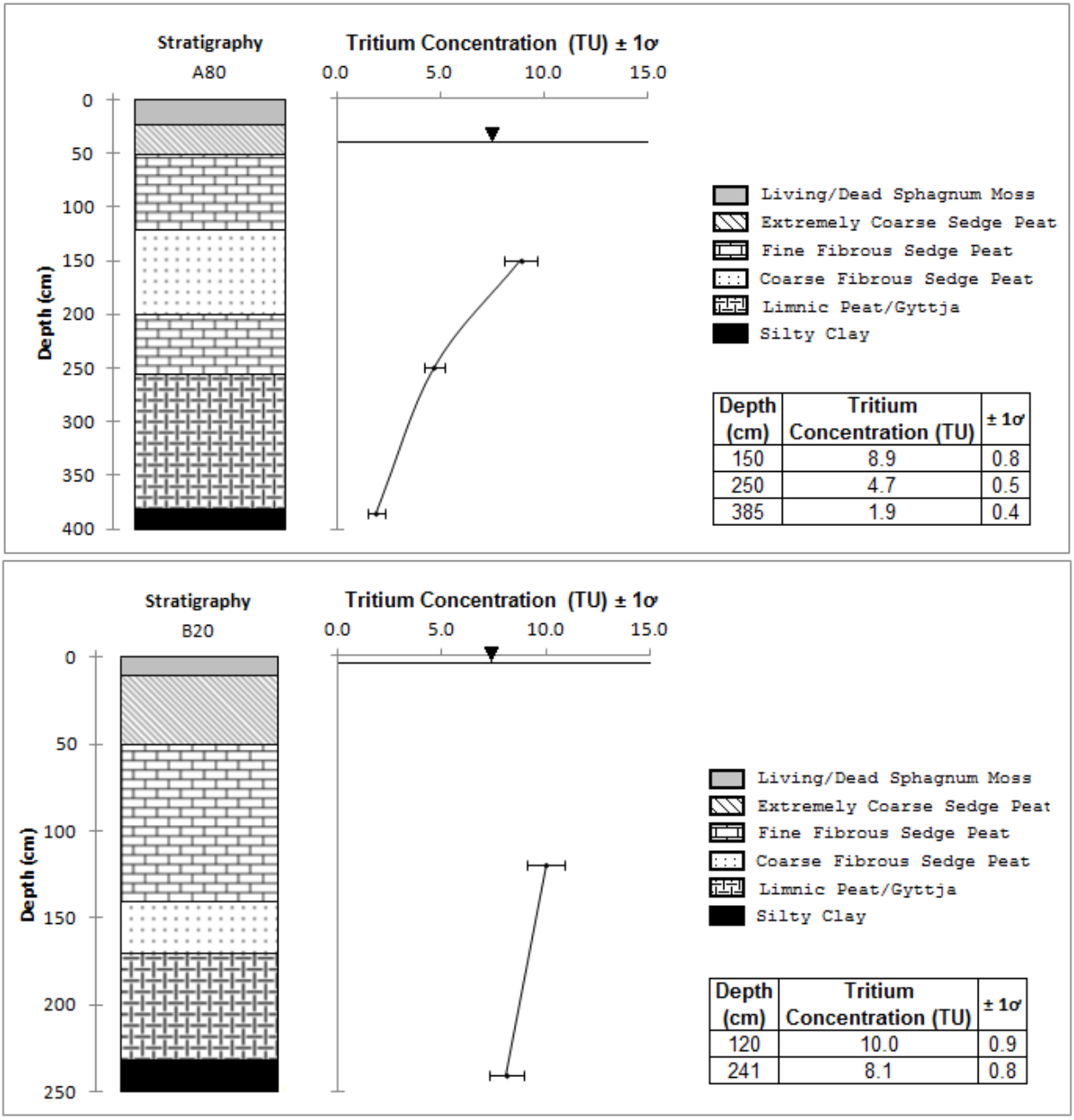

Figure 13. Sediment stratigraphy alongside tritium concentrations (TU) for the deep core in wetland 626A (A80 – Top), and wetland 626B (B20 – Bottom). Water table is shown by a line and a black triangle.

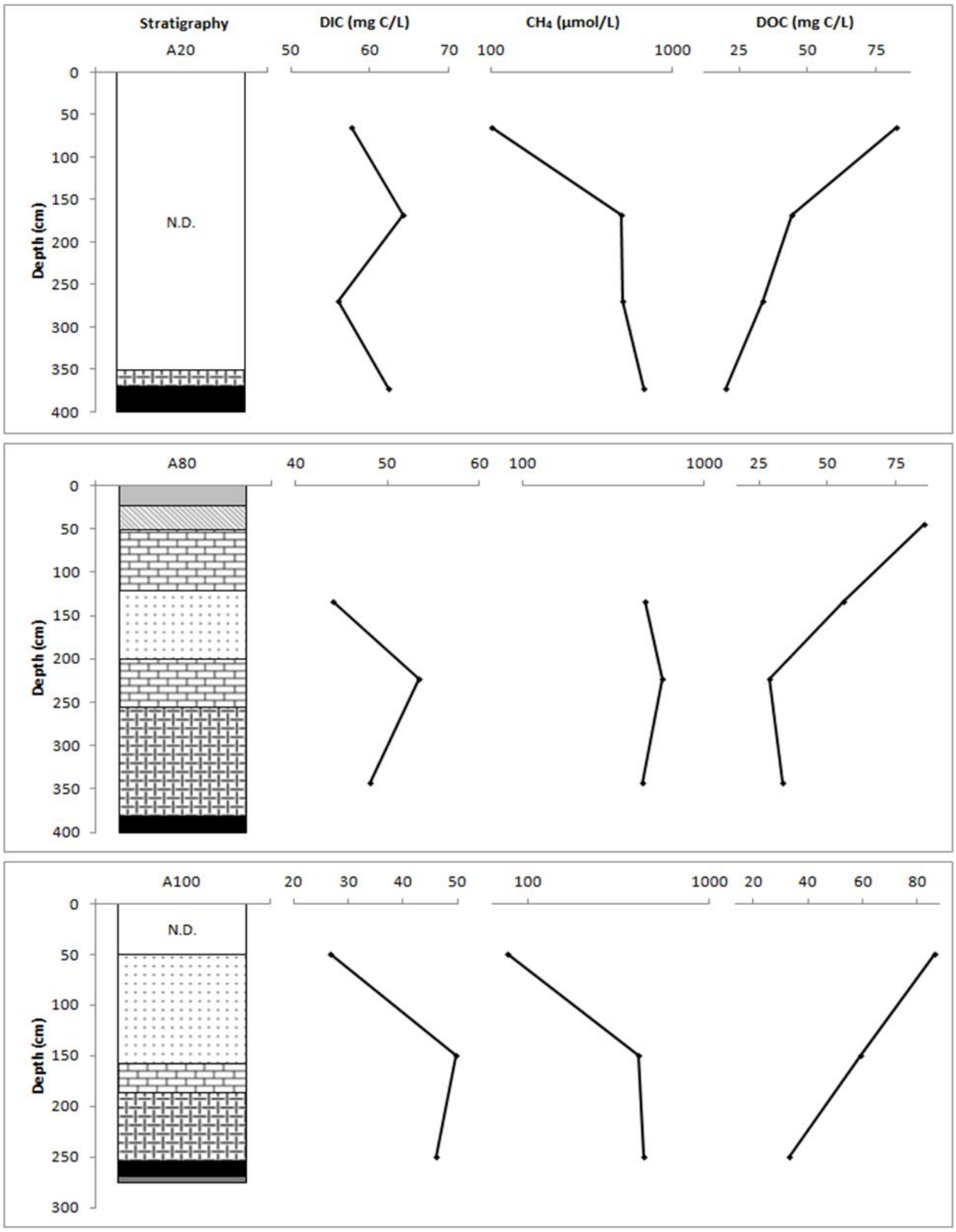

Figure 14. Core stratigraphy shown with DIC, CH_4, and DOC profiles for three cores in Wetland 626A, at 20 m (top), 80 m (middle), and 100 m (bottom) along the transect.

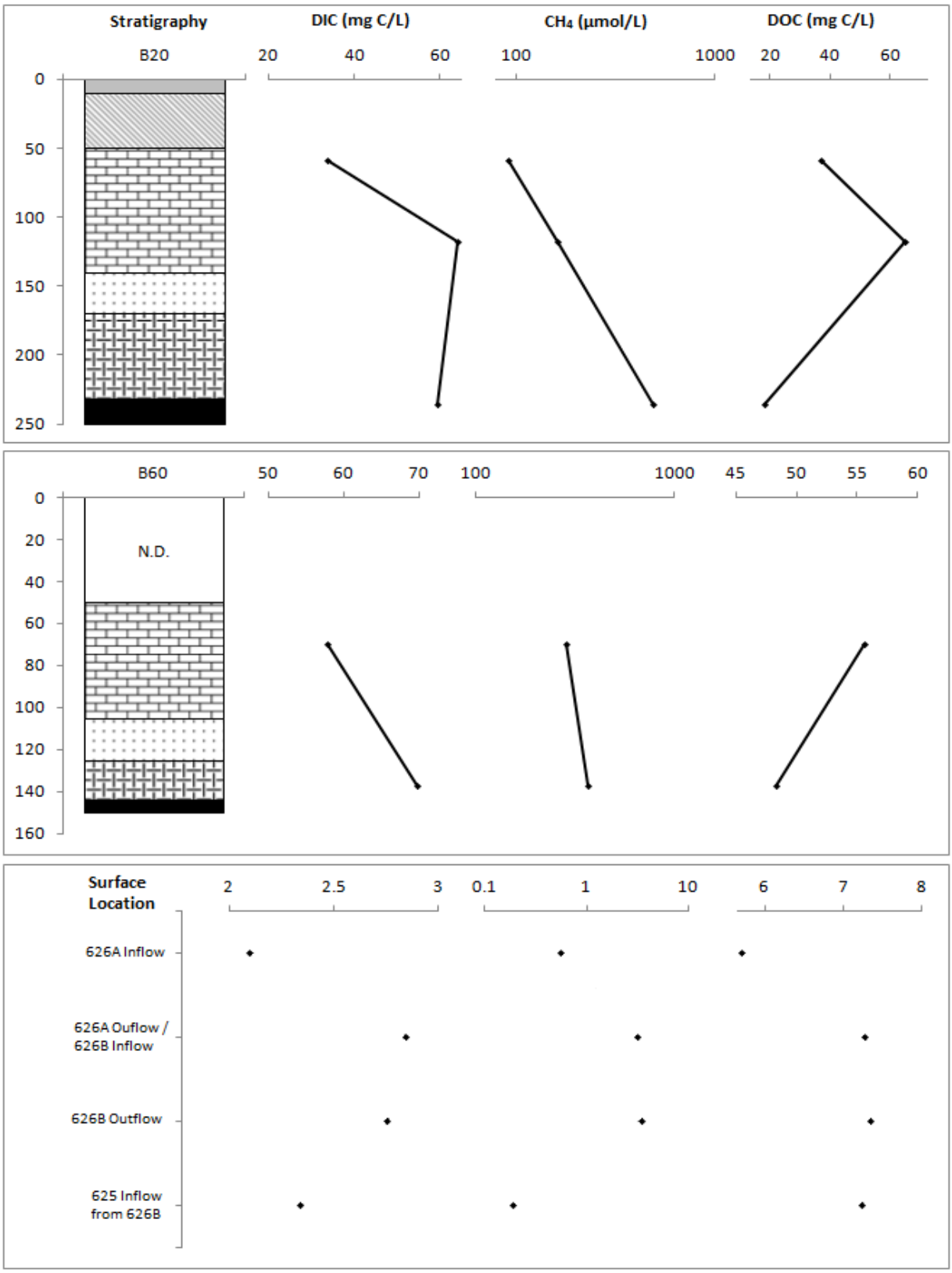

Figure 15. Core stratigraphy shown with DIC, CH_4, and DOC profiles for two cores in Wetland 626B, at 20 m (top) & 60 m (middle) along the transect. Surface metrics also shown (bottom).

4.7 Dissolved Inorganic Carbon & Methane

Water collection in the 626A piezometer at 80 m along the transect and 50 cm deep was extremely low, and unfortunately ended up being insufficient for this analysis. DIC concentrations tended to increase with depth to a certain point, and then remain constant or regress slightly with additional increases in depth. Concentrations also showed variation by location, with near surface values in 626A ranging from 27 to 58 mg C/L and basal values between 46 and 63 mg C/L (Fig. 14). Wetland 626B was similar, with near surface values ranging from 33 to 58 mg C/L and basal concentrations between 59 and 70 mg C/L (Fig. 15). The DIC concentrations of channelized surface water were very low and fairly consistent. Inflow from Lake 626 had a DIC of 2.09 mg C/L, while the three remaining sites were all slightly higher, ranging from 2.33 – 2.84 mg C/L (Fig. 15).

At all piezometer nests, methane concentrations increased with depth, growing sharply at first in shallow soils, then more gradually in deeper peats. In Wetland 626A, near surface values hovered between 75 and 100 μmol/L, while deeper water had methane concentrations ranging from 433 to 690 μmol/L (Fig. 14). In Wetland 626B, the shallow samples had CH_4 levels of 90 and 283 μmol/L, which increased to 489 and 363 μmol/L respectively at the base of each core (Fig. 15). Surface waters were generally very low in methane, but showed higher values at the outputs of both wetlands. Inflow from Lake 626 had a concentration of 0.55 μmol CH_4/L, while water exiting 626A and 626B had CH_4 values of 3.16 and 3.49 μmol/L respectively. By the time the surface water reached the downstream input to Lake 625, methane concentration had once again dropped to 0.19 μmol/L (Fig. 15).

4.8 Isotopes ($\delta^{13}C$) of DIC and Methane

The isotopic signatures for DIC, measured in $\delta^{13}C$ per mil, tended to become more positive with increasing depth. CH_4, on the other hand, became slightly more negative with depth.

In 626A, $\delta^{13}C$ signatures for CH_4 ranged from -62.5 ‰ to -68.5 ‰, with the more negative samples representing the deeper peats. DIC signatures were less consistent between nests, with some sites being more or less positive on a whole than others, but ultimately all values fell between -5.3 ‰ and +3.8 ‰ (Fig. 16). Wetland 626B showed a broader range of CH_4 signatures, ranging from -57.1 ‰ to – 73.3 ‰, and a slightly more negative DIC pool, with values between -6.2 ‰ and -0.9 ‰ (Fig. 17).

In surface water, there was no CH_4 detected at the inflow to 626A, nor the inflow to L625 downstream of the wetlands. However, both wetland outflows had similar signatures, between -57.7 ‰ and -59.3 ‰. The $\delta^{13}C$ signatures for DIC were also quite consistent, ranging from -12.0 ‰ to -15.9 ‰, with the most positive value at the 626A inflow and the most negative value at the L625 inflow downstream (Fig. 17).

4.9 Liquid Chromatography – Organic Carbon Detection

Surface waters, collectively, showed similar signal responses, with distinct peaks in the biopolymer, humic substances, building blocks, and low molecular weight acid regions (Fig. 18). Further analysis of the humic substance fraction is also shown in the form of an HS diagram (Fig. 19). In terms of carbon concentration by category, values were consistent across all surface samples, with biopolymers composing between 0.67 – 0.98 ppm, humic substances 2.56 – 3.73 ppm, building

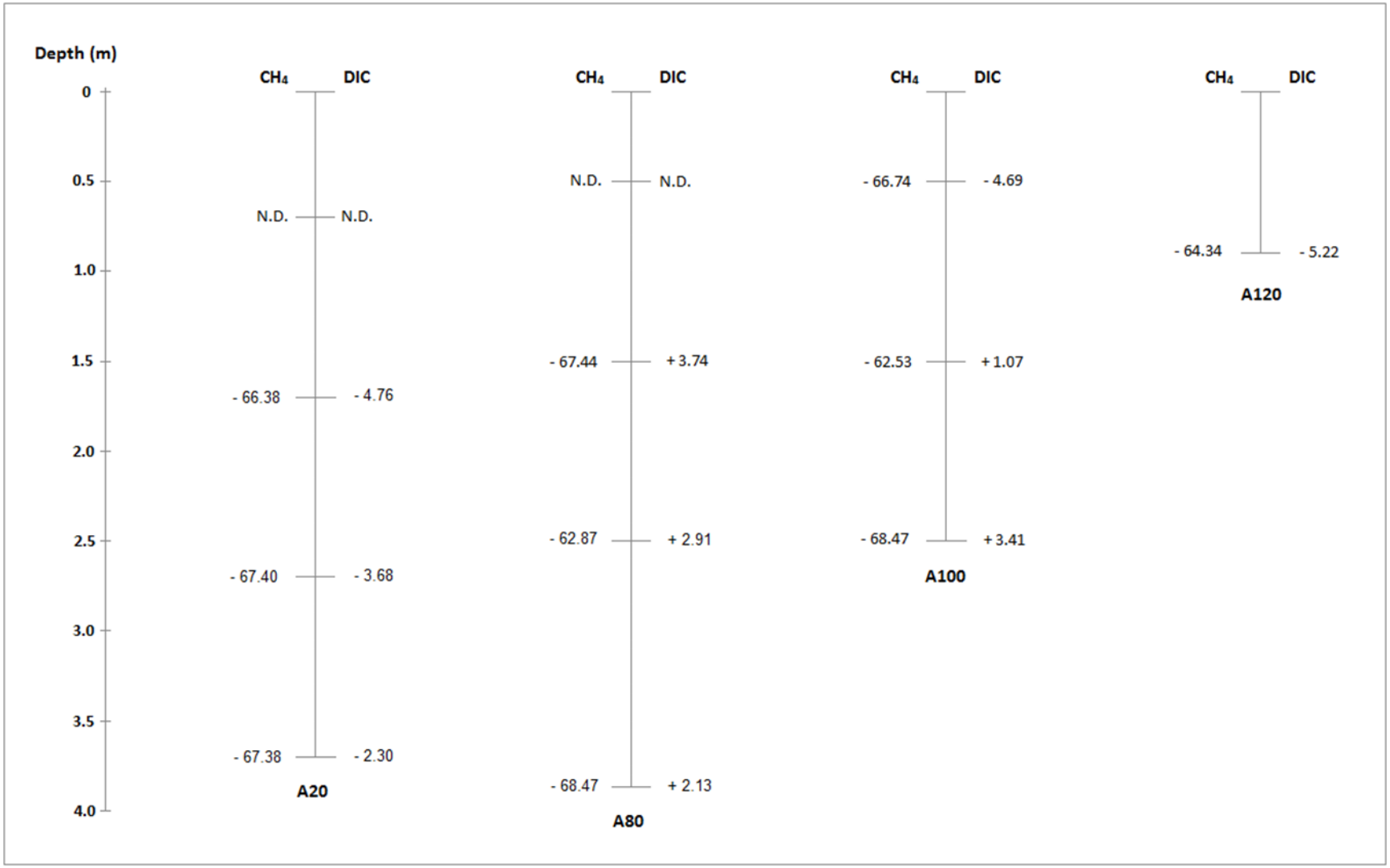

Figure 16. Isotopic signatures in $\delta^{13}C$ per mil for CH_4 and DIC versus relative depth for the four piezometer nests in Wetland 626A

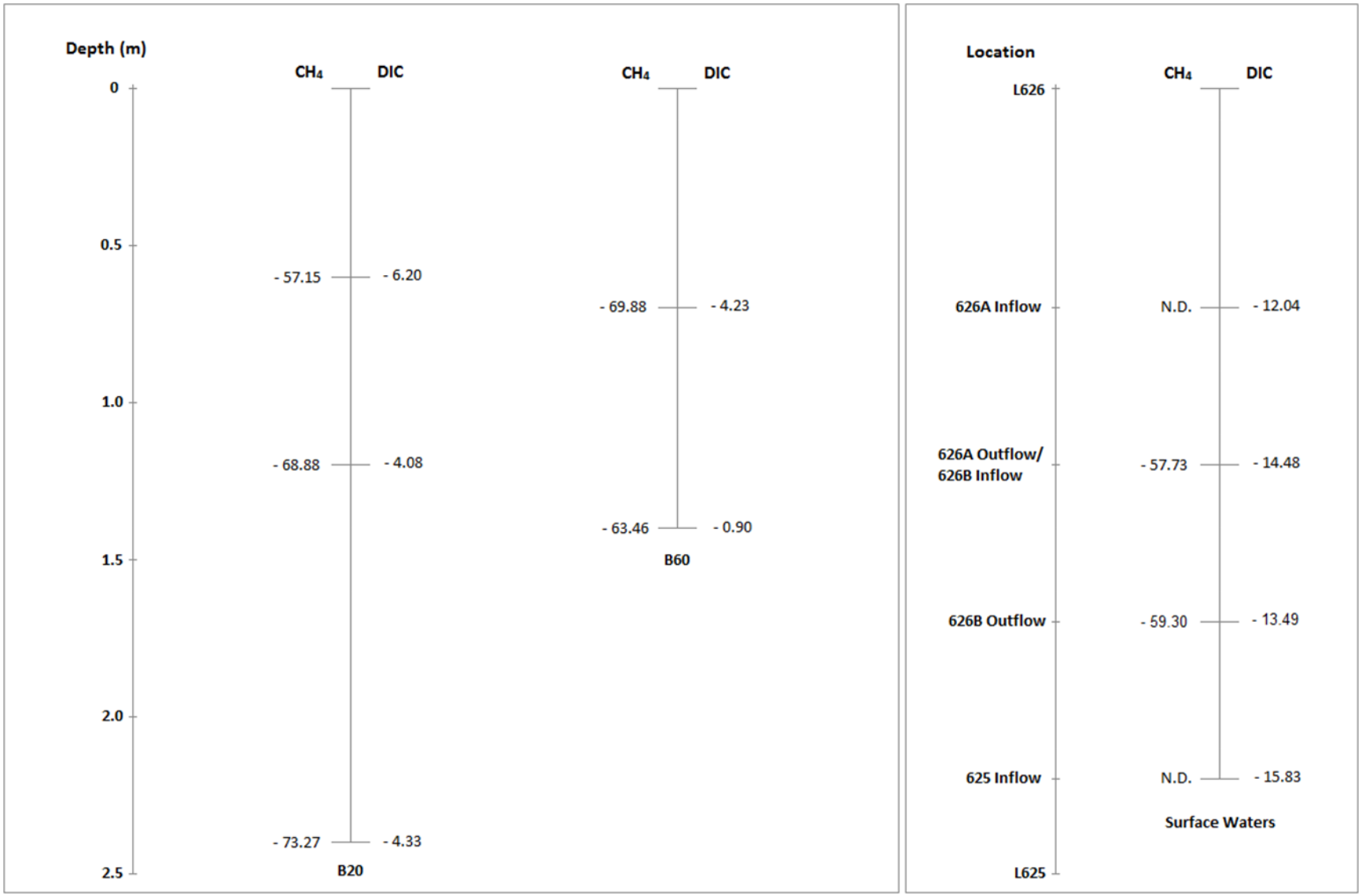

Figure 17. Isotopic signatures in $\delta^{13}C$ per mil for CH_4 and DIC versus relative depth for the two piezometer nests in Wetland 626B and the channelized surface waters flowing through the system.

blocks 1.12 – 1.54 ppm, low molecular weight neutrals 0.46 – 0.87, and low molecular weight acids making up 0.03 – 0.062 ppm (Table 3 & Fig. 20). A small increase in humic substance concentration was observed between the 626A inflow water and the remaining sampling points, which resulted in a slight increase to total DOC. Ultraviolet detection (UVD) shows moderately diminished signal response to biopolymer and building block peaks, with an accentuated response in the low molecular weight acid peak. The raw data can be seen in the appendix.

Piezometer samples showed significantly higher DOC concentrations than surface waters, and thus comparatively larger quantities of each fraction. Major differences were observed in the low molecular weight acids (LMWA), which in groundwater were inconsistent and without a discernible pattern, being undetected in half of all samples, and ranging from 1 ppb to over 4000 ppb in the remainder. In addition, low molecular weight neutrals (LMWN) were much higher in piezometer samples, with concentrations comparable to the humic substances fraction. As mentioned in section 4.6, DOC concentrations in groundwater samples almost exclusively decreased with depth. Based on LC-OCD analysis, this decline is primarily a result of decreasing humic substance concentrations in combination with slight to modest reductions in LMWN concentrations. The remaining fractions (biopolymers, building blocks, LMWAs, and hydrophobic) were more consistent, sometimes showing slight decreases or increases in concentration, but generally remaining the same. For a comparison to surface waters, plotted LC-OCD chromatograms have been shown for sampling site 626A – 20 m (Fig. 21) and an HS diagram further dissects the humic substance fraction (Fig. 22). Elution fraction concentrations for 626A – 20 m are also compared by depth (Fig. 23). The remaining plots can be found in the supplementary section. A tabular summary of elution fraction concentrations for all piezometer nests and all depths is shown in Table 4. In addition, the relative abundance of individual carbon

fractions as a percentage of total DOC is compared at each sampling location (Fig. 24 – 626A; Fig. 25 – 626B & surface waters).

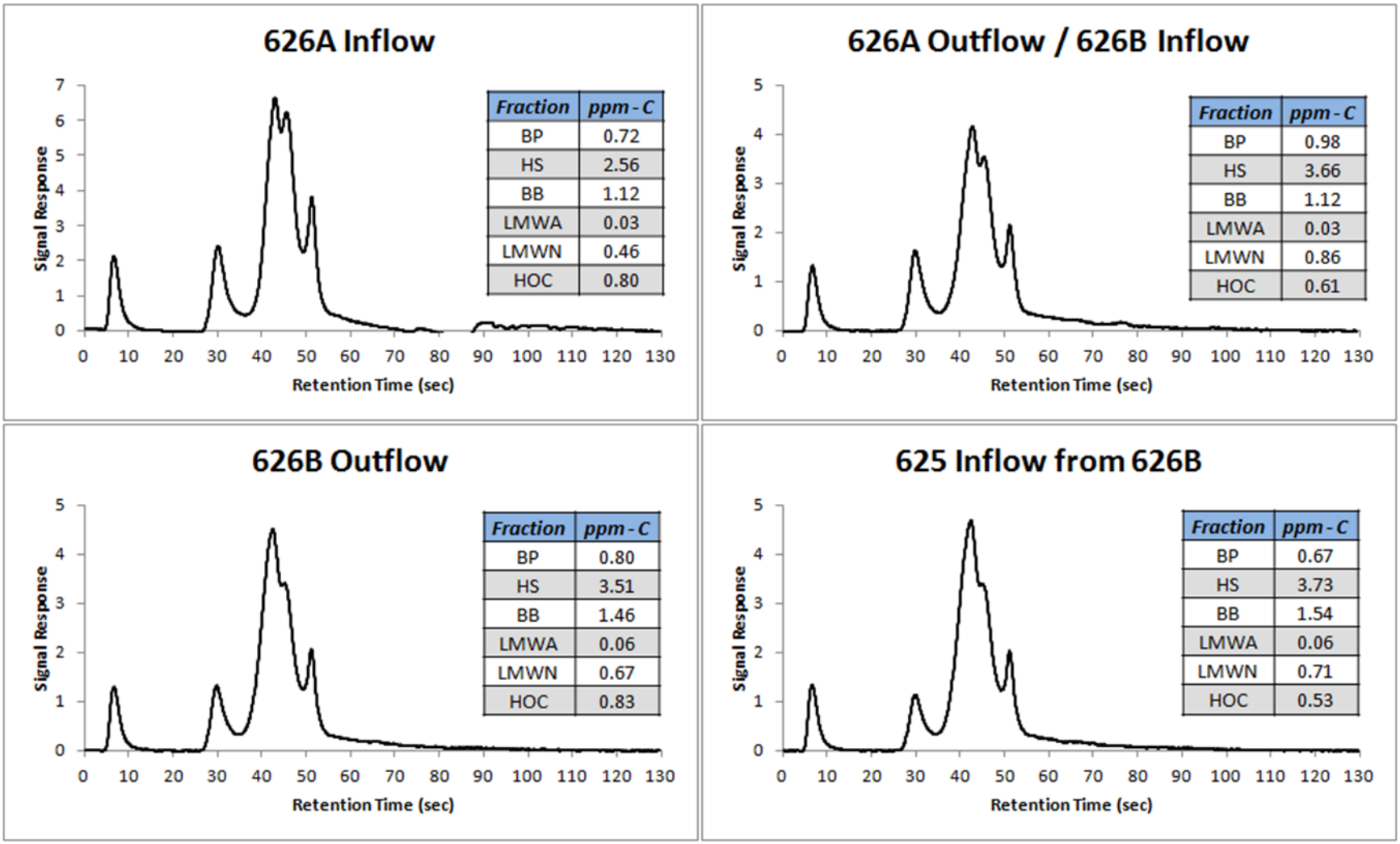

Figure 18. Plotted LC-OCD chromatograms for surface water samples in 626A and 626B. Carbon concentrations of eluted fractions are shown on the right (ppm). An explanation of fraction retention times pertaining to all LC-OCD plots can be found in section 5.3 of the discussion.

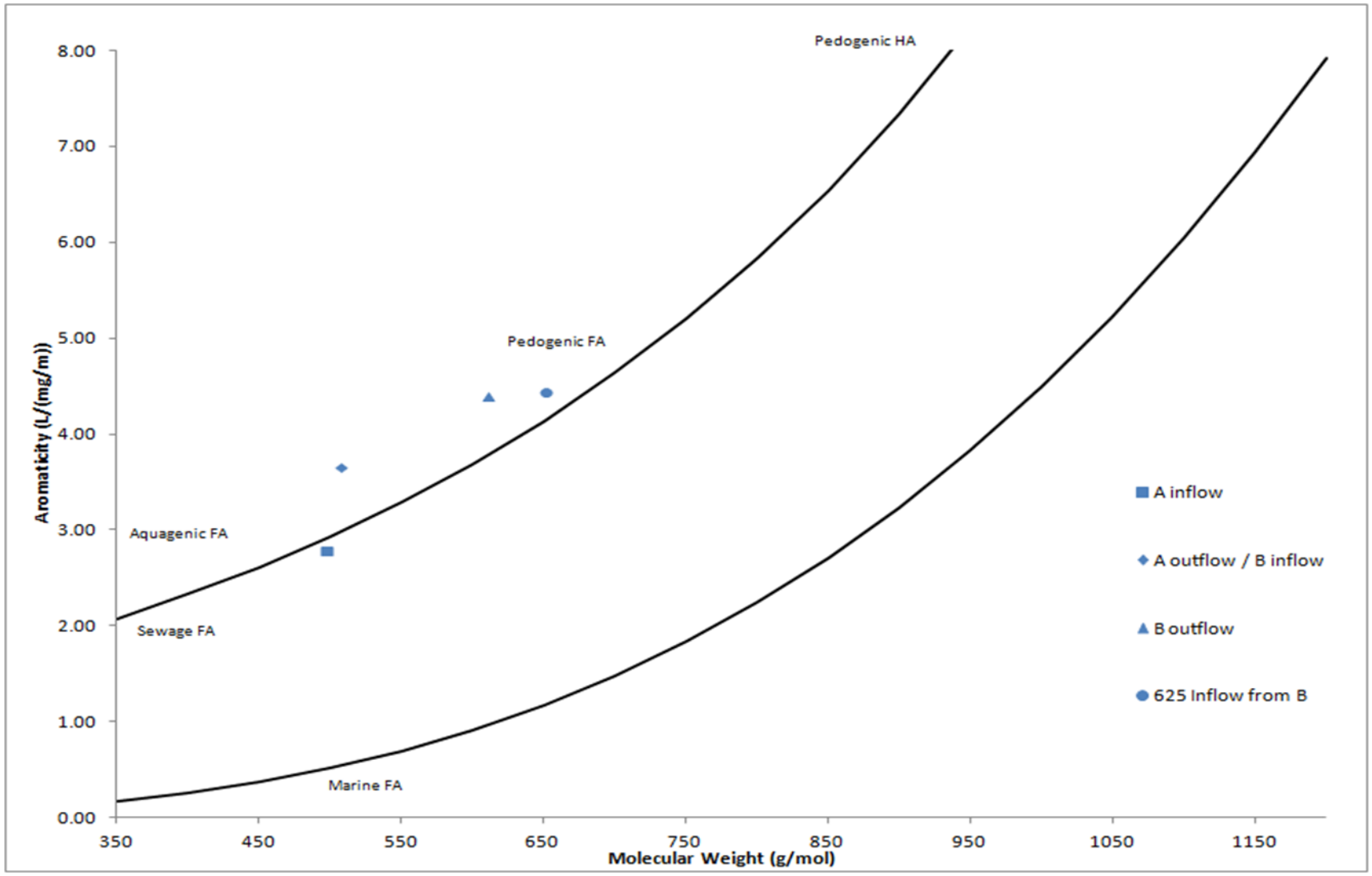

Figure 19. HS diagram, differentiating humic substances in surface water samples by aromaticity and molecular weight. Approximate zones, indicating the aquagenic to pedogenic balance, are shown.

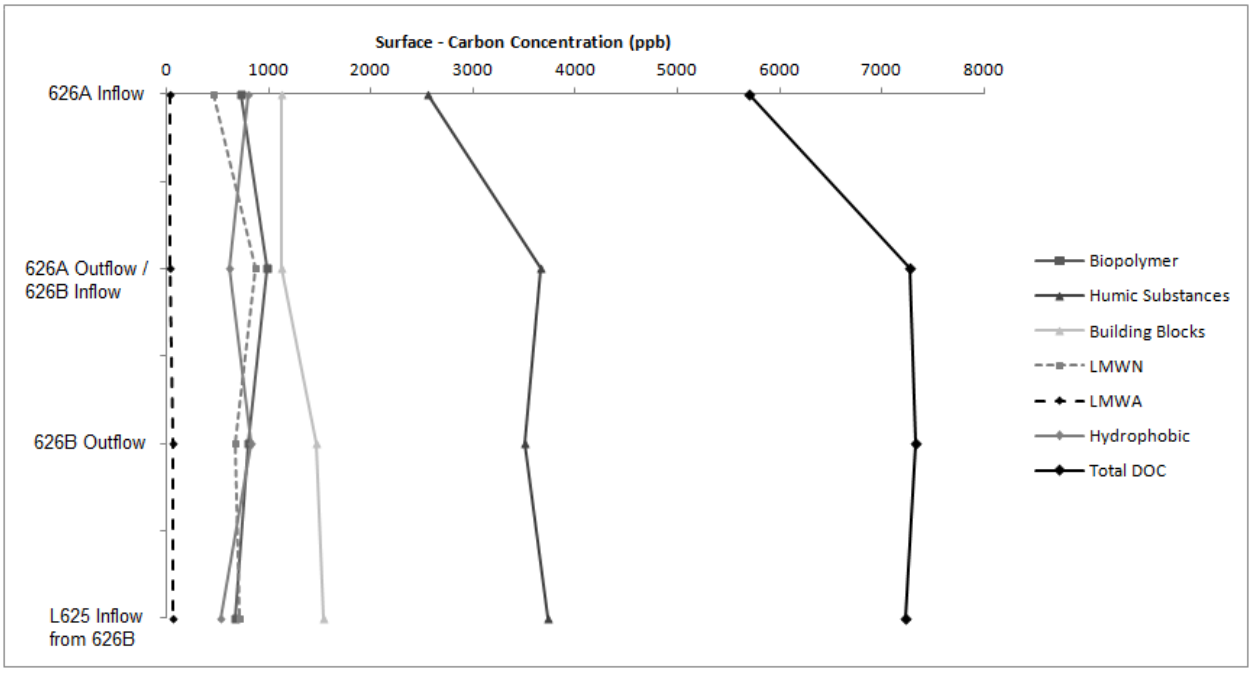

Figure 20. A comparison of elution fraction carbon concentrations for different surface sampling sites. LMWN & LMWA refer to Low Molecular Weight 'Neutrals' and 'Acids' respectively.

Table 3. Elution fraction carbon concentrations (in ppb) for differing surface sampling sites. LMWN & LMWA refer to Low Molecular Weight 'Neutrals' and 'Acids' respectively. SUVA values are also shown.

Surface Samples	Carbon Concentration (ppb)							
Location	Biopolymers	Humic Substances	Building Blocks	LMWN	LMWA	Hydrophobic	Total DOC	SUVA
Inflow to 626A	722	2561	1120	464	30	803	5700	2.36
Ouflow of 626A / Inflow to 626B	977	3662	1123	864	30	614	7270	2.94
Outflow of 626B	796	3507	1461	672	62	834	7332	3.29
Inflow to 625 from B	674	3729	1536	708	58	527	7232	3.49

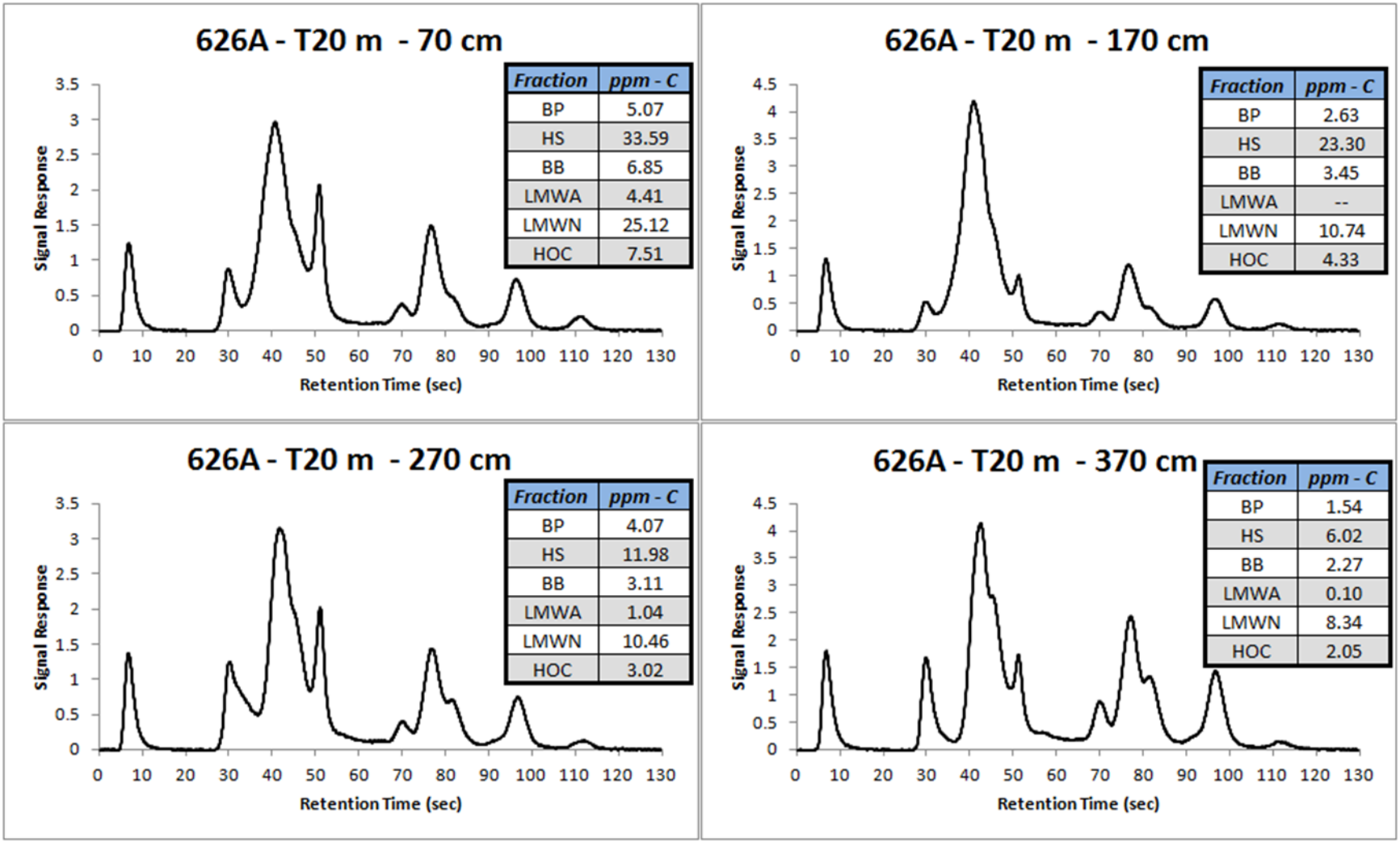

Figure 21. Plotted LC-OCD chromatograms for different depths within the 626A – 20 m piezometer sampling site. Carbon concentrations of eluted fractions are shown on the right (ppm). An explanation of fraction retention times pertaining to all LC-OCD plots can be found in section 5.3 of the discussion.

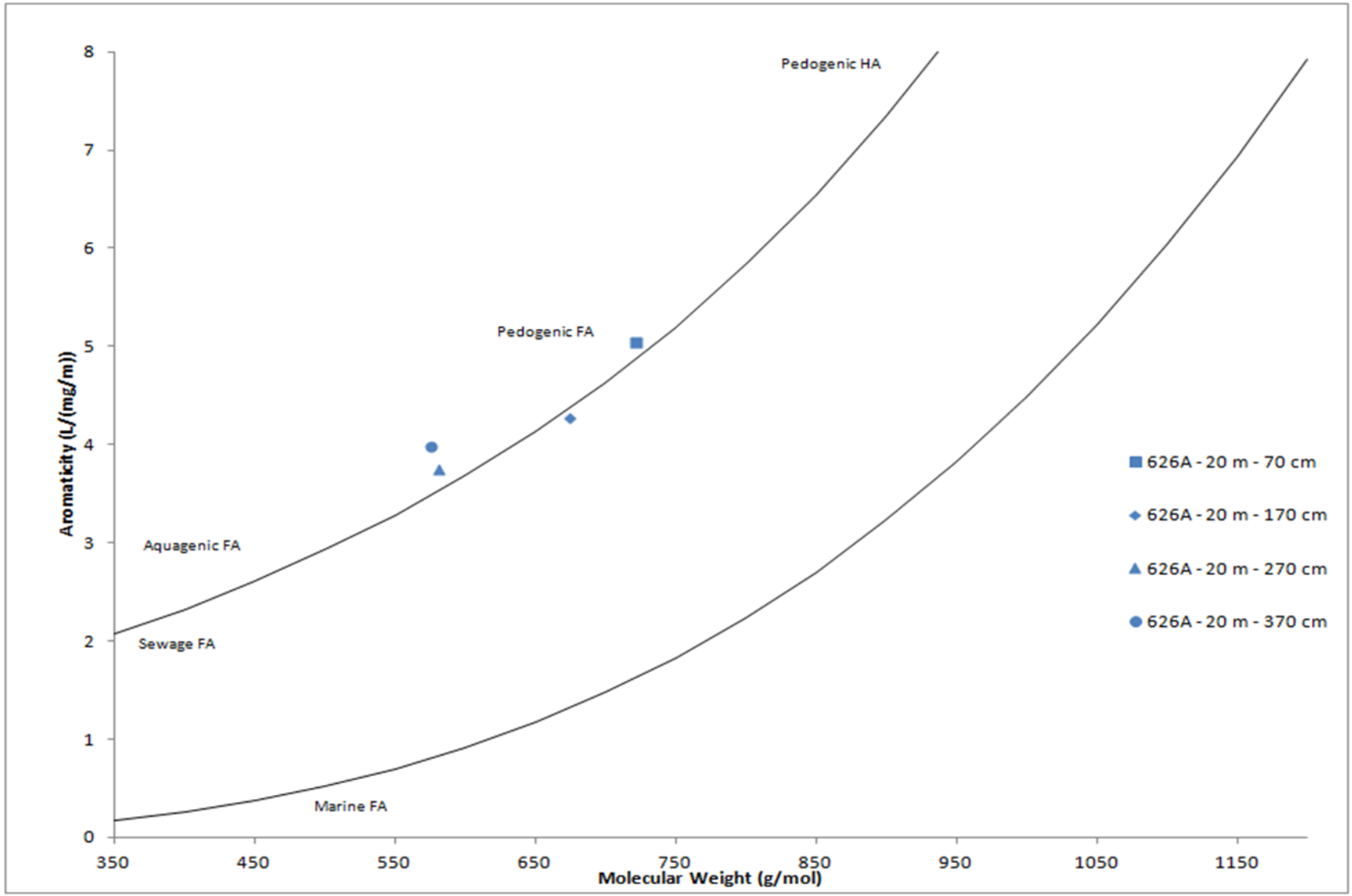

Figure 22. HS diagram, differentiating humic substances in the piezometer water samples of 626A – 20 m by aromaticity and molecular weight. Approximate zones, indicating the aquagenic to pedogenic balance, are shown.

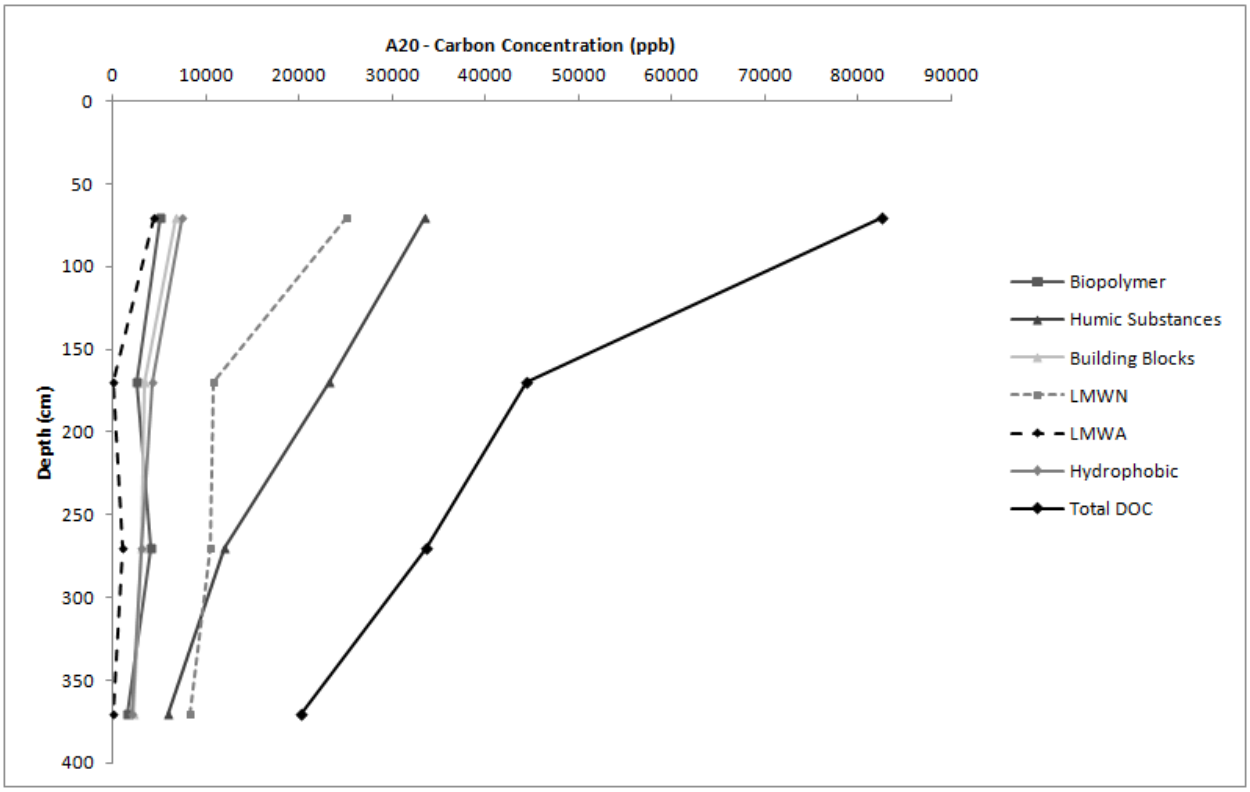

Figure 23. A comparison of elution fraction carbon concentrations for different depths within the 626A – 20 m piezometer sampling site. LMWN & LMWA refer to Low Molecular Weight 'Neutrals' and 'Acids' respectively.

Table 4. Elution fraction carbon concentrations (in ppb) for all piezometer sampling sites and depths. LMWN & LMWA refer to Low Molecular Weight 'Neutrals' and 'Acids' respectively. SUVA values are also shown.

Core Samples		Carbon Concentration (ppb)							
Location	Depth (cm)	Biopolymers	Humic Substances	Building Blocks	LMWN	LMWA	Hydrophobic	Total DOC	SUVA
626A 20 m	*70*	5066	33586	6851	25121	4410	7513	82547	2.93
	170	2633	23304	3451	10743	0	4329	44460	3.73
	270	4066	11981	3114	10464	1040	3023	33687	3.65
	370	1537	6017	2269	8335	100	2051	20308	4.12
626A 80 m	*50*	3779	34579	3975	35857	0	7209	85400	2.92
	150	2077	31420	4295	13088	25	4895	55800	3.80
	250	3328	13932	2675	6272	0	2603	28812	4.62
	385	2523	8724	2945	15582	0	3944	33720	3.25
626A 100 m	*50*	4124	27736	3686	40858	0	9735	86135	2.24
	150	2726	23259	3387	24735	0	5124	59228	2.81
	250	2601	13716	2497	10833	0	3663	33309	2.65
626A 120 m	*90*	1886	3576	1752	13406	347	3314	24282	2.40
626B 20 m	*60*	1618	10975	1128	19441	11	3958	37130	2.13
	120	2878	7727	2521	41771	0	10142	65040	1.23
	241	605	3822	1808	9294	73	2377	17980	2.19
626B 60 m	*70*	3245	16219	2416	25889	1	7856	55627	2.67
	137	3588	9137	2772	25964	713	6126	48300	2.34

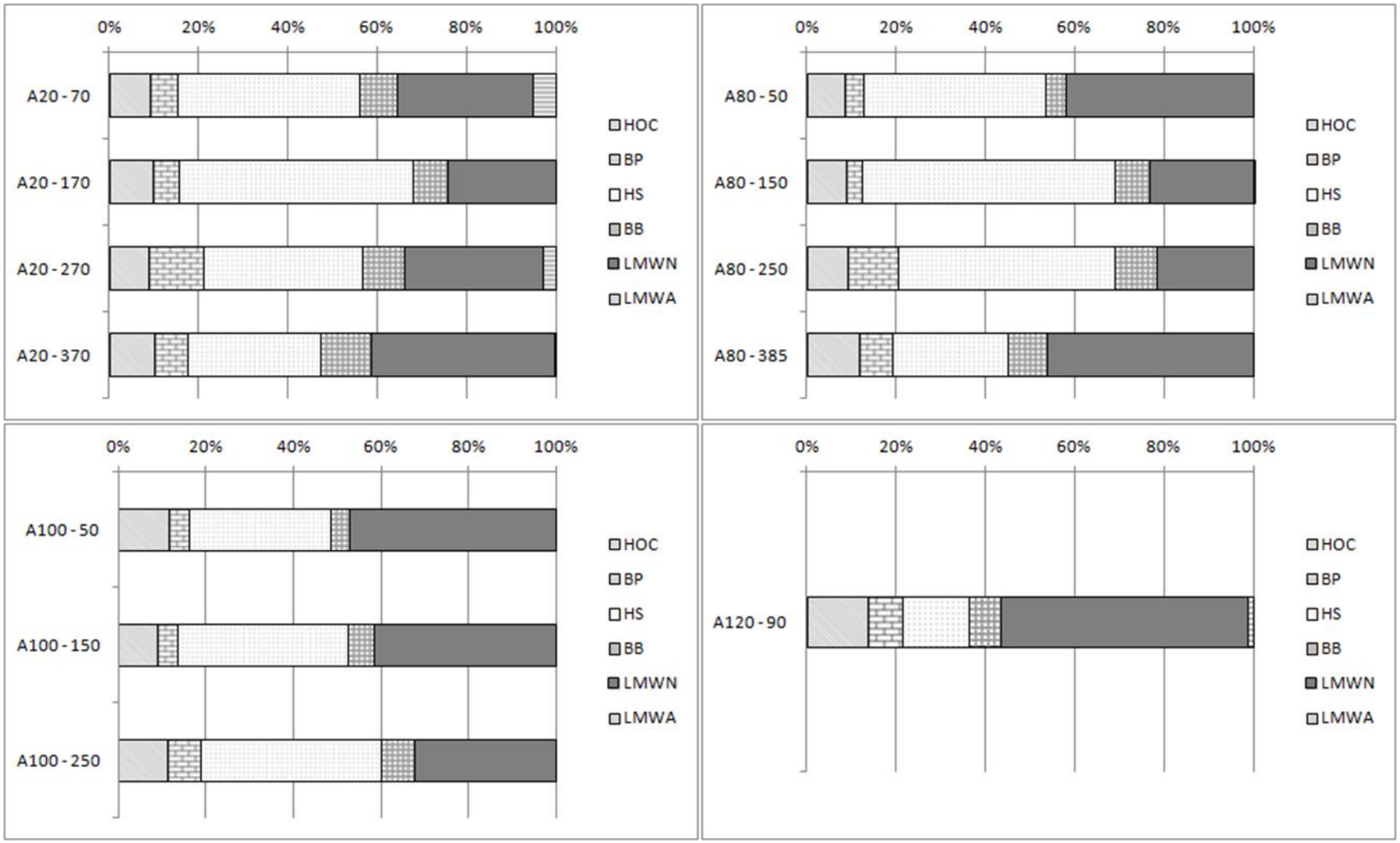

Figure 24. Relative abundance of individual carbon fractions as a percentage of total DOC for samples in wetland 626A (HOC = hydrophobic organic carbon, BP = biopolymers, HS = humic substances, BB = building blocks, LMWN = low molecular weight neutrals, LMWA = low molecular weight acids).

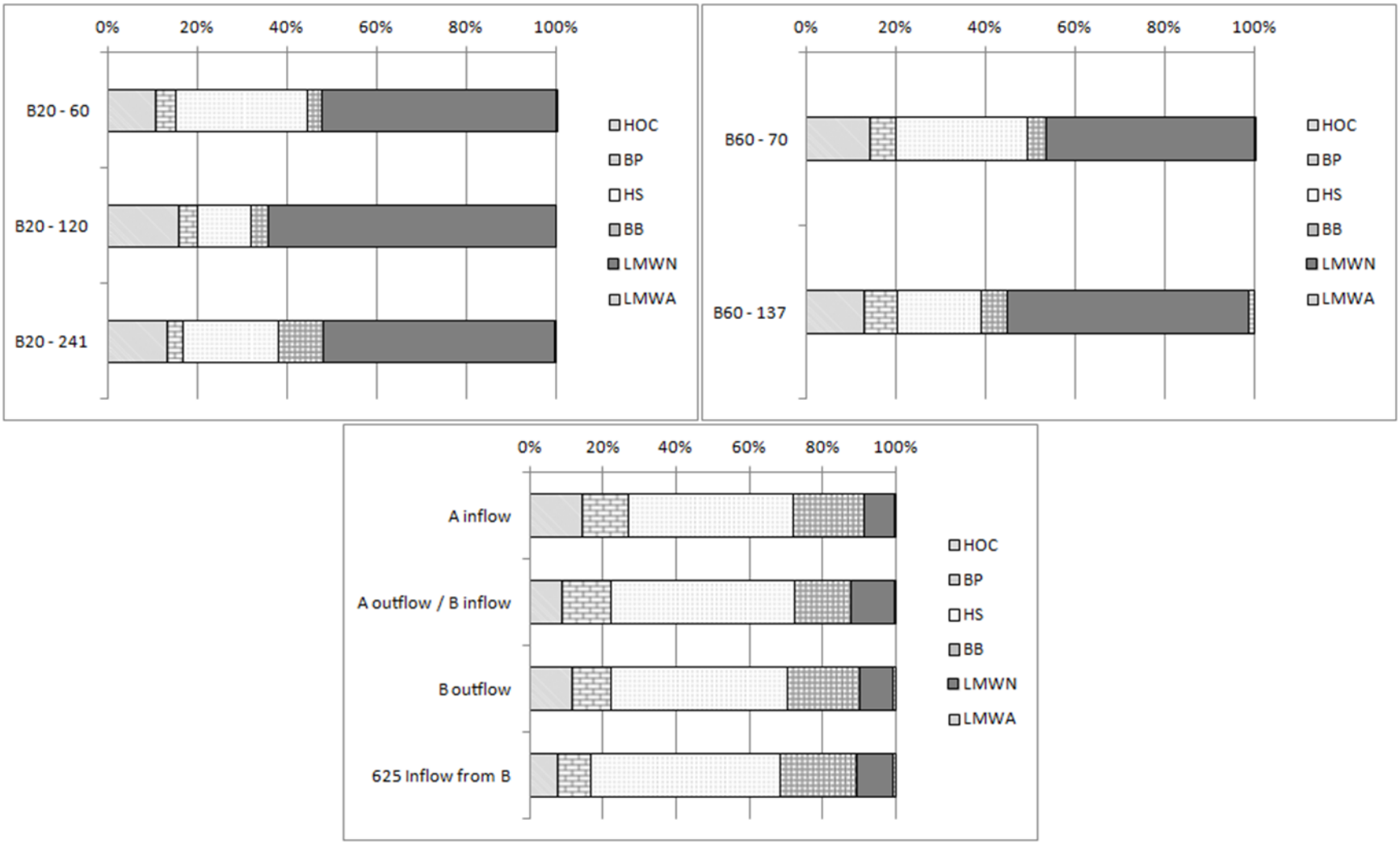

Figure 25. Relative abundance of individual carbon fractions as a percentage of total DOC. Comparisons are made for 626B (top left & top right) and all surface waters (bottom) (HOC = hydrophobic organic carbon, BP = biopolymers, HS = humic substances, BB = building blocks, LMWN = low molecular weight neutrals, LMWA = low molecular weight acids).

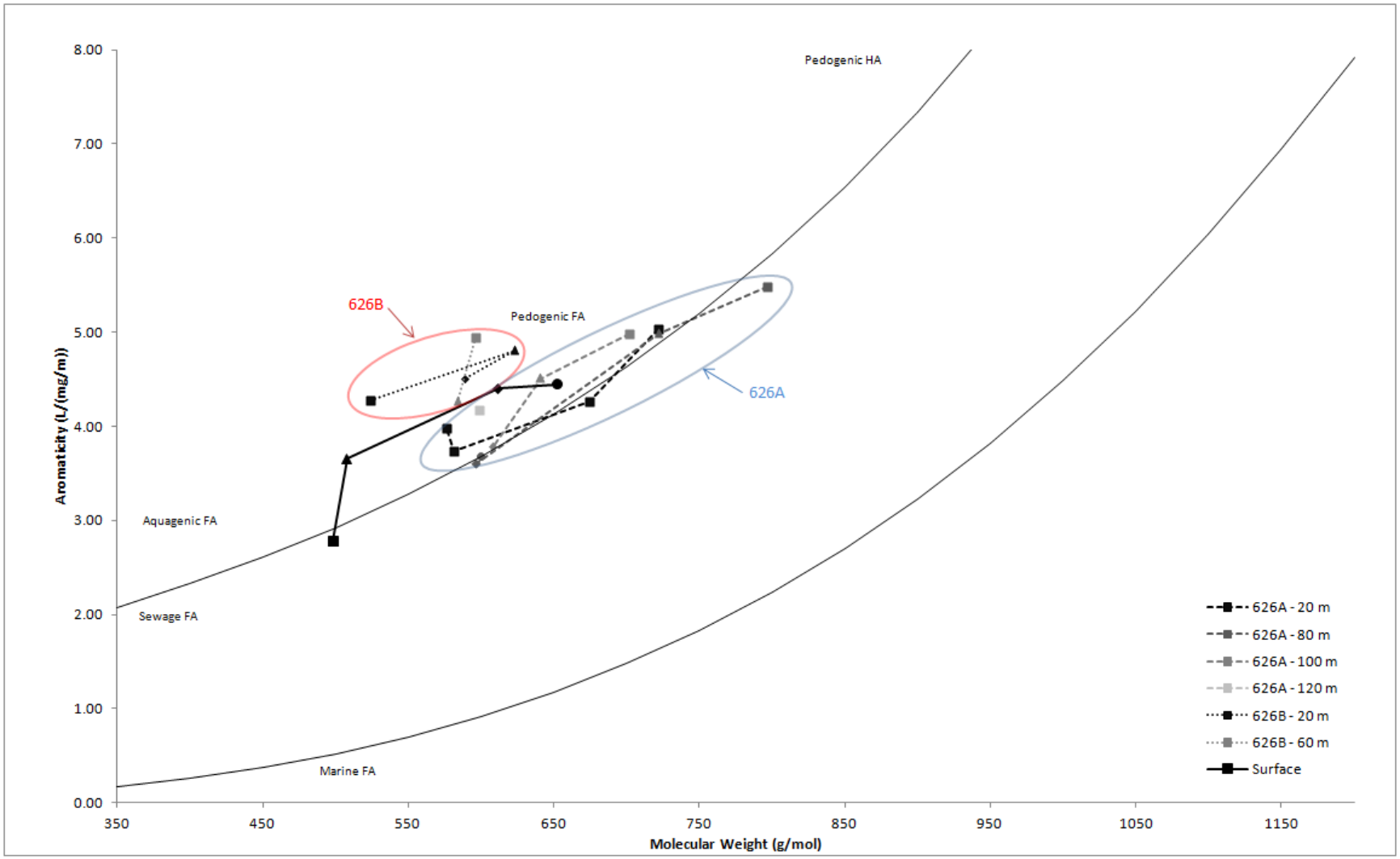

Figure 26. HS diagram, differentiating humic substances in all water samples by aromaticity and molecular weight. Approximate zones, indicating the locations of 626A vs 626B samples, are shown. Within each piezometer location, near surface water is represented by a 'square' and samples progress towards a 'circle' as depth increases (Square, Triangle, Diamond, Circle). For surface samples, the 'square' represents L626 water, and other data points are downstream at the wetland outlets and L625 inflow.

CHAPTER 5

Discussion

5.1 Local Peatland Development

Local peatland development can be reconstructed using basin stratigraphy and sediment composition, radiocarbon dating and local climate information collected during this study. Open water probably occupied the local bedrock basins around 13850 - 11000 calendar years ago when Glacial Lake Agassiz flooded the area, laying down silty clay. Around 11100 years BP, each of the wetland basins became isolated as Glacial Lake Agassiz waters receded. Small lakes and then shallow water wetlands occupied each basin as evidenced by the gyttja and limnic peat in the stratigraphic profiles of both wetlands. A combination of allogenic and autogenic influences suggests that both basins underwent substantial infilling, eventually transforming into sedge dominated fens. Site 626B is shallower (2.5 m) and is thought to have undergone this transition around 9800 years BP, much earlier than 626A (4.0 m), which became a sedge fen around 8000 years BP.

In 626B, a coarse band of sedge peat formed over the limnic layer, suggesting that rapid accumulation rates during this period forced sediment into the anoxic zone before significant decomposition could occur. The texture of this sedge peat became finer and more fibrous around 9000 years BP and remained so for several millennia, before becoming extremely fibrous around 4000 to 3500 years BP (Fig. 9). Low lake levels in nearby L239 between 5500 and 8900 calendar years BP indicate high temperatures and arid conditions, which would limit deposition of sediment (Laird and Cumming, 2008). As a result, the vegetation in this basin likely shifted from a sedge and *T. latifolia* marsh to a marsh with shrubs, such as *M. gale, R. groenlandicum, and C. calyculata*.

Accumulation and build up of peat over the last 3500 years has been quite slow, growing at a rate of about 0.014 cm/yr. Neoglacial cooling and an increase in precipitation should have encouraged continued expansion of the peatland; however, it is possible that sustained peat formation and peatland growth has been hampered by increased aerobic decay of the near-surface peat layers (Rydin and Jeglum, 2006). During this period, much of the peatland surface became dry except for a small open water channel through the centre of each basin. Present day vegetation on the peatlands shows *Carex* and *T. latifolia* dominated zones in the wettest areas of wetland, primarily along the main stream channel. Drier areas beyond the stream channel and along the outer perimeter contain some sedge species, but with dense shrub cover. The presence of *Sphagnum* in many of these areas suggests that 626B could be undergoing a succession into a poor fen and bog complex. Dry conditions brought on by the upstream water diversion are expected to accelerate this process, encouraging loss of sedge dominance, expansion of shrub communities and encroachment of other terrestrial vegetation.

Upon becoming a fen around 8000 calendar years BP, wetland 626A would have looked very similar to 626B, supporting *T. latifolia* and a wide abundance of sedge species. Over the next 1000 years, warming temperatures would have allowed for relatively normal accumulation of sediments, which showed a fine and fibrous texture. Between 7000 and 5800 years BP, local conditions must have become ideal, and a layer of hastily buried coarse fibrous sedge peat was laid down. Around 5600 cal yr BP, perhaps a result of the arid mid-Holocene conditions, accumulation slowed and peat texture became finer. Vegetation in the wetland would have still been similar to 626B, dominated by sedge species, but with intrusions of shrubs and some *Sphagnum* species. This section of the peat core ends about 50 cm from the surface, which represents approximately the last 2500 years BP. The lower half is made up of extremely coarse

peat, followed by a 25 cm layer of dense *Sphagnum* and highly decomposed peat, representing a hollow within the poor fen and bog portion of the wetland. Therefore, the modern *Sphagnum* mosses established and started expansion across the peatland surface between 1500 and 2500 years ago, developing into a system of hummocks and hollows more recently.

Yazvenko *et al*. (1994) studied the long-term history and formation of the nearby wetland in L979 and found a similar timeline for major transitions. Initial deposition began around 8700 ^{14}C years BP and culminated with the formation of the modern *Sphagnum* peat layer between 2000 and 3000 years BP. Work by Mewhinney (1996) at L632, another ELA study site, dated basal gyttja to 9600 ^{14}C years BP and showed emergence of *Sphagnum* species around 1250 – 1500 years BP. Species distribution in 626A has probably not changed immensely in the recent geological past. The *Sphagnum* peatland, while initially smaller, would have still supported a variety of shrubs, including *A. glaucophylla, V. oxycoccos, Drosera rotundifolia, Maianthemum trifolium, M. gale, C. calyculata* and *R. groenlandicum* all of which occur in the peatland at present. The fen shrunk over time and is currently broken into two sections, one that is sedge dominated and the other that is shrub dominated. *Dulichium arundinaceum*, *Eriophorum* species, *C. rostrata* and *C. lasiocarpa* dominate the vegetation close to the main stream channel. In particularly wet areas, *T. latifolia*, *Hypericum virginicum* and *Equisetum fluviatile* are also common. Drier areas around the basin perimeter feature a mixture of sedges amongst more dominant shrub species.

The redirection of water through the constructed diversion channel will reduce the amount of water flow through the 626A wetland. A lower water table will initially result, causing a nutrient decline that will strain the existing sedge communities. This will pave the way for encroachment of terrestrial vegetation, such as shrubs and trees along the basin edges. Both

of these scenarios are expected side-effects of the hydrological alteration if conditions remain unchanged.

5.2 Developmental History of Upland Forest and Regional Climate

Deglaciation of the ELA region occurred approximately 11500 ^{14}C yr BP (13350 calendar years BP). Mixed herbaceous shrub and forested tundra characterized the new landscape as the ice sheet continued to recede (Björck, 1985; McAndrews, 1982; Dyke, 2005). Pollen records show that around 10400 ^{14}C yr BP (12300 cal. yr BP), a transition towards boreal forest began with the northern expansion of mixed *Picea* forest containing hardwoods such as *Larix*, *Betula*, *Populus* and *Ulmus* (Björck, 1985). By 10000 ^{14}C yr BP (11550 cal. yr BP), the *Picea* dominated forests were replaced by *Pinus* dominated forests with other hardwoods, such as *Betula* species. Study of nearby L239 showed that these forests remained relatively unchanged for the remainder of the early Holocene, as local temperatures and precipitation levels gradually increased (Moos, 2010).

During the mid-Holocene, beginning ~8600 ^{14}C yr BP and progressing to ~4500 ^{14}C yr BP (9550 – 5150 cal. yr BP), forests continued to change, growing into more open, *Pinus banksiana* and *Populus* dominated woodlands with an abundance of herbaceous species such as Cupressaceae, Chenopodiaceae, *Artemisia* and *Ambrosia* (Björck, 1985; Moos, 2010). These changes are thought to have occurred gradually with an eastward shift of prairie grassland (Björck, 1985). This shift was brought on by increasingly warm, arid conditions, which peaked approximately 6000 – 3000 ^{14}C yr BP (6850 – 3200 cal. yr BP) (Viau *et al*., 2006). Laird and Cumming (2008) proposed that conditions during this period increased evapotranspiration significantly in the ELA region, causing an ~8 m drop in the water level of a small headwater lake. By 5900 ^{14}C yr BP (6700 cal. yr BP), local forests were changing once more as prairie

pollen influx declined leaving a *Pinus*, *Betula*, and *Alnus* dominated mixed forest (Björck, 1985; Dyke, 2005). Warm conditions allowed both mixed and boreal forests to push much further north than their present day limits, a situation which held until the advent of the recent Neoglacial period (Dyke, 2005). This brought a cooler, wetter climate, forcing a southward retreat of the existing biomes, and returning the ELA region from parkland to closed-canopy boreal forest by around 3000 ^{14}C yr BP (3200 cal. yr BP) (Dyke, 2005; Moos, 2010). Björck (1985) found a decrease in pollen from pine, herb and deciduous species, coupled with an increase in *Larix laricina*, *Abies balsamea*, and a sharp rise in *Picea* species. Moos (2010) found a similar shift in Lake 239 records, a small headwater lake also located in the ELA, leaving a distribution that has been kept more or less constant to the present day. The upland vegetation development of the L626 study site can be considered equivalent to that seen around L239, due to their proximity and the fact that they shared an identical climate history.

Current global temperatures are actually 2-4 ºC cooler than peak mid-Holocene levels, indicating that continued anthropogenic warming from increased atmospheric CO_2 concentrations, according to IPCC and NRC predictions, could return temperatures to similar heights or even exceed them (Kaufman *et al*., 2004; Dyke, 2005; IPCC, 2007; NRC, 2010). Thus, a comprehensive paleoecologic understanding of all postglacial periods featuring large temperature and biome shifts could provide a rough template for potential future biome shifts (Houghton *et al*., 1996; Dyke, 2005).

5.3 Wetland Organic Carbon and Response of Wetlands to Diversions

5.3.1 Surface Organic Carbon

Sampling and analysis of surface water from strategic points along the study sites central stream channel found low overall levels of DOC. Water entering the wetlands from L626 showed the lowest DOC concentration, which increased by about 1.5 mg/L (26%) by the outflow of wetland 626A, suggesting a small input from peatland DOC. This value leveled off, remaining approximately constant at the outflow of 626B and at the inflow to L625 further downstream. This suggests that the majority of influence to the central stream channel came from wetland 626A, and that this influence was fairly small, indicating minimal exchange of water between the channel and the adjacent peat. One caveat to this conclusion is that it only represents conditions prevalent in the summer season when water levels are naturally lower. Seasonal sampling of surface waters, spread over the course of a year, would be expected to show a higher rate of DOC exchange during periods with heavier precipitation and higher flow rates.

Analysis of surface waters by LC-OCD showed remarkably similar chromatograms between sampling sites. Biopolymer peaks are almost identical, with carbon concentrations remaining roughly the same despite a slight increase in total DOC after water enters 626A. This suggests that the largest compounds within the water, primarily polysaccharides, do not breakdown or accumulate during the passage of surface water through the two wetlands. After this, the differences within the chromatograms are subtle. Water samples taken from the L626 outflow show a distinct separation between the humic substance peak and the building block peak, but progressing downstream, the two peaks converge until the building block signal

appears as a shoulder to the humic substances, similar to the example in figure 2. The carbon concentrations representing both peaks increase roughly 40% from the 626A inflow to the L625 inflow, with increases in the building block contingent lagging behind increases to the humic substances. While the concentration of humic substances reaches a maximum at the 626A outflow/626B inflow before plateauing, building block carbon accumulates gradually. This indicates that decomposing organic material from 626A is a primary contributor of humic substances, which leach into the channel of passing surface water. In 626B, there is a small addition to the humic substances pool, but only sufficient to replace that which is lost to further degradation, becoming building blocks. This breakdown process continues on the short journey to L625, leading to a slight increase in building blocks, with humic substances replenished from surrounding soils.

Analysis of an HS diagram featuring surface samples illustrates a progression towards greater molecular mass and aromaticity (Fig. 19). This suggests that humic substances in the 626A inflow sample were of terrestrial origin, but underwent UV and microbial degradation while in the lake. Contributions from less altered soil derived carbon in both 626A and 626B produced a shift towards more pedogenic fulvic acids, as well as pedogenic humic acids. The gravity of this shift could be due solely to the unaltered pedogenic HS input, but is also likely affected by the breakdown, and thus loss, of the older, more degraded humic substances. There is a notable increase in the concentration of low molecular weight acids between the 626A outflow/626B inflow sample point and the 626B outflow. Although the concentration approximately doubles, the overall contribution of LMW-acids to total DOC only increases from about 0.50% to 0.80%. The reason for this increase is uncertain. However, while sampling it was observed that 626B was significantly wetter than 626A, and consequently, the main surface

flow channel was far less constrained and most likely slower moving. This greater exposure could have increased leaching of low molecular weight acids from wetland peat into the surface flow, but due to the lack of increase in other fractions, this theory could easily prove incorrect. Another more likely possibility is the same one that describes the increase in building blocks. If the concentration of low molecular weight acids are contributed from the breakdown of humic and fulvic acid, as well as other humic substances, then it stands to reason that they would show the same lag in formation as the building blocks. There is a wide array of actual acids that could exist within this fraction, but work by Ruhl and Jekel (2012) on individual acids and their elution behaviour suggests that acetic acid and pyruvic acid correspond to the peak labeled as low molecular weight acids in typical surface waters. Common contributing aromatic acids are thought to include benzentetracarbonic acid, benzenetricarbonic acid, and phthalic acid. For surface waters, the elution of low molecular weight neutrals from the column was fairly low, at least compared to pore water samples, but was proportional to changes in total DOC, making up 8-12% of all carbon. The representation of LMW-neutrals on the chromatogram was shown by an asymptotic curve to the baseline, indicating a relatively small, but complex mixture of compounds.

Specified ultraviolet absorption (SUVA), determined at 254 nm and normalized for DOC concentration, is an analytical technique used to estimate the fraction of dissolved aromatic carbon in a water sample. It serves as a good indicator of the humic fraction of total DOC, which can be compared to values obtained from the LC-OCD analysis (Weishaar *et al*., 2003). Surface samples at the outflow of L626 indicated a low aromatic content, but samples taken at the outlets of each wetland and the downstream inflow to L625 showed a higher SUVA,

suggesting an increase in aromatic dissolved carbon (Table 3). This increase was reflected in the LC-OCD data, showing a modest jump in the humic substance fraction.

Overall, the total DOC and LC-OCD fractions of the analyzed surface waters suggest that there is minimal interaction between the bulk of water in each wetland and the central stream of channelized lake water during the summer season. While a modest increase in DOC was observed between the surface water of the L626 outflow and the L625 inflow, near-surface pore water was up to 12 times more concentrated (86 ppm vs 7 ppm). This discrepancy could be achieved through low hydraulic conductivity peats, allowing minimal leaching of wetland DOC into the central channel. A second possibility arises during periods of elevated water levels, where rapid flow of water downstream prevents any substantial collection of DOC.

The increased dryness of both wetlands is an anticipated effect of the diversion and is also a simulation of expectations from climate change. Although the diversion does not influence direct precipitation or run-off into the basin as climate change could, it produces a net reduction in overall water input. This net reduction in flow is expected to slow the progression of surface water through the wetland, allowing more time for dissolved compounds to diffuse into the channel. In addition, a lower net flow rate would make the wetland more vulnerable to fluxes in precipitation, both daily and seasonal. In dry periods, flow rates could literally diminish to near zero, causing parched peat on either side of the channel to draw water out of the stream. Decomposing vegetation would elevate the concentration in DOC in the former stream water, which could promptly be discharged back into the channel during precipitation events. Samples taken during this time would be drastically different from samples obtained in periods of consistently wet, saturated conditions, which would maintain a much lower level of TDS. This phenomenon should also occur under regular flow conditions, but to a lesser degree.

Consequently, a more careful account of precipitation events will have to be taken for future surface sampling.

5.3.2 Sub-surface Organic Carbon

A profile of LC-OCD analyses from piezometer samples shows that total DOC, as well as the concentration of various DOC fractions, can undergo substantial change with depth. The near surface acrotelm of peatlands is a more aerobic zone where water table fluctuates and the majority of vegetation decay occurs. While a large quantity of carbon escapes into the atmosphere, the remainder is dissolved in water or becomes trapped in the peat itself. Thus, high levels of total DOC are a standard feature of the upper layers of a peatland. As peat is compressed over time and the water table is drawn higher to support new growth, the peat enters a permanently flooded zone referred to as the catotelm. Decay is slowed by anaerobic conditions, but continues, producing a profile of declining DOC concentration with depth. Wetland 626A is a good example of this process, while 626B shows some variability that will be speculated at. By studying the different LC-OCD fractions, a better grasp of the procedure of decomposition can be attained.

Chromatograms of 626A pore water show similarities in the location of peaks, but high variation in the strength of signal responses. This suggests that while the prevailing conditions at different sites or depths may change, altering concentrations, the presence of all fundamental compounds that make up the DOC pool remains consistent. In 626A, the hydrophobic carbon contingent decreased with depth, but showed very little change with respect to percentage of the total DOC pool. Biopolymer concentrations showed a general decrease with depth, perhaps due to increased breakdown of polysaccharides, such as starch and cellulose, into monomeric units or smaller chains. Biopolymers also represented a lower portion of total DOC compared to surface

waters. However, they appeared to rise in relative abundance for samples obtained within the limnic/gyttja based strata of the wetland, between roughly 2.0 – 4.0 m depth. Each of these samples was more similar in representation to surface waters, supporting the idea that either more lacustrine conditions existed during this period, or that surface waters are reaching this layer through a groundwater source. However, low basal tritium concentrations, approximately equal to cosmogenic background levels, agree with the former theory (Osborne, 2002). Pore water uninfluenced by tritium from the testing of nuclear weapons has not been recharged in at least 60 years, suggesting that the surrounding peat is highly compact with low hydraulic conductivity, allowing minimal movement of water into or out of this peat layer. A study of basin hydrology would shed more light on this concept. Mewhinney (1996) found low basal tritium values at another nearby ELA site, L632 – an 8 m basin, in the mid 1990s. Concentrations above 3 m were between 10-30 TU, having been recharged in the recent past. However, deep pore water below 4 m was consistently below 6 TU, suggesting that this water had not been recharged since before atmospheric nuclear weapons testing began. Slightly more than one tritium half-life has occurred since those samples were taken, so unaffected samples within 626A would be expected to have a concentration < 3 TU. This was the case for the basal sample in lake 626A, but not 626B, suggesting the potential for significantly different hydrology in each basin.

Low molecular weight acids ranged from a small component of DOC to being non-existent. For half of the samples taken, analysis failed to detect any LMW acids. For those few samples where they were present, there was no discernible pattern observed. Humic substances, usually representing the majority of the DOC pool, declined with depth in all cases. The HS diagram used to differentiate humic substances (see fig. 26) shows that water within the

shallower peat of 626A has a more pedogenic signature, a result of the higher decay and DOC formation in this layer. Basal samples are more aquagenic, showing a signature that is much closer to L626 water. This could indicate that the humic substances within the DOC are being heavily degraded as they move down through the peat. It could also suggest that basal water is very old, and that more recent near-surface water isn't penetrating the tight layer of limnic peat and gyttja at the bottom of the basin. The main exception to this rule, was at the 120 m station along the transect, which showed aquagenic humic substances at only 90 cm depth. The presence of fen community at this site, the proximity to the central stream, and a slightly lower DOC is the probable cause, as all other sampling points were located in the *Sphagnum* bog with high near surface DOC.

SUVA values obtained from piezometer waters in 626A show no discernible overall patterns and imply a minimal relationship with LC-OCD measurements taken for the humic substance fraction (Table 4). Calculations of DOC aromaticity for the HS fraction revealed a decrease with depth. This matches humic substance concentrations, which also decreased with depth, alongside total DOC. However, in some profiles SUVA showed a tendency to increase with depth, indicating that humic substances composed a higher percentage of total DOC. This was not the case, as seen in figure 24, and so suggests that SUVA values are incorporating aromatic features from a different DOC fraction. Therefore, while SUVA is a useful tool in drinking water analysis, its application to differentiating DOC in pore water from wetland sitess is difficult to ascertain. As Weishaar *et al*. (2003) summarized, conclusions obtained from SUVA values are useful predictors of general water chemistry, but caution should be exercised when applying them.

Building blocks and low molecular weight neutrals showed the same general trend as humic substances with slight exceptions. However, the interaction between these three fractions as a percentage of total DOC shows an interesting relationship. In wetland 626A, representation of humic substances actually increased between the shallowest sample and the next depth before beginning to decline. The maximum observed percentage of humic substances around 1.5 m may indicate a balance point between formation and microbial decomposition of the fraction. Accompanying this, building block representation grew with depth, implying that decay over time produces lower strata that are typically more decomposed than upper strata. The section of the chromatograms representing low molecular weight neutrals was less complex than for surface water samples, showing distinct peaks centered at approximately 70, 78, 82, 96, and 113 minutes. According to Ruhl and Jekel (2012), methanol (t_{max} = 77.7) and isopropyl alcohol (t_{max} = 82.2) could be good matches for the elution signals at 78 and 82 minutes respectively. There were no other obvious matches, but Ruhl and Jekel (2012) were also able to show that hydroxyl functional groups accelerate elution, methyl groups decelerate it and that hydrodynamic volume can also influence the process. The remaining peaks could therefore be a variety of individual compounds with such modifications or a mixture of them.

The LMW neutral concentrations in 626A piezometers were drastically higher than in surface waters, but more importantly, their representation as a percentage of total DOC was greatly enhanced, from a low range of 8 – 12 % in surface waters to a high of 21 – 55% in peat pore water. Such small compounds are likely one of the last stages in decomposition of organic matter, hence their significant presence in a wetland ecosystem. They should form most readily in areas showing high rates of decomposition, such as the aerobic zone of near surface peat, and in areas where decomposition has been allowed to proceed for extended periods of time, such as

deep basal peats. Their size should also render them fairly labile, so as a fraction of total DOC, they should be smaller in areas less conducive to their formation. This could partially explain the fluctuation in their percentage abundance, as seen in figure 25.

Wetland 626B has less data to work with, but shows a slightly different scenario with respect to DOC. Total DOC varies sharply in samples taken at the 20 m station, almost doubling before declining to half the original concentration. Further along the transect at 60 m, there is no significant change with depth. This might normally imply uniform peat, but cores taken at both of these stations reveal different layers of peat with varying make-up and texture. Tritium values provide more insight into these peculiar numbers, indicating that water in basal sediments have been recharged since the advent of bomb tritium. This suggests that hydraulic conductivity is higher within 626B, perhaps a result of a shallower basin, wetland classification (fen vs. bog/fen complex in 626A), or a difference in development of peat strata. With higher levels of advection and transport within and between peat layers, DOC and LC-OCD data could, and in fact does, appear fairly homogenous. In the wetter central area of 626B at 60 m, biopolymers, building blocks, and low molecular weight neutrals were almost identical between middle and basal depth samples. Hydrophobic carbon decreased slightly in deeper sediments, and humic substances showed a modest decrease as well. On the deeper, western side of the basin, only the humic substances responded in an anticipated pattern, decreasing with depth. An HS diagram (see fig. 26), plotting the samples taken from 626B shows a more compact aquagenic signature, closer in similarity to the surface waters passing through the central stream channel. Therefore, decaying vegetation has a small impact on the nature of humic substances in wetland 626B when compared to 626A. The difference in aromaticity of humic substances in 626B in relation to

surface waters is due to photo-bleaching on the surface, while pore water within the peat is shielded from sunlight.

As with wetland 626A, there was no discernible pattern with depth for SUVA readings in 626B (Table 4). However, values for wetland 626B were generally lower than 626A, and in most cases, also lower than surface values. This is likely a result of DOC fractions as opposed to DOC concentrations, and shows that the overall DOC signature of 626B is more degraded than the DOC of passing surface water. Lower mobility of water within the peat, and thus a longer residence time, would permit more extensive degradation of all DOC. However, it should be noted that the aromaticity of the specific humic substance fraction in 626B is higher than that of surface water, implying that the lower SUVA values in 626B are a byproduct of already broken down humic substances (not current HS), most likely in the form of low molecular weight acids and neutrals.

The remaining major fractions, biopolymers, hydrophobic carbon, building blocks, and low molecular weight neutrals, all had dramatic peaks in concentration at 120 cm depth, more than doubling values from 60 cm. The cause of this discrepancy is difficult to determine, but it is unlikely that suddenly reduced hydraulic conductivity or some method of surficial DOC stripping is to blame. The most likely explanation is supported by radiocarbon data and peat accumulation rates. Deposition of organic matter occurred at a much higher rate during the period when the high DOC layer was formed. If rates were rapid enough, aerobic decay could have been minimized, resulting in an aged, but quickly buried and less decomposed segment of peat. Likewise, recent deposition has been much slower, and thus a greater percentage of plant material would have been allowed to decay and escape as CO_2 or CH_4 before subsequent detrital vegetation could bury it, leaving a lower organic carbon concentration in the peat. A glance at

the loss on ignition profile for wetland 626B – 20 m shows some support for these conclusions, as organic carbon is less abundant in a band between 55 and 115 cm depth. This reduced carbon content suggests that accumulation rates were lower during this period and that the wetland could have functioned as a carbon source, as opposed to a carbon sink. Likewise, lower organic carbon content within the 626B – 20 m sediments at this depth could also indicate the position of a former stream channel. Wetland 626B is currently much wetter than 626A, and is thought to have been even more marsh-like in its early history. A wider, more dominant stream channel would have left more minerogenous deposits in the sediment, which could serve to reduce organic matter content, and in turn, reduce the amount of DOC produced within that layer of peat.

The construction of the diversion channel is expected to have a profound effect on the organic carbon balance of wetlands 626A and 626B. Reduced flow from L626 will simulate a drought effect, drying out the wetland through lowering of the water table. Litter and underlying vegetation will be exposed to entirely aerobic conditions and undergo full decomposition, releasing more carbon into the atmosphere. Due to compression of buried sediments, a thin band of peat can represent the concentrated carbon remnants of hundreds of years of deposition. A large enough drop in the water table could even provide an oxic zone to the former upper catotelm.

If dry, drought like conditions exist for a prolonged period, accumulation rates will be stunted or reversed, converting the wetlands to greater potential carbon sources. Futuristic DOC, LOI or ^{14}C radiocarbon profiles would show a sharp boundary in the peat where organic carbon concentrations suddenly declined. This boundary would represent an age gap between

unaffected peats from before the dry period and those that were deposited after carbon sink conditions were restored.

5.4 Wetland Inorganic Carbon

Northern peatlands rarely show much variation in the $\delta^{13}C$ isotopic signatures of solid carbon or DOC. These values are typically around -26 ‰ ± 2 ‰ and thus do not offer much insight into the carbon cycling processes that occur within the depths of a peatland (Schiff *et al*., 1997). DIC and CH_4 isotopes however, presented in figures 16 and 17, vary quite a bit, and are more useful tools in differentiating such processes.

The $\delta^{13}C$ isotopic DIC signals ranged from –5.22 ‰ to +3.74 ‰ in basin 626A and –6.20 ‰ to –0.90 ‰ in 626B, while all surface flows were between –12.0 ‰ and –16.0 ‰. More negative DIC is indicative of aerobic conditions that favour peat oxidation, while more positive signatures imply the presence of anaerobic conditions and the production of methane via methanogenesis. Biogenic methane production in northern peatlands, as discussed in chapter 1, is primarily formed by the CO_2 reduction pathway. The $\delta^{13}C$ isotopic CH_4 signatures for wetlands 626A and 626B ranged from –62.5 ‰ to –68.5 ‰ and from –57.1 ‰ to -73.3 ‰ respectively.

DIC concentration was low at the outflow of L626, but increased due to wetland contributions at both peatland outlets, thereby making the $\delta^{13}C$-DIC signature more negative. While traversing the downhill route to L625, the channel water underwent degassing of CO_2, reducing DIC concentration once more.

Surface flows for both wetlands, where detected, had $\delta^{13}C$-CH_4 signals between –57.7 ‰ and –59.3 ‰. The more positive signals indicated more aerobic zones where old methane is

undergoing oxidation, while more negative signals suggest anaerobic conditions and the formation of new methane. Although methane isotopes could not be determined at the L626 outflow or the L625 inflow, signatures at both sites would be expected to be more positive than values from the wetland outflows. This is due to a lack of wetland influence at the former site, which reflects lake conditions, and a sufficient opportunity for degassing of isotopically lighter methane by the time channel water reaches the latter site. Reduced concentration at both sites, relative to the wetland outflows, supports this conclusion.

In both wetland 626A and 626B, the upper ~1.0 m of sedge and sphagnum peat shows low, but increasing concentrations of DIC and CH_4, and comparatively high, though decreasing, amounts of DOC from decomposing organic matter. The δ^{13}C-DIC isotopic signature is relatively negative, while the CH_4 signal is more positive. This data indicates that the upper meter of peat is primarily aerobic, permitting decomposition and the formation of DOC, while preventing significant methanogenesis. The δ^{13}C signature of DIC entering the wetland from the outflow of Lake 626 is –12.0 ‰, which is set by lake processes. Within the wetlands, a δ^{13}C signature of –22.0 ‰ provides a good baseline value at which methanogenesis is not occurring and peat oxidation is at a maximum. As Mewhinny (1996) found at L632, another site within the ELA, any DIC signature that was more positive than –22.0 ‰ indicated the onset of methanogenesis. These values peaked at roughly +10.0 ‰ for areas with the most anoxic conditions. Thus, even in shallow peats along the main transect of the L626 wetlands, the more negative DIC signals suggest that a methanogenesis gradient still exists, producing small amounts of the gas. However, the prevailing oxic environment ensures that most CH_4 is promptly reoxidized, making the remaining methane pool more positive.

In the mid-depth ranges, around 1.0 – 2.0 m, increasingly anoxic conditions, coupled with significantly less degradable organic matter, leads to sharply declining DOC concentrations. Elevation of methanogenesis also occurs, producing an increase in both DIC and CH_4 concentrations. This has the effect of making the $\delta^{13}C$ signal of the DIC pool more positive, while simultaneously making the $\delta^{13}C$ of the methane pool more negative.

Amongst the deep peat layers the majority of easily degraded organic material has already been decomposed (Rydin and Jeglum, 2006). There is still organic matter present, but the rate at which DOC is lost from the system now exceeds its rate of formation, leading to a concentration minimum. While much of this DOC is being converted to DIC and CH_4, it could also be removed by gradual diffusion or ebullition to upper layers. DIC concentrations also declined slightly in most basal samples, while methane concentrations stayed roughly the same or continued to increase. Progressively more anoxic conditions in the catotelm encourage an increase in both fermentation and CO_2 reduction, which is the probable cause for increasing methane concentrations. The slight decrease in DIC seen in most profiles could be due to a combination of factors. As a reactionary intermediate, a decrease in the initial DOC concentration will induce a similar decrease in the amount of DIC formed, while the subsequent reduction to CH_4 will promote a further loss. Most basal samples were also extracted from compact limnic peats which feature a lower hydraulic conductivity, preventing DIC from diffusing upwards before it can be reduced. Isotopic signatures support this model, with more negative $\delta^{13}C$ in CH_4 and more positive $\delta^{13}C$ in DIC within most basal samples. One key exception was the series of DIC signatures in core A80, which became slightly more negative with depth. It is quite feasible that DIC production from DOC was outpacing the rate of reduction to CH_4, signified by the scarcely changing methane concentration in the profile.

Another peculiarity was core B60, which showed a $\delta^{13}C$-CH_4 signature that became more positive from 70 cm to 137 cm depth. It is possible that rapid preferential diffusion of negative CH_4 from the base of the core could result in a more positive reading. It is also possible that fermentation plays a greater role than expected at this specific location. However, as Lansdown *et al*. (1992) were able to determine that acetate fermentation was responsible for less than 1% of methane production at their study site, it is unlikely that the situation is so significantly different in wetlands 626A or 626B.

Construction of the diversion is expected to decrease the flow rate of water through each wetland, effectively lowering the water table and accelerating decomposition of newly exposed sediments. Dry conditions will prevent accumulation of new peat, initially producing a sharp increase in DOC within the oxic layer. This DOC will be converted almost exclusively to CO_2 gas, before escaping via diffusion or ebullition to the atmosphere. This would produce an increase in near surface DIC concentration, which would become more isotopically negative. The expansion of the oxic zone will not necessarily lead to a decrease in methane production, but rather, will provide a larger oxidizing region where methanotrophic bacteria can convert CH_4 gas to CO_2 before it escapes. This will cause a decrease in overall methane emissions from the wetland. With roughly equivalent formation and loss of methane in the anoxic zone, the isotopic signature of the deep, dissolved $\delta^{13}C$ CH_4 would be expected to remain relatively constant.

5.5 Conclusions & Recommendations for Future Research

Construction of a diversion channel that effectively reduces water flow to a small wetland system is expected to influence the diversity of prevailing vegetation and the dynamics of carbon in basin sediments – the nature of both disturbances being primarily negative. Lower water levels will also reduce nutrient availability, favouring more swamp or bog-like conditions and

encouraging terrestrialization, expansion of bog species and loss of fen vegetation. A reduced water table is also expected to play havoc on the carbon dynamics of both wetlands, causing the aerobic decay of upper peat sediments and the subsequent release of large amounts of carbon dioxide to the atmosphere. Under natural succession, these processes could take hundreds to thousands of years to occur, spreading any negative side effects over long periods of time, and giving floral and faunal species adequate time to adapt. However, through man-made allogenic forcing, an acceleration of these processes runs the risk of upsetting the balance, diversity and evolutionary path of these wetlands. On a world wide scale the rapidity and severity of these shifts could contribute to the production of a climatic feedback loop, further worsening the existing impacts. These adjustments represent some of the consequences anticipated from callous establishment of hydrological alterations around the world. In addition, they can provide an analog for future anthropogenic warming scenarios where rapid changes to temperature and the abundance of precipitation put and the health of boreal peatlands at risk on a global scale. Some of the anticipated impacts of the L626 water diversion are depicted in the schematic below.

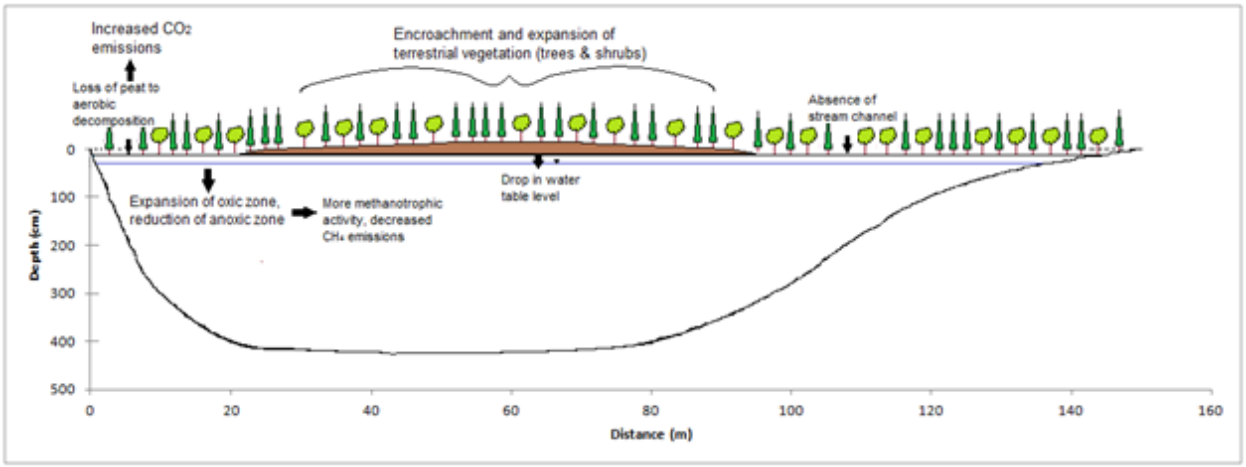

Figure 27. Schematic of anticipated impacts to wetland 626A after 5+ years of diversion. Wetland 626B would experience similar changes, minus the effects to the bog.

One recommendation for future research would in regards to timing of a return to the site. While yearly sampling would be ideal, five years post diversion presents a good window for a second look at the wetlands. This will allow for multiple seasons, mitigating the influence that any one season might have on the site in terms of temperature and precipitation. Additionally, five years is sufficient time to see a shift in major vegetative communities, specifically the encroachment of terrestrial shrubs and trees, converting the site towards swamp conditions.

Despite the variety of information collected regarding wetlands 626A and 626B, there are many other analyses that could have been done to improve their characterization. Improvement to the depth of the study could be achieved through additional quantities of data. Creation of a second or third transect at each site, an increase in piezometer nests, and more frequent sampling would all provide additional data, enhancing the conviction of every conclusion. Specifically, obtaining a ^{14}C date on the basal DOC in wetland 626A would be beneficial in determining the age of deep pore water and showing how it is moving within the peat. Additional ^{14}C dates in the solid peat around major stratigraphic boundaries and at specific time periods would help define whether historic wetland development was influenced more strongly by basin hydrology or by climate. A more complete view of the central streams influence could be found by performing additional sampling and spacing it over the span of an entire year, to include all seasons. However, improvement to the study could also come from a broader approach, utilizing a more numerous suite of analyses.

More rigorous analysis of the solid peat would have improved this researchers understanding of the formation and evolution of the ecosystem. Pollen identification and C/N isotope analysis within the cores would improve conclusions regarding paleoecology and paleoclimate within the basin and in the surrounding uplands. Collection of vegetation and peat

samples from the randomly selected plots used for percent cover analysis could have been used to calculate biomass and predict total carbon content of the wetlands. Investigation of greenhouse gas emissions with enclosed chambers, like those used by Alm *et al*. (1997), could be used to establish CO_2 and CH_4 releases from the wetland. This would allow direct measurement of any emission changes and would help determine whether the study sites were becoming greater sources of greenhouse gases.

The nature of pre-existing vegetation is one determinant in the hydrology and geochemistry of a peatland. However, the nature of the water body is equally indicative of what kind of vegetation will grow in the future. The tandem of these two properties helps control the evolution of the wetland, and disruption to either will ultimately affect both. Thus, research into the hydrology of both basins, using methods similar to Mewhinney (1996), could have improved conclusions related to carbon dynamics and would show whether hydrology played a significant role in the development of both sites.

Finally, having used LC-OCD analysis to help characterize both study sites, an interesting follow up could involve using the technique to try and differentiate vegetation as DOC sources. Whether this could be performed to separate different sections of a plant, different species of plant, different communities of vegetation, or whether it could be done at all is the first question. The mobile nature of water in an ecosystem would be one challenge, while the nature of vegetation decomposition pathways could provide another hurdle. However, if possible in some form, this would certainly be a significant tool in determining the influence of vegetation on local water chemistry, while also providing additional options for recent paleoecologic research.

Implementation of any of these techniques would improve the overall characterization of both wetlands. In addition, chronological application of such methods could help demonstrate how swift and severe the impacts of water flow diversions and climate warming can be on wetland ecosystems.

REFERENCES

Alm, J., Talanov, A., Saarnio, S., Silvola, J., Ikkonen, E., Aaltonen, H., Nykänen, H. and Martikainen, P.J. 1997. Reconstruction of the carbon balance for microsites in a boreal oligotrophic pine fen, Finland. *Oecologia* **110**: 423-431.

Alm, J., Schulman, L., Walden, J., Nykänen, H., Martikainen, P.J. and Silvola, J. 1999. Carbon balance of a boreal bog during a year with an exceptionally dry summer. *Ecology* **80**: 161-174.

Asada, T., Warner, B.G., Schiff, S.L. 2005. Effects of shallow flooding on vegetation and carbon pools in boreal peatlands. *Applied Vegetation Science* **8**: 199-208.

Beaty, K.G. 2010. Lake 626 diversion study at the Experimental Lakes Area: Scope of work 2010. Annual Report. Winnipeg, MB. 17 pp.

Beaty, K.G., and Lyng, M.E. (1989). *Hydrometerological data for the Experimental Lakes Area, northwestern Ontario, 1982 to 1987*. Canadian Data Report of Fisheries and Aquatic Sciences. No. 759. Winnipeg, CA.

Berglund, B.E. (editor). Handbook of Holocene Paleoecology and Palaeohydrology. John Wiley and Sons (1986). 869 pp.

Björck, S. 1985. Deglaciation chronology and revegetation in northwestern Ontario. *Canadian Journal of Earth Science* **22**: 850-871.

Boelter, D.H., and Verry, E.S. (1977). Peatland and water in the northern lake states. U.S. Department of Agriculture and Forestry Servive General Technical Report NC-31.

Bridgham, S.D., Megonigal, J.P., Keller, J.K., Bliss, N.B. and Trettin, C. 2006. The carbon balance of North American wetlands. *Wetlands* **26**: 889-916.

Canada Soil Survey Committee. 1978. The Canadian System of Soil Classification. Research Branch, Canada Department of Agriculture. Publication No. 1646. Ottawa, Ontario. 164 p.

Canadian Association of Petroleum Producers (CAPP). June 2010. Responsible water management in Canada's oil and gas industry. http://www.capp.ca/getdoc.aspx?DocID=173950

Canadian Association of Petroleum Producers (CAPP). June 2012. Crude Oil: Forecast, Markets & Pipelines. http://www.capp.ca/getdoc.aspx?DocId=209546&DT=NTV

Chanton, J.P., Martens, C.S. and Kelley, C.A. 1989. Gas transport from methane-saturated tidal, freshwater and wetland sediments. *Limnology and Oceanography* **34**: 807-819.

Chanton, J.P. and Dacey, J.W.H. 1991. Effects of Vegetation on Methane Flux, Reservoirs and Carbon Isotopic Composition. In: Mooney, H., Holland, E., Sharkey, T. (Eds.), For Trace Gas Emissions from Plants. Academic Press, pp. 65-92.

Chanton, J.P. 2005. The effect of gas transport on the isotope signature of methane in wetlands. *Organic Geochemistry* **36**: 753-768.

Clark, P.U., Dyke, A.S., Shakun, J.D., Carlson, A.E., Clark, J., Wohlfarth, B., Mitrovica, J.X., Hostetler, S.W. and McCabe, A.M. 2009. The last glacial maximum. *Science* **325**: 710-714.

Clayton, L. and Moran, S.R. 1982. Chronology of late Wisconsinan glaciations in middle North America. *Quaternary Science Reviews* **1**: 55-82.

Crill, P.M. 1991. Seasonal patterns of methane uptake and carbon dioxide release by a temperate woodland soil. *Global Biogeochemical Cycles* **5**: 319-334.

Dean, W.E. 1974. Determination of carbonate and organic matter in calcareous sediments and sedimentary rocks by loss on ignition: comparison with other methods. *J. Sed. Pet*. **44**: 242–248.

Domenico, P.A. and Schwartz, F.W. 1990. Physical and Chemical Hydrogeology. John Wiley and Sons, Inc. USA. pp. 369.

Dyck, B.S. 1998. *The species composition, aboveground biomass and carbon content of vegetation in two basin bogs in the Experimental Lakes Area, north-western Ontario.* M. Sc. Thesis, University of Manitoba, Winnipeg, CA.

Dyck, B.S. and Shay, J.M. 1999. Biomass and carbon pool of two bogs in the Experimental Lakes Area, northwestern Ontario. *Canadian Journal of Botany* **77**: 291-304.

Dyke, A.S. 2005. Late quaternary vegetation history of northern North America based on pollen, macrofossil, and faunal remains. *Géographie physique et Quaternaire* **59**: 211-262.

ECO. 2010. Annual Greenhouse Gas Progress Report 2011: Meeting Responsibilities: Creating Opportunities. Toronto, ON: Environmental Commisioner of Ontario. pp. 3-14.

Environment Canada. 2007. Water use: withdrawal uses. http://www.ec.gc.ca/eau-water/default.asp?lang=En&n=851B096C-1. Updated July, 2011.

Fairbanks, R.G., Mortlock, R.A., Chiu, T., Cao, L., Kaplan, A., Guilderson, T.P., Fairbanks, T.W., and Bloom, A.L. 2005. Marine radiocarbon calibration curve spanning 0 to 50,000 years B.P. based on paired 230^{Th}/234U/238U and 14C dates on pristine corals. *Quaternary Science Reviews* **24**: 1781-1796.

Foster, D.R., Wright Jr., H.E., Thelaus, M. and King, G.A. 1988. Bog development and landform dynamics in central Sweden and South-eastern Labrador, Canada. *Journal of Ecology* **76**: 1164-1185.

Fry, B. 2006. Stable Isotope Ecology. New York, Springer Science+Business Media, LLC. 316 pp.

Gat, J.R., Mook, W.G., and Meijer, H.A.J. (2001). "Volume II: Atmospheric Water", In: W.G. Mook (Ed.), *Environmental isotopes in the hydrological cycle: Principles and applications.* UNESCO, Paris, pp. 63-74.

Glaser, P.H., Chanton, J.P., Rosenberry, D.O., Morin, P.J., Siegel, D.I., Ruud, O., Reede, A.S. and Chasar, L. 2004. Surface deformations as indicators of deep ebullition fluxes in a large northern peatland. *Global Biogeochemical Cycles* **18**: 1-15.

Gorham, E. and Hofstetter, R.H. 1971. Penetration of bog peats and lake sediments by tritium from atmospheric fallout. *Ecology* **52**: 898-902.

Gorham, E. 1991. Northern peatlands: Role in the carbon cycle and probable responses to climatic warming. *Ecological Applications* **1**: 182-195.

Gorham, E. and Janssens, J. 1992. Concepts of fen and bog re-examined in relation to bryophyte cover and the acidity of surface waters. *Acta Societatis Botanicorum Poloniae* **61**: 7-20.

Graf, W.L. (2006). Downstream hydrologic and geomorphic effects of large dams on American rivers. *Geomorphology* **79**: 336-360.

Hebert, P.D.N. and McGinley, M. 2010. "Wetland classifications". In: Encyclopedia of Earth. Eds. Cutler J. Cleveland (Washington, D.C.: Environmental Information Coalition, National Council for Science and the Environment). [First published in the Encyclopedia of Earth May 24, 2010; Last revised Date May 24, 2010; Retrieved June 17, 2012 <http://www.eoearth.org/article/Wetland_classifications>

Hornibrook, E.R.C. Longstaffe, F.J. and Fyfe, W.S. 2000. Evolution of stable isotope compositions for methane and carbon dioxide in freshwater wetlands and other anaerobic environments. *Geochimica et Cosmochimica Acta* **64**: 1013-1027.

Houghton, J.T., Meira Filho, L.G., Callander, B.A., Harris, N., Kattenberg, A. and Maskell, K. 1996. Climate Change 1995: The Science of Climate Change. Intergovernmental Panel on Climate Change. Cambridge University Press, Cambridge. pp. 572.

Huber, S.A. and Frimmel, F.H. 1996. Gelchromatographie mit Kohlenstoffdetektion (LC-OCD): Ein rasches und aussagekräftiges Verfahren zur Charakterisierung hydrophiler organischer Wasserinhaltsstoffe. *Vom Wasser* **86**: 277-290.

Huber, S.A., Balz, A., Abert, M. and Pronk, W. 2011. Characterization of aquatic humic and non-humic matter with size-exclusion chromatography – organic carbon detection – organic nitrogen detection (LC-OCD-OND). *Water Research* **45**: 879-885.

IPCC, *Fourth Assessment Report: Climate Change*. 2007, Intergovernmental Panel on Climate Change, Geneva, Switzerland; Retrieved June 2, 2012. http://www.ipcc.ch/publications_and_data/ar4/wg1/en/tssts-2-5.html

Johnson, W.C., Millett, B.V., Gilmanov, T., Voldseth, R.A., Guntenspergen, G.R., and Naugle, D.E. 2005. Vulnerability of northern prairie wetlands to climate change. *BioScience* **55**: 863-872.

Kaufman, D.S., Ager, T.A., Anderson, N.J., Anderson, P.M., Andrews, J.T., Bartlein, P.J., Brubaker, L.B. Coats, L.L., Cwynar, L.C., Duvall, M.L., Dyke, A.S., Edwards, M.E., Eisner, W.R., Gajewski, K., Geirsdottir, A., Hu, F.S., Jennings, A.E., Kaplan, M.R., Kerwin, M.W., Lozhkin, A.V., MacDonald G.M., Miller, G.H., Mock, C.J., Oswald, W.W., Otto-Bliesner, B.L., Porinchu, D.F., Ruhland, K., Smol, J.P., Steig, E.J. and Wolfe, B.B. 2004. The Holocene thermal maximum in the Western Arctic. *Quaternary Science Reviews* **23**: 529-560.

Keller, M. and Stallard, R.F. 1994. Methane emissions by bubbling from Gatun Lake, Panama. *Journal of Geophysical Reasearch* **99**: 8307-8319.

Kelly, C.A. and Rudd, J.W.M. 1993. Fluxes of CH_4 and CO_2 to the atmosphere from hydroelectric reservoirs. Environment Canada. CO_2/Climate Report, Winter 1993

Kelly, C.A., Rudd, J.W.M., Bodaly, R.A., Roulet, N.P., St. Louis, V.L., Heyes, A., Moore, T.R., Schiff, S., Aravena, R., Scott, K.J., Dyck, B., Harris, R., Warner, B., and Edwards, G. 1997. Increases in fluxes of greenhouse gases and methyl mercury following flooding of an experimental reservoir. *Environmental Science & Technology* **31**: 1334-1344.

Kendall, C. and Caldwell, E.A. (1998). "Fundamentals of Isotope Geochemistry", In: C. Kendall and J.J. McDonnell (Eds.), *Isotope Tracers in Catchment Hydrology.* Elsevier Science, Amsterdam, pp. 51-86.

Keppler, F., Hamilton, J.T.G., Brab, M. and Rockmann, T. 2006. Methane emissions from terrestrial plants under aerobic conditions. *Nature* **439**: 187-191.

Kussow, W.R. Wisconsin Soils Report: Humate and Humic Acid. University of Wisconsin-Madison: Department of Soil Science; 1994. http://archive.lib.msu.edu/tic/groot/article/1994mar18.pdf.

Laine, J. and Vasander, H. 1996. Ecology and vegetation gradients of peatlands. In: *Peatlands in Finland*, (ed. H. Vasander), pp. 10-19, Finnish Peatland Society, Helsinki.

Laird, K.R. and Cumming, B.F. 2008. Reconstruction of Holocene lake level from diatoms, chrysophytes and organic matter in a drainage lake from the Experimental Lakes Area (northwestern Ontario, Canada). *Quaternary Research* **69**: 292-305.

Lal, R. 2008. Sequestration of atmospheric CO_2 in global carbon pools, *Energy & Environmental Science* **1**: 86-100.

Lansdown, J.M., Quay, P.D. and King, S.L. 1992. CH_4 production via CO_2 reduction in a temperate bog: A source of ^{13}C-depleted CH_4. *Geochimica et Cosmochimica Acta* **56**: 3493-3503.

Lucas, L.L. and Unterweger, M.P. 2000. Comprehensive review and critical evaluation of the half-life of tritium. *J. Res. Natl. Stand. Technol.* **105**: 541-549.

McAndrews, J.H. 1982. Holocene environment of a fossil bison from Kenora, Ontario. *Ontario Archeology* **37**: 41-51.

Mewhinney, E.J. 1996. *The importance of hydrology to carbon dynamics in a small boreal forest wetland.* M. Sc. Thesis, University of Waterloo, Ontario, CA.

Mitsch, W.J., and Gosselink, J.G. (2007). Wetlands (4th ed.). New Jersey, John Wiley & Sons, Inc. 582 pp.

Moos, M.T. 2010. *Tracking long-term Holocene climate trends in Lake 239 (Experimental Lakes Area, NW Ontario) using diatoms, pollen, and charcoal.* PhD Thesis, Queen's University, Kingston, Ontario, CA.

National Atlas Information Service. 1993. Canada: Terrestrial Ecoregions. The National Atlas of Canada. 5th Edition. Department of Energy, Mines and Resources Canada, Environment Canada, Ottawa, CA.

National Wetlands Working Group. 1988. Wetlands of Canada. Sustainable Development Branch, Environment Canada, Ottawa, Ont., and Polyscience Publications Inc., Montreal, Que. Ecological Land Classification Survey No. 24.

National Wetlands Working Group. 1997. The Canadian Wetland Classification Systerm, 2nd Edition. Warner, B.G. and C.D.A. Rubec (eds.), Wetlands Research Centre, University of Waterloo, Waterloo, ON, Canada. p. 9, 19-24, 27-35.

Neal, C., Smith, C.J. and Hill, S. 1992. Forestry Impact on Upland Water Quality. Institute of Hydrology. Wallingford. Report No. 119.

Newmaster, S.G., Harris, A.G. and Kershaw, L.J. 1997. Wetland plants of Ontario. Edmonton. Lone Pine Publishing. 240 pp.

NOAA, *Trends in Atmospheric Carbon*. 2011, National Oceanic & Atmospheric Administration, Washington, DC, 2011, http://www.esrl.noaa.gov/gmd/ccgg/trends/.

NOAA, *Carbon dioxide levels reach milestone at Arctic sites*. 2012, National Oceanic & Atmospheric Administration, Washington, DC, 2012, http://researchmatters.noaa.gov/news/Pages/arcticCO2.aspx.

NRC, *Advancing the Science of Climate Change*. 2010, National Research Council. The National Academies Press, Washington, DC, USA.

Oechel, W.C., Hastings, S.J., Vourlitis, G., Jenkins, M., Riechers, G. and Grulke, N. 1993. Recent change of Arctic tundra ecosystems from a net carbon dioxide sink to source. *Nature* **361**: 520-523.

Osborne, R.V. Tritium in the Canadian Environment: Levels and Health Effects. Ottawa, Canada: Canadian Nuclear Safety Commission; Report (in press); 2002. http://www.odwac.gov.on.ca/standards_review/tritium/Osborne_CNSC-RSP-0153-2.pdf.

Prest, V.K. 1969. Retreat of Wisconsin and recent ice in North America. Geological Survey of Canada, Ottawa, Ont. Map No. 1257A

Prowse, T.D., Wrona, F.J., and Power, G. 2004. Dams, reservoirs and flow regulation. In Environment Canada. 2004. Threats to Water Availability in Canada – Chapter 2. National Water Research Institute, Burlington, Ontario. NWRI Scientific Assessment Report Series No. 3 and ACSD Science Assessment Series No. 1. 128 p.

Ptacek, C., Price, W., Smith, J.L., Logsdon, M. and McCandless, R. 2004. Land-use practices and changes: Mining and petroleum production. In Environment Canada. 2004. Threats to Water Availability in Canada – Chapter 9. National Water Research Institute, Burlington, Ontario. NWRI Scientific Assessment Report Series No. 3 and ACSD Science Assessment Series No. 1. 128 p.

Quay, P.D., King, S.L., Lansdown, J.M. and Wilbur, D.O. 1988. Isotopic composition of methane released from wetlands: Implications for the increase in atmospheric methane. *Global Biogeochemical Cycles* **2**: 385-397.

Quinn, F., Day, J.C., Healey, M., Kellow, R., Rosenberg, D., and Saunders, J.O. 2004. Water allocations, diversion and export. In Environment Canada. 2004. Threats to Water Availability in Canada – Chapter 1. National Water Research Institute, Burlington, Ontario. NWRI Scientific Assessment Report Series No. 3 and ACSD Science Assessment Series No. 1. 128 p.

Robichaud, A. and Bégin, Y. 2009. Development of a raised bog over 9000 years in Atlantic Canada. *Mires and Peat* **5 (4)**: 1-19.

Rosenberg, D.M., Berkes, F., Bodaly, R.A., Hecky, R.E., Kelly, C.A., Rudd, J.W.M. 1997. Large-scale impacts of hydroelectric development. *Environmental Review* **5**: 27-54.

Rosenberg, D.M., McCully, P. and Pringle, C.M. 2000. Global-Scale Environmental Effects of Hydrological Alterations: Introduction. *Bioscience* **50**: 746-751.

Roulet, N.T. 2000. Peatlands, carbon storage, greenhouse gases, and the Kyoto Protocol: Prospects and significance for Canada. *Wetlands* **20**: 605-615.

Rowe, J.S. 1972. Forest Regions of Canada. Fisheries and Environment Canada, Canadian Forest Service, Headquarters, Ottawa. 172 pp.

Ruhl, A.S. and Jekel, M. 2012. Elution behaviour of low molecular weight compounds in size exclusion chromatography. *Journal of Water Supply: Research and Technology – AQUA* **61**: 32-40.

Rydin, H. and Jeglum, J. (2006). The Biology of Peatlands. New York, Oxford University Press Inc. 343 pp.

Schiff, S.L., Aravena, R., Trumbore, S.E., Hinton, M.J., Elgood, R. and Dillon, P.J. 1997. Export of DOC from forested catchments on the Precambrian Shield of Central Ontario: Clues from ^{13}C and ^{14}C. *Biogeochemistry* **36**: 43-65.

Schindler, D.W. and Donahue, W.F. 2006. An impending water crisis in Canada's western prairie provinces. *Proc. Natl. Acad. Sci. USA* **103**: 7210-7216.

Schindler, D.W., Donahue, W.F. and Thompson, J.P. 2007. Future water flows and human withdrawals in the Athabasca River. In D.J. Davidson & A.M. Hurley (Eds.), *Running out of steam? Oil sands development and water use in the Athabasca River-watershed: Science and market based solutions* (pp. 1-38). Environmental Research and Studies Centre, University of Alberta. http://www.ualberta.ca/~ersc/water.pdf

Schindler, D.W. 2009. A personal history of the Experimental Lakes Project. *Canadian Journal of Fisheries and Aquatic Sciences* **66**: 1837-1847.

Schwintzer, C.R. 1981. Vegetation and nutrient status of northern Michigan bogs and conifer swamps with a comparison to fens. *Can. J. Bot.* **59**: 842-853.

Shotyk, W. 1988. Review of the inorganic geochemistry of peats and peatland waters. *Earth-Science Reviews* **25**: 95-176.

Silvola, J., Alm, J., Ahlholm, U., Nykänen, H., and Martikainen, P.J. 1996. CO_2 fluxes from peat in boreal mires under varying temperature and moisture conditions. *Journal of Ecology* **84**: 219-228.

Steinmann, P., Eilrich, B., Leuenberger, M. and Burns, S.J. 2008. Stable carbon isotope composition and concentrations of CO_2 and CH_4 in the deep catotelm of a peat bog. *Geochimica et Cosmochimica Acta* **72**: 6015-6026.

Stokstad, E. 2008. Canada's Experimental Lakes. *Science* **322**: 1316-1319.

Tarnocai, C. 2006. The effect of climate change on carbon in Canadian peatlands. *Global and Planetary Change* **53**: 222–232

Tarnocai, C. 2009. The impact of climate change on Canadian peatlands. *Canadian Water Resources Journal* **34**: 453-466.

Teller, J.T. and Clayton, L., eds, 1983, Glacial Lake Agassiz; Geological Association of Canada, Special Paper 26, p. 451

Thormann, M.N., Bernier, P.Y., Foster, N.W., Schindler, D.W. and Beall, F.D. 2004. Land-use practices and changes: Forestry. In Environment Canada. 2004. Threats to Water Availability in Canada – Chapter 8. National Water Research Institute, Burlington, Ontario. NWRI Scientific Assessment Report Series No. 3 and ACSD Science Assessment Series No. 1. 128 p.

Turetsky M., Wieder K., Halsey L., Vitt D. 2002. Current disturbance and the diminishing peatland carbon sink. *Geophy. Res. Lett.* **29**: 1526-1529.

Tyler, S.C., Bilke, R.S., Sass, R.L. and Fisher, F.M. 1997. Methane oxidation and pathways of production in a Texas paddy field deduced from measurements of flux, $\delta^{13}C$ and δD of CH_4. *Global Biogeochemical Cycles* **8**: 1-12.

USGS, *Resources on Isotopes: Fundamentals of Stable Isotope Geochemistry.* 2004, U.S. Geological Survey, Reston, VA; Retrieved June 23, 2012. < http://wwwrcamnl.wr.usgs.gov/isoig/res/funda.html>

Viau, A.E., Gajewski, K., Sawada, M.C. and Fines, P. 2006. Millennial-scale temperature variations in North America during the Holocene. *Journal of Geophysical Research* **111**: D09102, doi: 10.1029/2005JD006031.

Vitt D. H., Halsey L. A., Bauer I. E., Campbell C. 2000. Spatial and temporal trends in carbon storage of peatlands of continental western Canada through the Holocene. *Can. J. Earth Sci.* **37**: 683–693.

Vitt, D.H. and Bayley, S. 1984. The vegetation and water chemistry of four oligotrophic basin mires in northwestern Ontario. *Canadian Journal of Botany* **62**: 1485-1500.

Vitt, D.H. 2006. Functional characteristics and indicators of boreal peatlands. In: Boreal Peatland Ecosystems. R.K. Wieder and D.H. Vitt eds. Springer, Berlin. pp. 9-24.

Waddington, J.M. and Roulet, N.T. 1997. Groundwater flow and dissolved carbon movement in a boreal peatland. *Journal of Hydrology* **191**: 122-138.

Wall, A.J. and Blanchfield P.J. 2012. Habitat use of lake trout (Salvelinus namaycush) following species introduction. *Ecology of Freshwater Fish* **21**: 300-308.

Warner, B.G. 2003. Peat. In Encyclopedia of sediments and sedimentary rocks. Ed. By G.V. Middleton. Kluwer Academic Publishers, Dordrecht. pp. 514-516.

Weishaar, J.L., Aiken, G.R., Bergamaschi, B.A., Fram, M.S., Fujii, R., and Mopper, K. 2003. Evaluation of specific ultraviolet absorbance as an indicator of the chemical composition and reactivity of dissolved organic carbon. *Environmental Science and Technology* **37**: 4702-4708.

Whiticar, M.J., Faber, E. and Schoell, M. 1986. Biogenic methane formation in marine and freshwater environments: CO_2 reduction *vs*. acetate fermentation – Isotope evidence. *Geochimica et Cosmochimica Acta* **50**: 693-709.

Williams, J.W., Shuman, B. and Bartlein, P.J. 2009. Rapid responses of the prairie-forest ecotone to the early Holocene aridity in mid-continental North America. *Global Planetary Change* **66**: 195-207.

Yamamoto, S., Alcauskas, J. and Crozier, T. 1976. Solubility of methane in distilled water and seawater. *Journal of Chemical Engineering Data* **21**: 78-80.

Yazvenko, S.B., B.G. Warner and R. Aravena. 1994. Long-term history and formation of the Lake 979 wetland. ELARP 3rd Annual Report. Winnipeg, MB. 8 pp.

Zoltai, S.C. and Pollett, F.C. (1983). Wetlands in Canada: their classification, distribution and use. In Ecosystems of the world, vol. 4B, Mires: Swamp, Bog, Fen and Moor, A.J.P. Gore (ed.), NY: Elsevier Science.

SUPPLEMENTARY

LC-OCD Chromatograms:

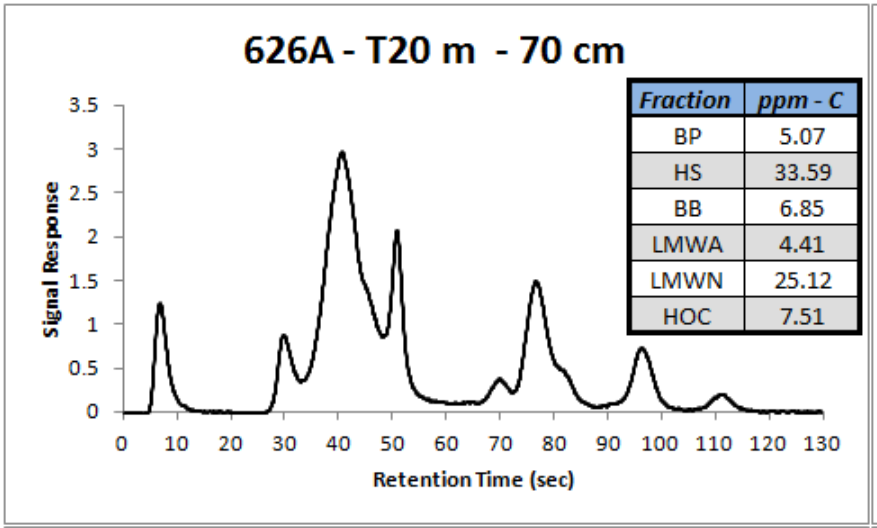

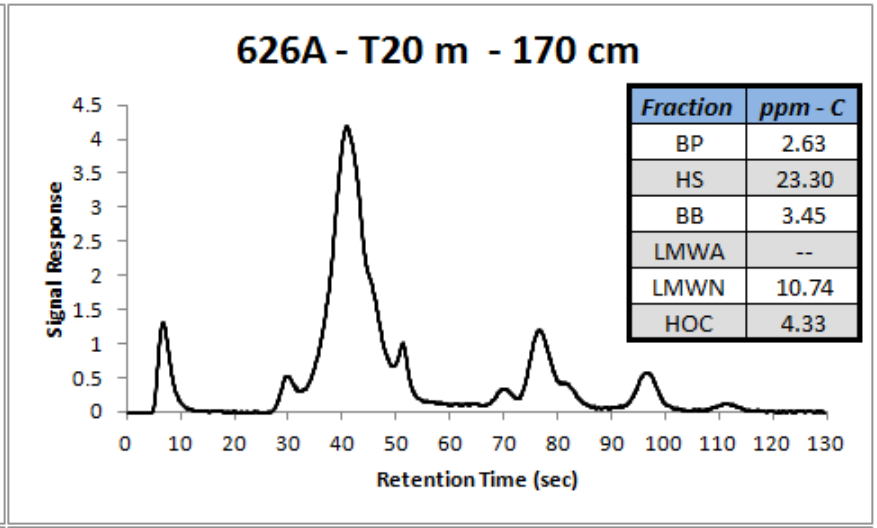

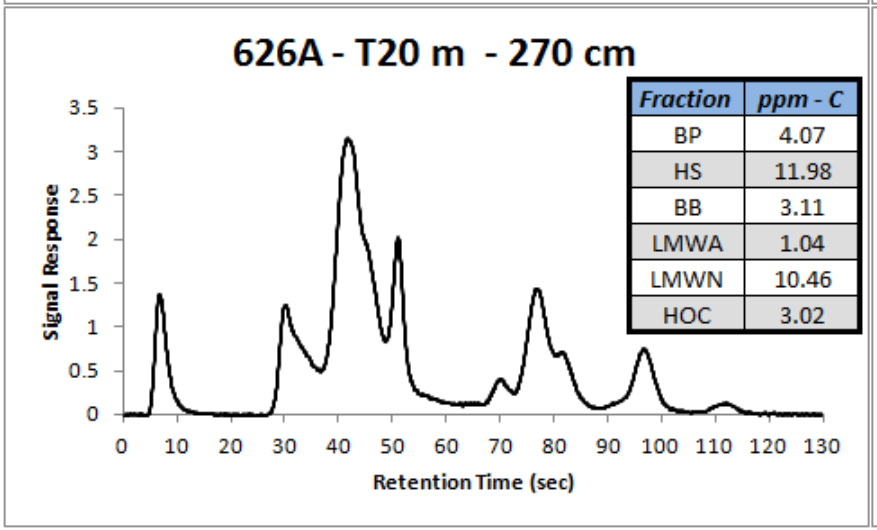

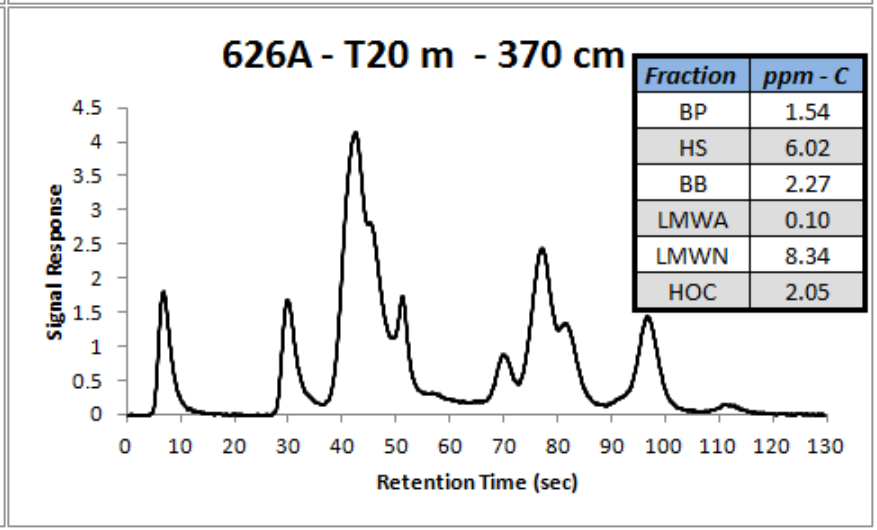

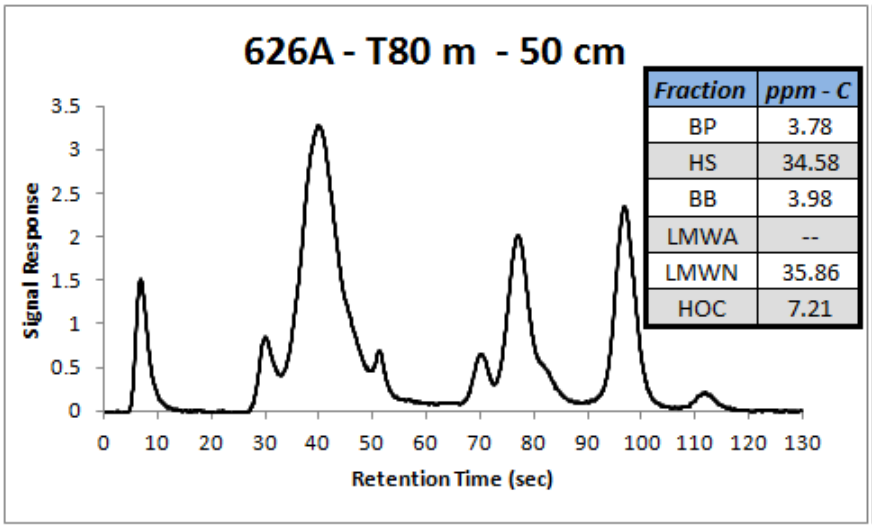
626A - T80 m - 50 cm
Signal Response
Retention Time (sec)
Fraction | ppm - C
BP | 3.78
HS | 34.58
BB | 3.98
LMWA | --
LMWN | 35.86
HOC | 7.21

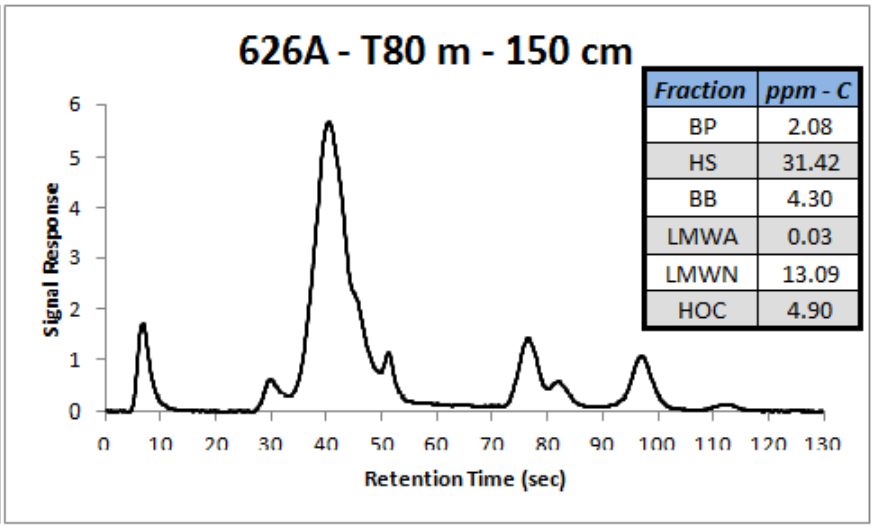
626A - T80 m - 150 cm
Signal Response
Retention Time (sec)
Fraction | ppm - C
BP | 2.08
HS | 31.42
BB | 4.30
LMWA | 0.03
LMWN | 13.09
HOC | 4.90

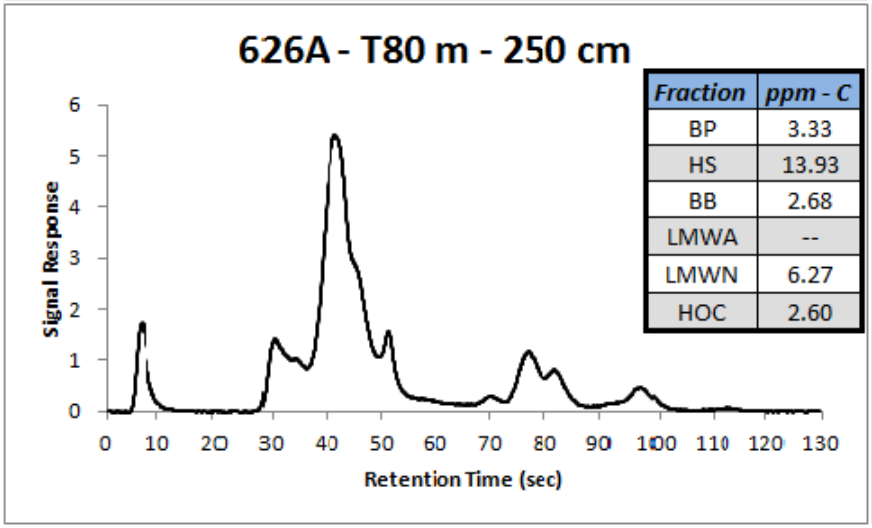
626A - T80 m - 250 cm
Signal Response
Retention Time (sec)
Fraction | ppm - C
BP | 3.33
HS | 13.93
BB | 2.68
LMWA | --
LMWN | 6.27
HOC | 2.60

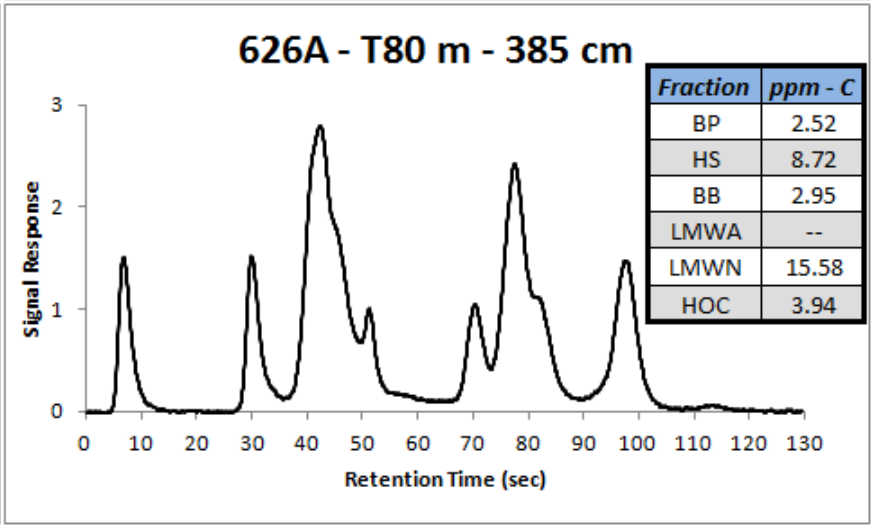
626A - T80 m - 385 cm
Signal Response
Retention Time (sec)
Fraction | ppm - C
BP | 2.52
HS | 8.72
BB | 2.95
LMWA | --
LMWN | 15.58
HOC | 3.94

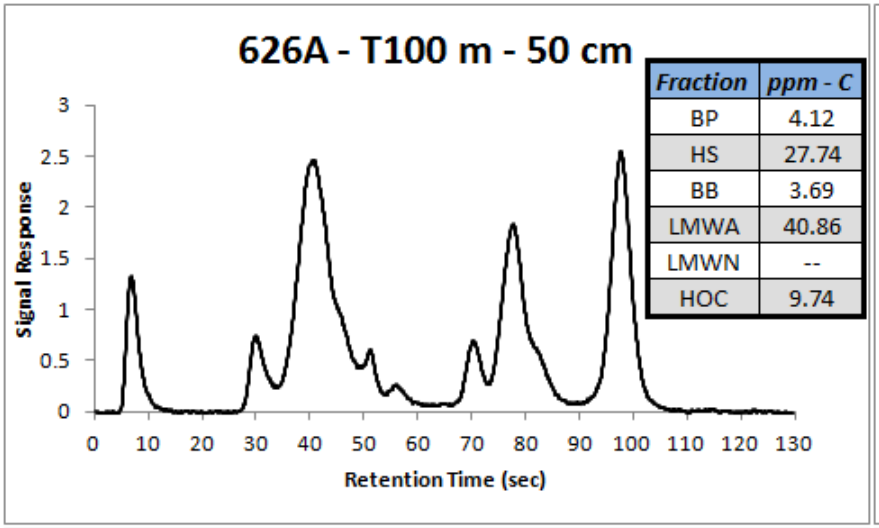
626A - T100 m - 50 cm
Signal Response
Retention Time (sec)
Fraction | ppm - C
BP | 4.12
HS | 27.74
BB | 3.69
LMWA | 40.86
LMWN | --
HOC | 9.74

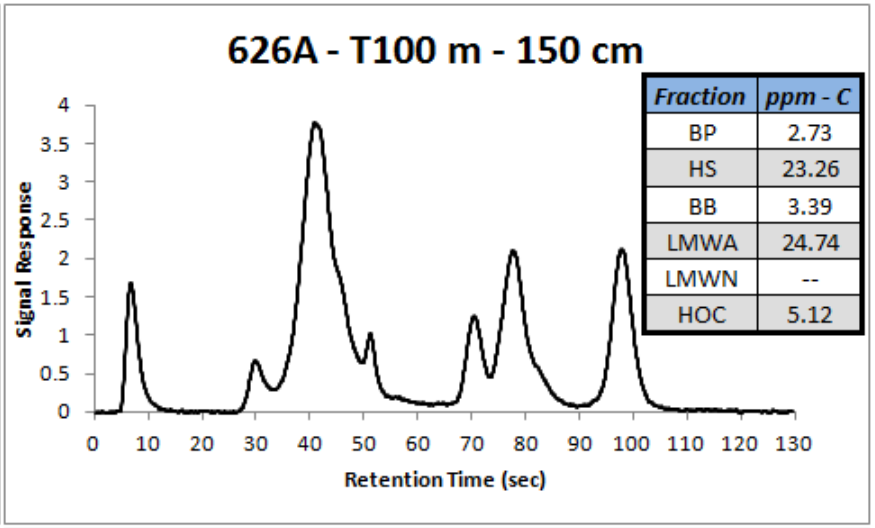
626A - T100 m - 150 cm
Signal Response
Retention Time (sec)
Fraction | ppm - C
BP | 2.73
HS | 23.26
BB | 3.39
LMWA | 24.74
LMWN | --
HOC | 5.12

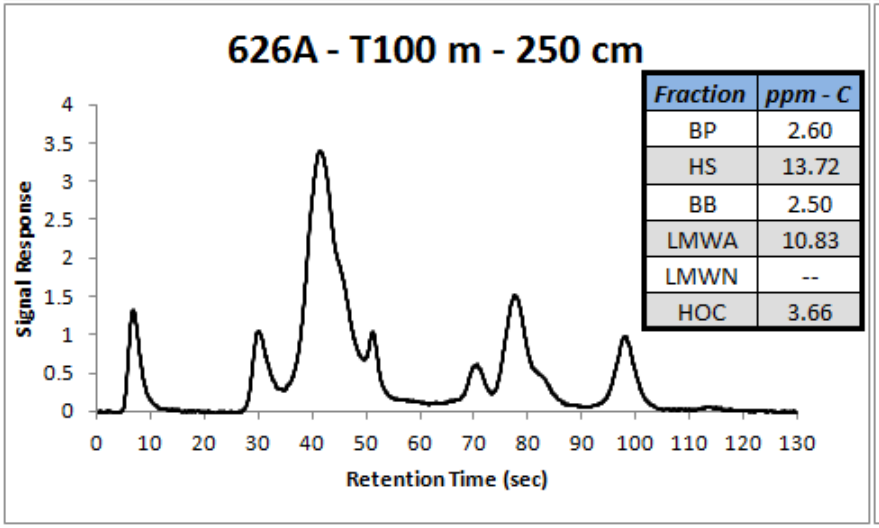
626A - T100 m - 250 cm
Signal Response
Retention Time (sec)
Fraction | ppm - C
BP | 2.60
HS | 13.72
BB | 2.50
LMWA | 10.83
LMWN | --
HOC | 3.66

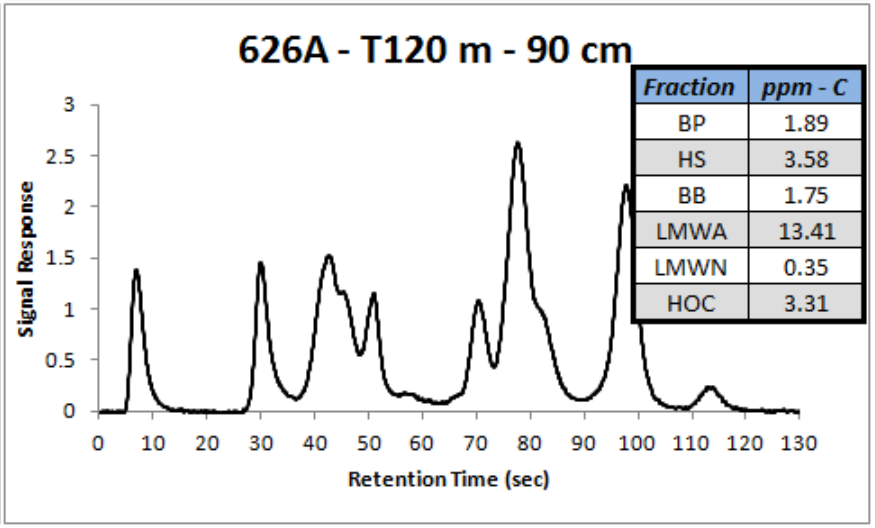
626A - T120 m - 90 cm
Signal Response
Retention Time (sec)
Fraction | ppm - C
BP | 1.89
HS | 3.58
BB | 1.75
LMWA | 13.41
LMWN | 0.35
HOC | 3.31

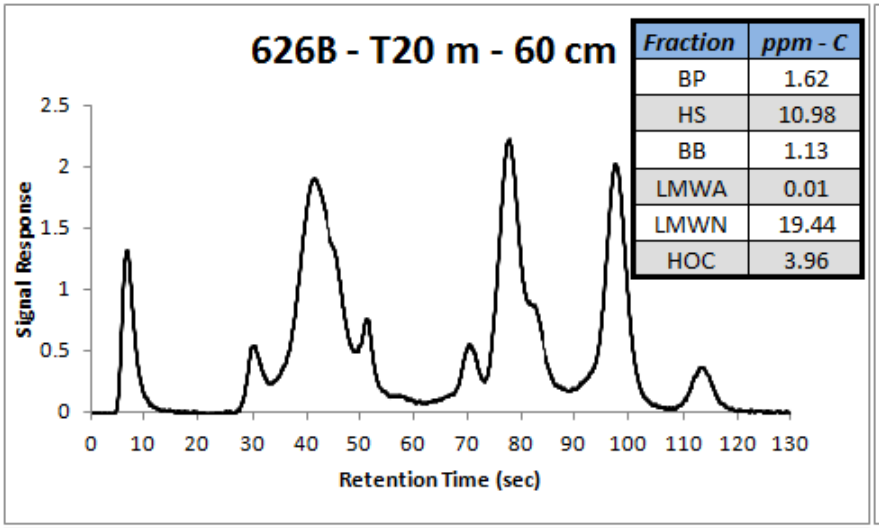

Fraction	ppm - C
BP	1.62
HS	10.98
BB	1.13
LMWA	0.01
LMWN	19.44
HOC	3.96

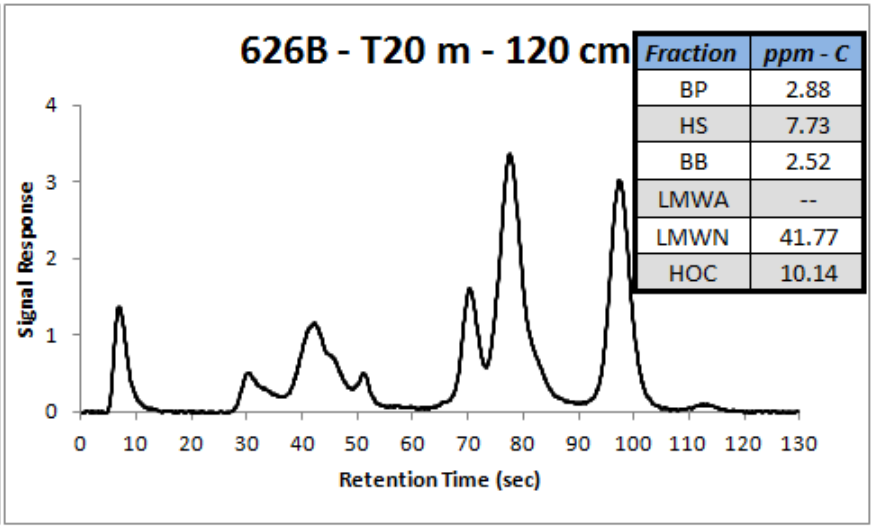

Fraction	ppm - C
BP	2.88
HS	7.73
BB	2.52
LMWA	--
LMWN	41.77
HOC	10.14

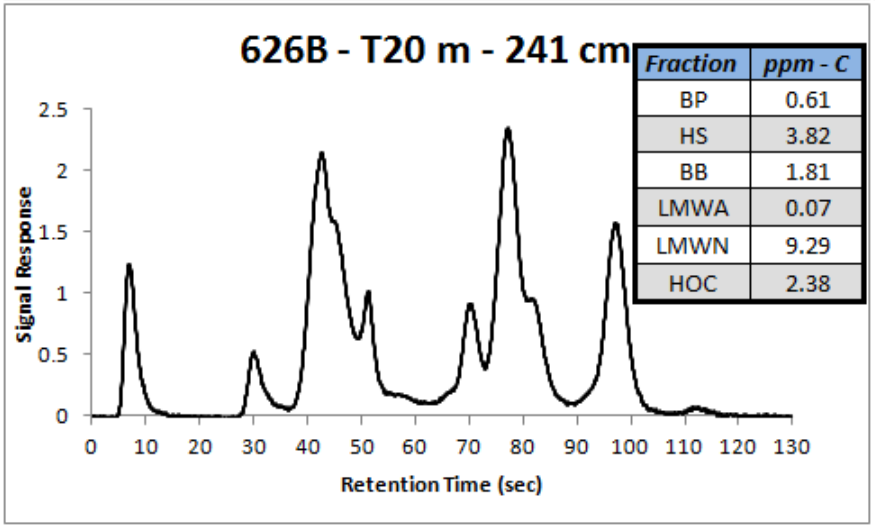

Fraction	ppm - C
BP	0.61
HS	3.82
BB	1.81
LMWA	0.07
LMWN	9.29
HOC	2.38

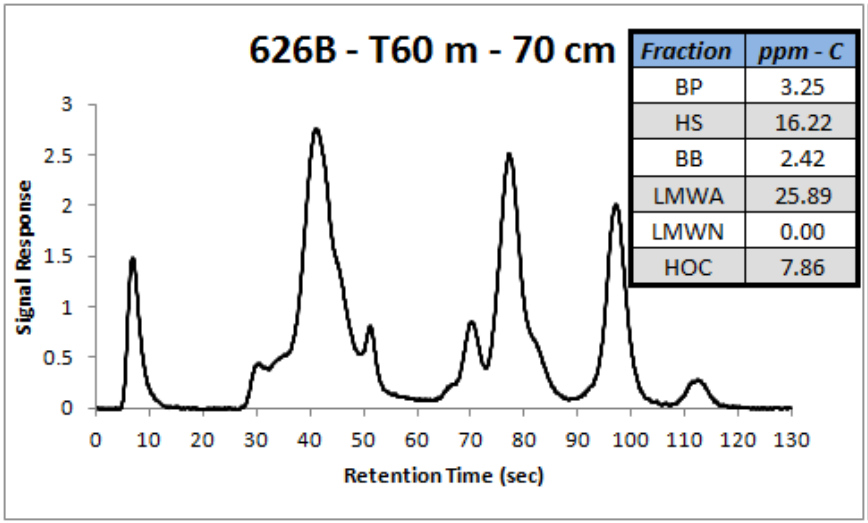
626B - T60 m - 70 cm
Fraction
ppm - C
BP
3.25
HS
16.22
BB
2.42
LMWA
25.89
LMWN
0.00
HOC
7.86
Signal Response
Retention Time (sec)

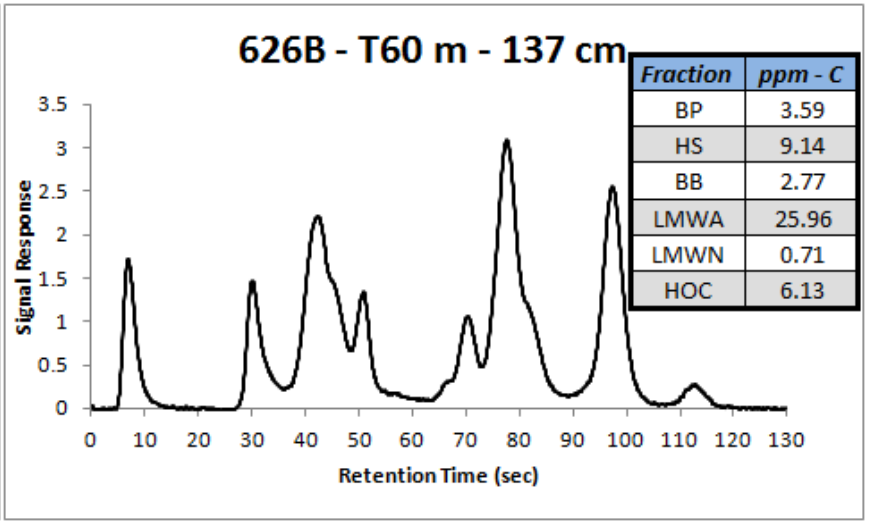
626B - T60 m - 137 cm
Fraction
ppm - C
BP
3.59
HS
9.14
BB
2.77
LMWA
25.96
LMWN
0.71
HOC
6.13
Signal Response
Retention Time (sec)

626A Inflow

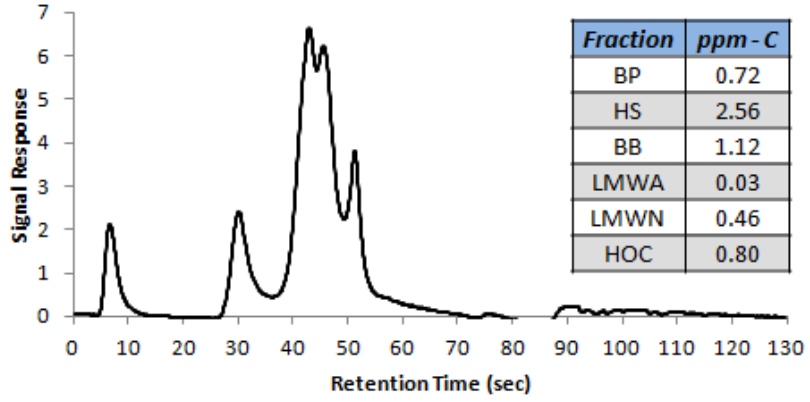

Fraction	ppm - C
BP	0.72
HS	2.56
BB	1.12
LMWA	0.03
LMWN	0.46
HOC	0.80

626A Outflow / 626B Inflow

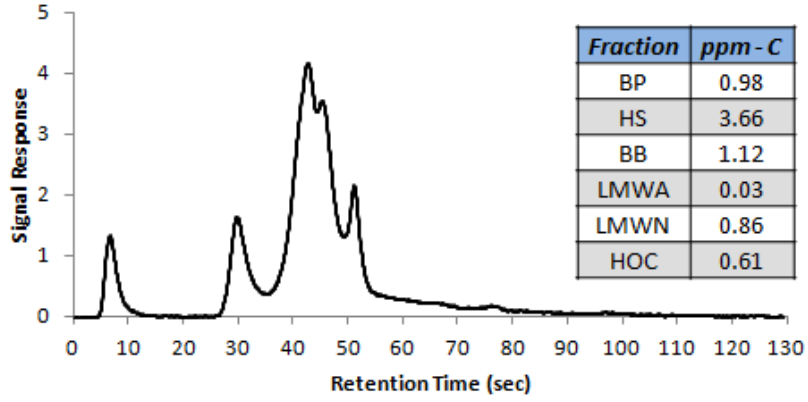

Fraction	ppm - C
BP	0.98
HS	3.66
BB	1.12
LMWA	0.03
LMWN	0.86
HOC	0.61

626B Outflow

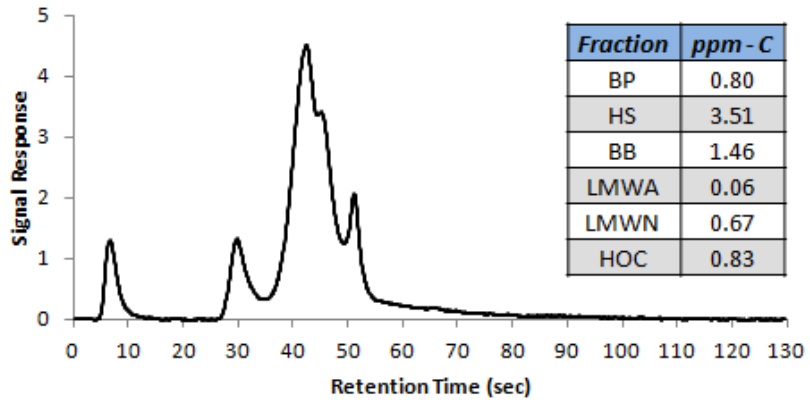

Fraction	ppm - C
BP	0.80
HS	3.51
BB	1.46
LMWA	0.06
LMWN	0.67
HOC	0.83

625 Inflow from 626B

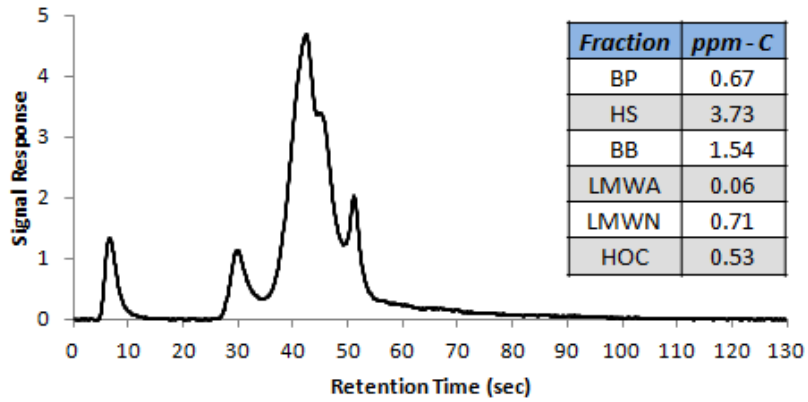

Fraction	ppm - C
BP	0.67
HS	3.73
BB	1.54
LMWA	0.06
LMWN	0.71
HOC	0.53

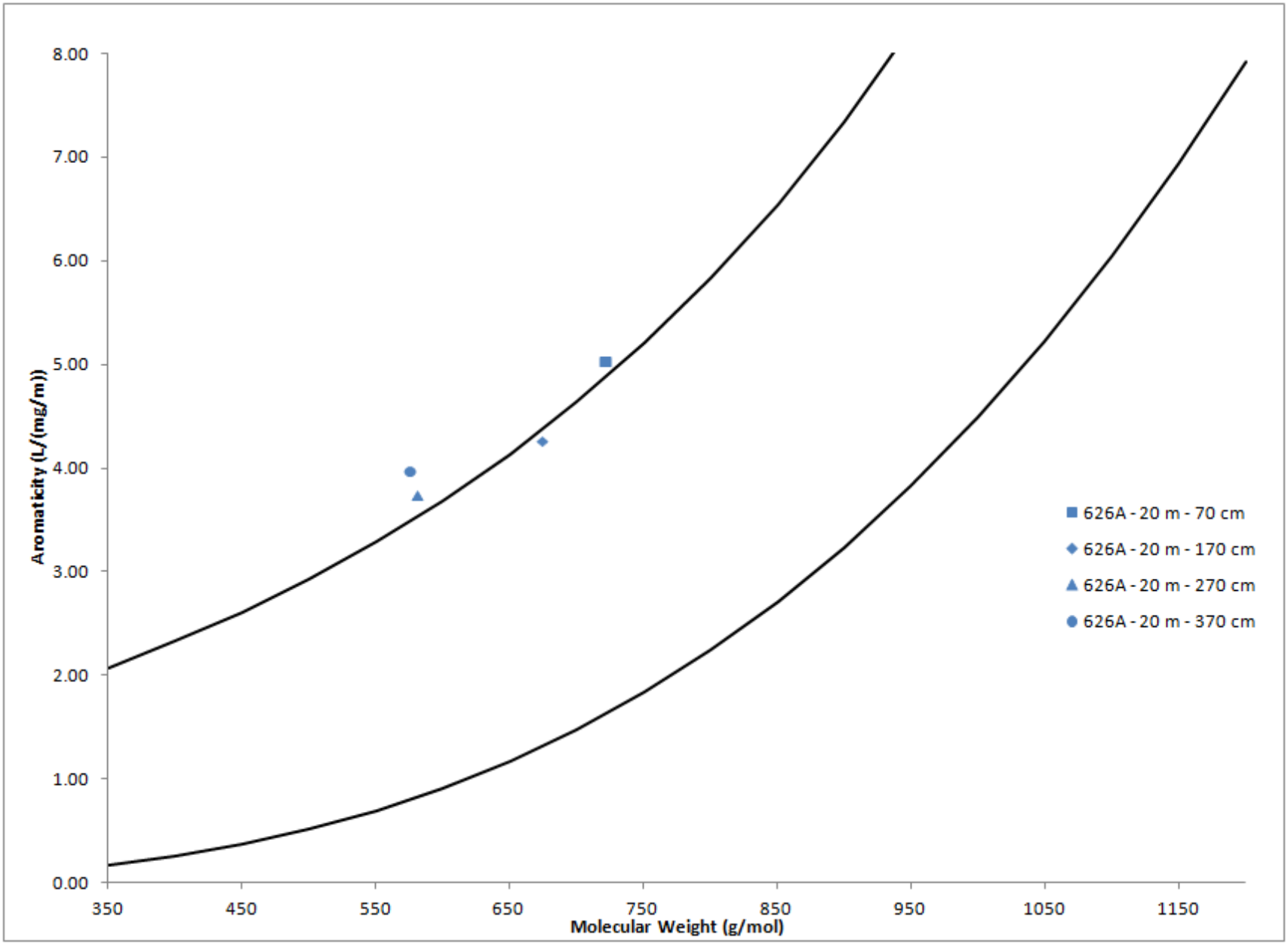
8.00
7.00
6.00
5.00
4.00
3.00
2.00
1.00
0.00
Aromaticity (L/(mg/m))
350
450
550
650
750
850
950
1050
1150
Molecular Weight (g/mol)
626A - 20 m - 70 cm
626A - 20 m - 170 cm
626A - 20 m - 270 cm
626A - 20 m - 370 cm

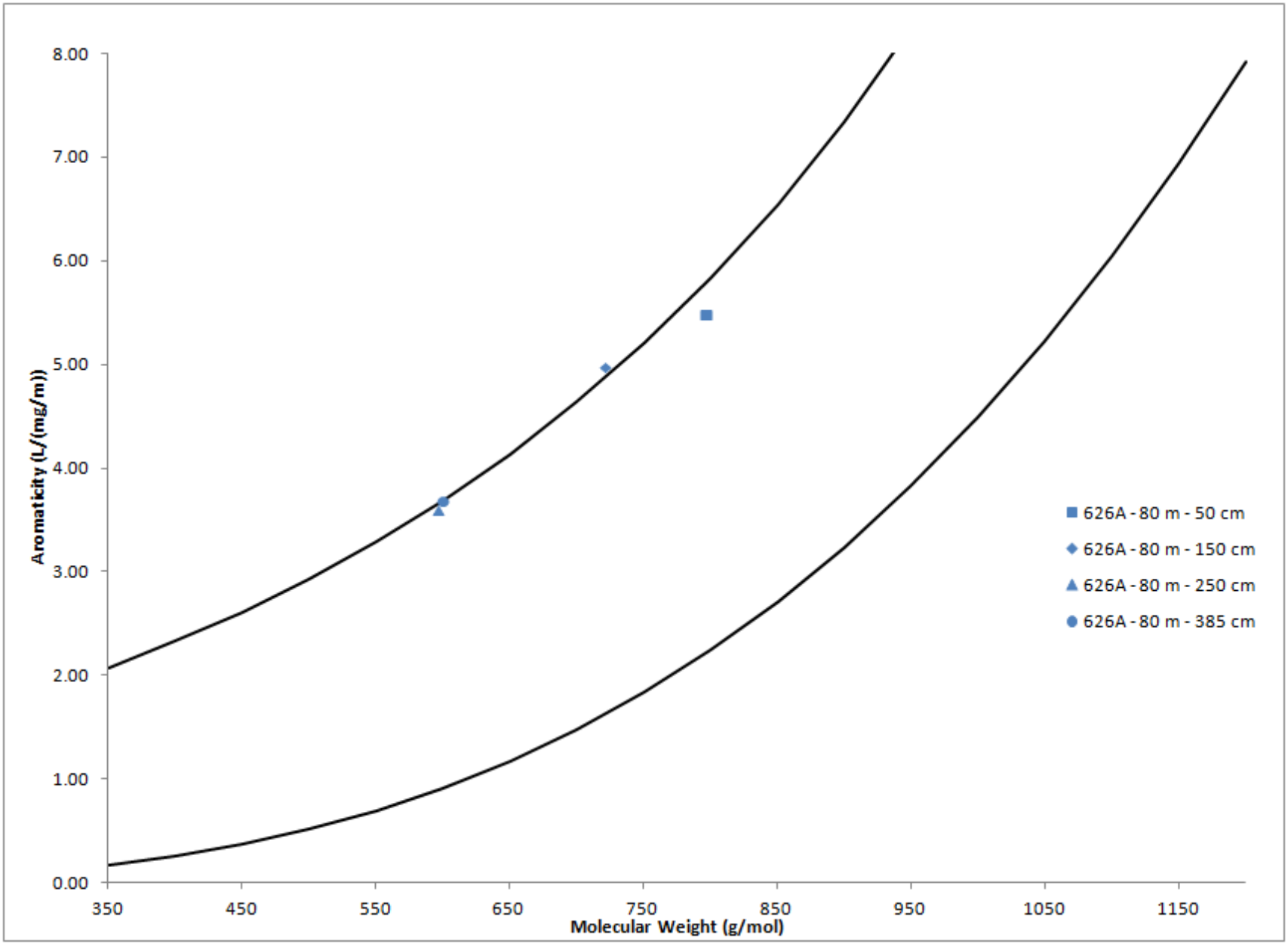
8.00
7.00
6.00
5.00
4.00
3.00
2.00
1.00
0.00
Aromaticity (L/(mg/m))
350
450
550
650
750
850
950
1050
1150
Molecular Weight (g/mol)
626A - 80 m - 50 cm
626A - 80 m - 150 cm
626A - 80 m - 250 cm
626A - 80 m - 385 cm

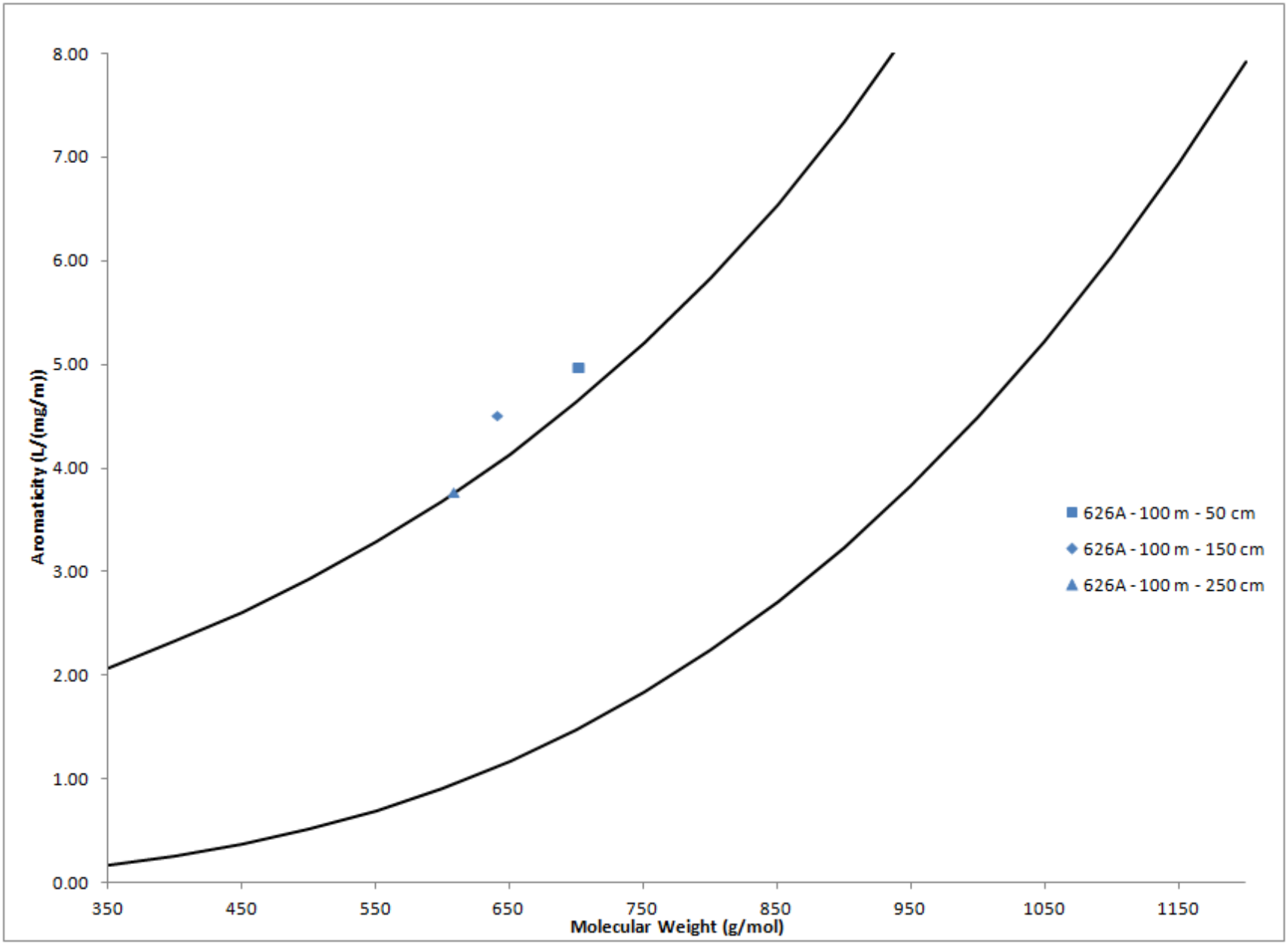
8.00
7.00
6.00
5.00
4.00
3.00
2.00
1.00
0.00
Aromaticity (L/(mg/m))
350
450
550
650
750
850
950
1050
1150
Molecular Weight (g/mol)
626A - 100 m - 50 cm
626A - 100 m - 150 cm
626A - 100 m - 250 cm

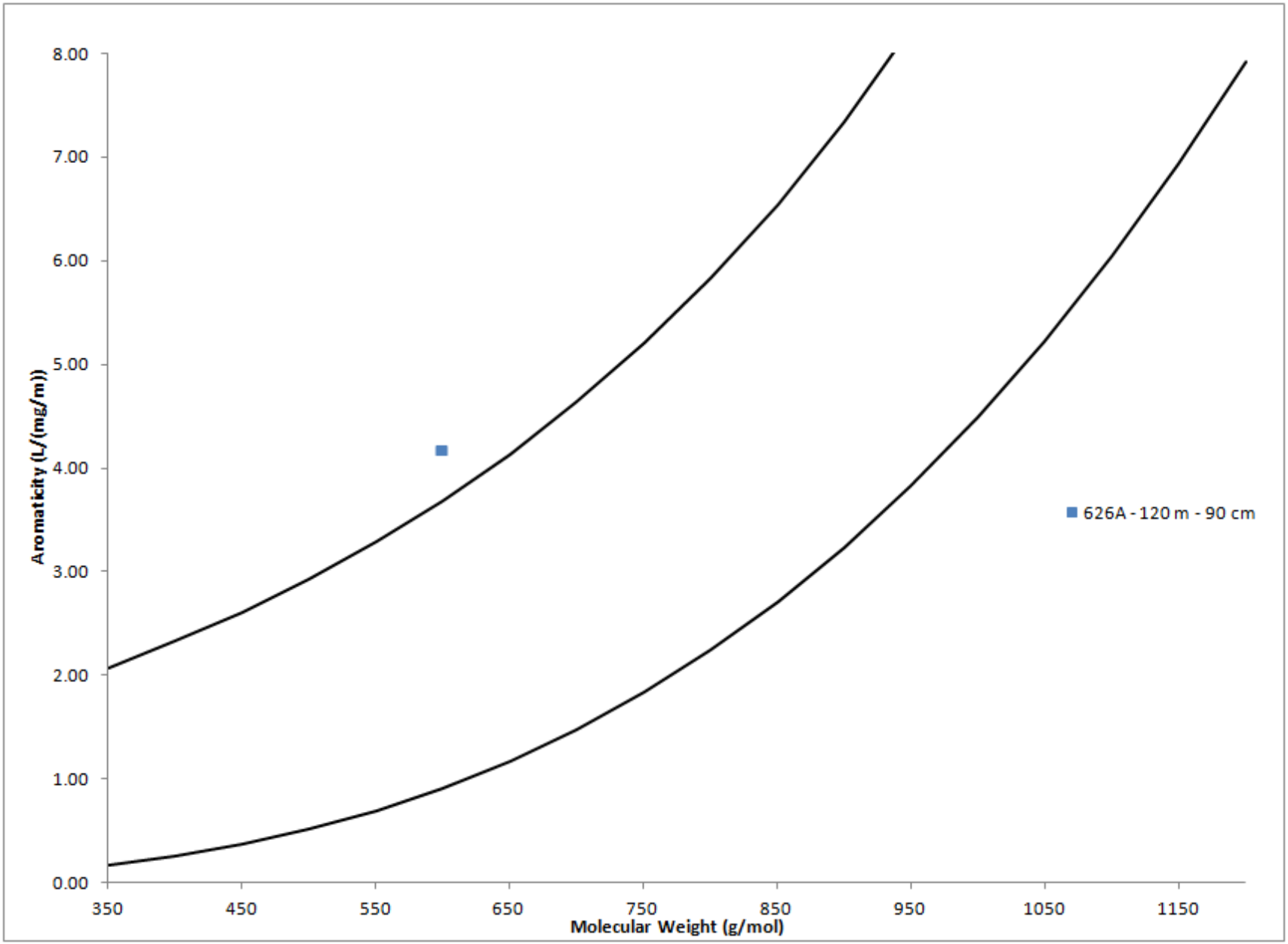
8.00
7.00
6.00
5.00
4.00
3.00
2.00
1.00
0.00
Aromaticity (L/(mg/m))
350
450
550
650
750
850
950
1050
1150
Molecular Weight (g/mol)
626A - 120 m - 90 cm

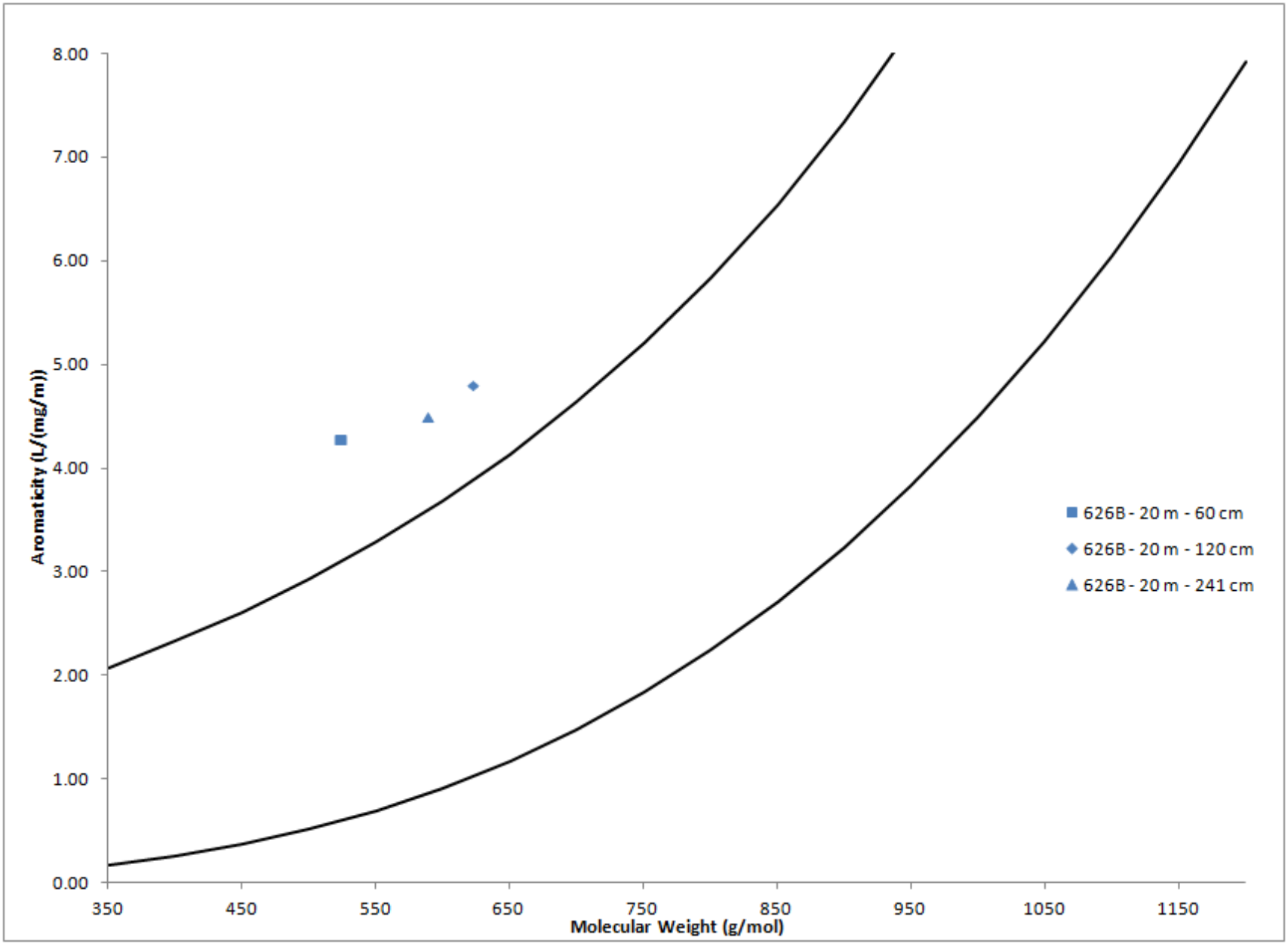
8.00
7.00
6.00
5.00
4.00
3.00
2.00
1.00
0.00
Aromaticity (L/(mg/m))
350
450
550
650
750
850
950
1050
1150
Molecular Weight (g/mol)
626B - 20 m - 60 cm
626B - 20 m - 120 cm
626B - 20 m - 241 cm

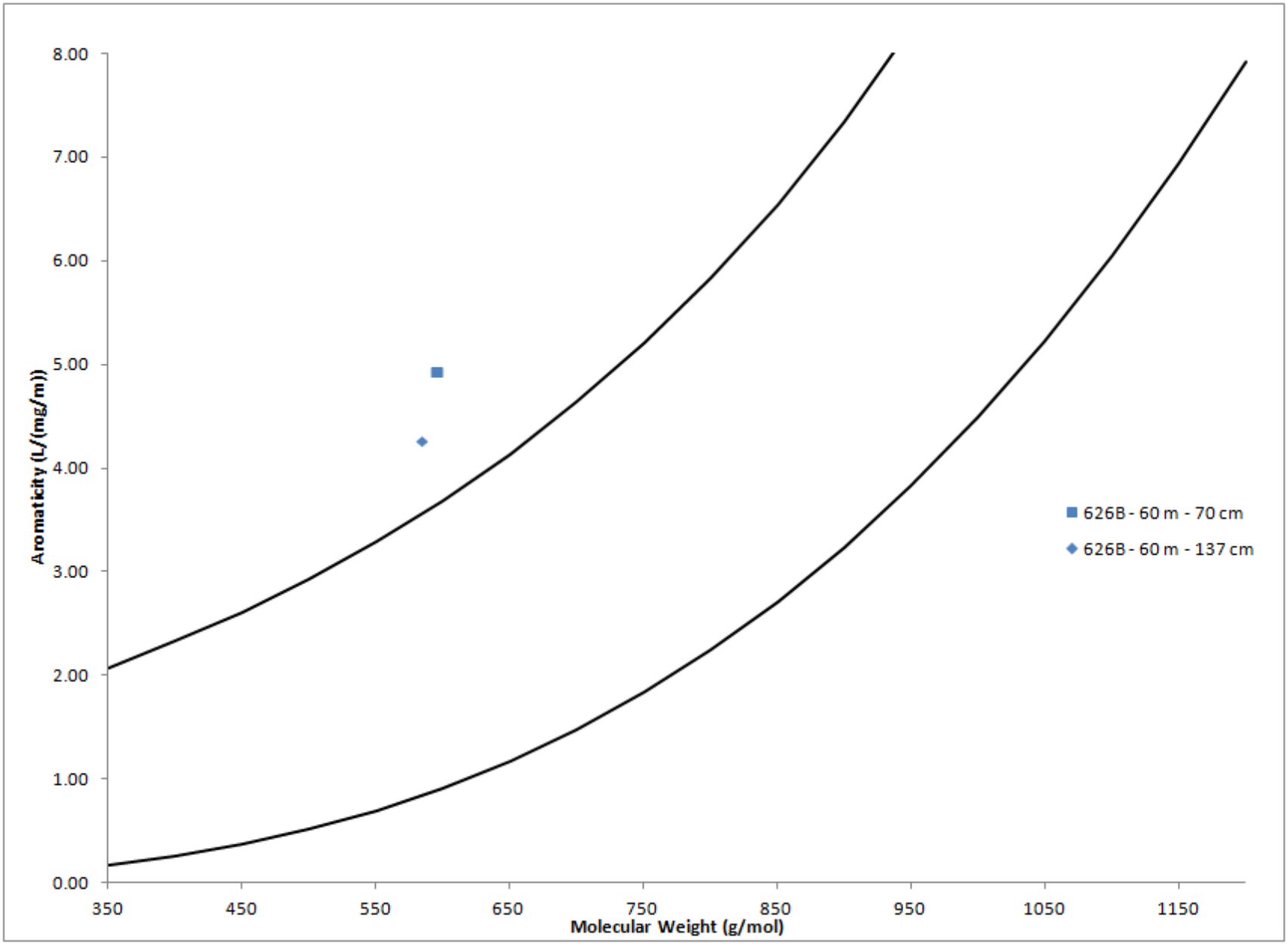
8.00
7.00
6.00
5.00
4.00
3.00
2.00
1.00
0.00
Aromaticity (L/(mg/m))
350
450
550
650
750
850
950
1050
1150
Molecular Weight (g/mol)
626B - 60 m - 70 cm
626B - 60 m - 137 cm

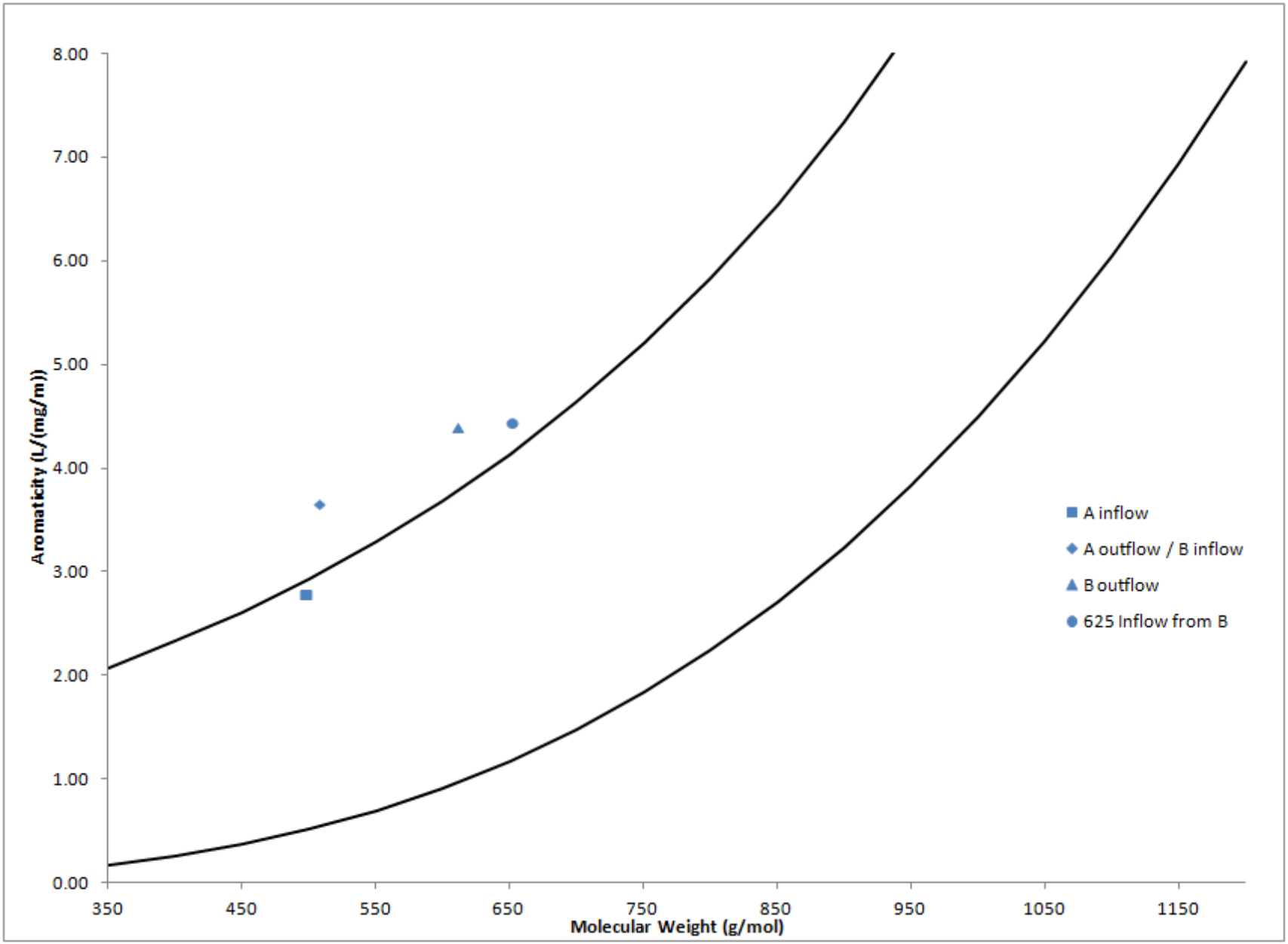
8.00
7.00
6.00
5.00
4.00
3.00
2.00
1.00
0.00
Aromaticity (L/(mg/m))
350
450
550
650
750
850
950
1050
1150
Molecular Weight (g/mol)
A inflow
A outflow / B inflow
B outflow
625 Inflow from B

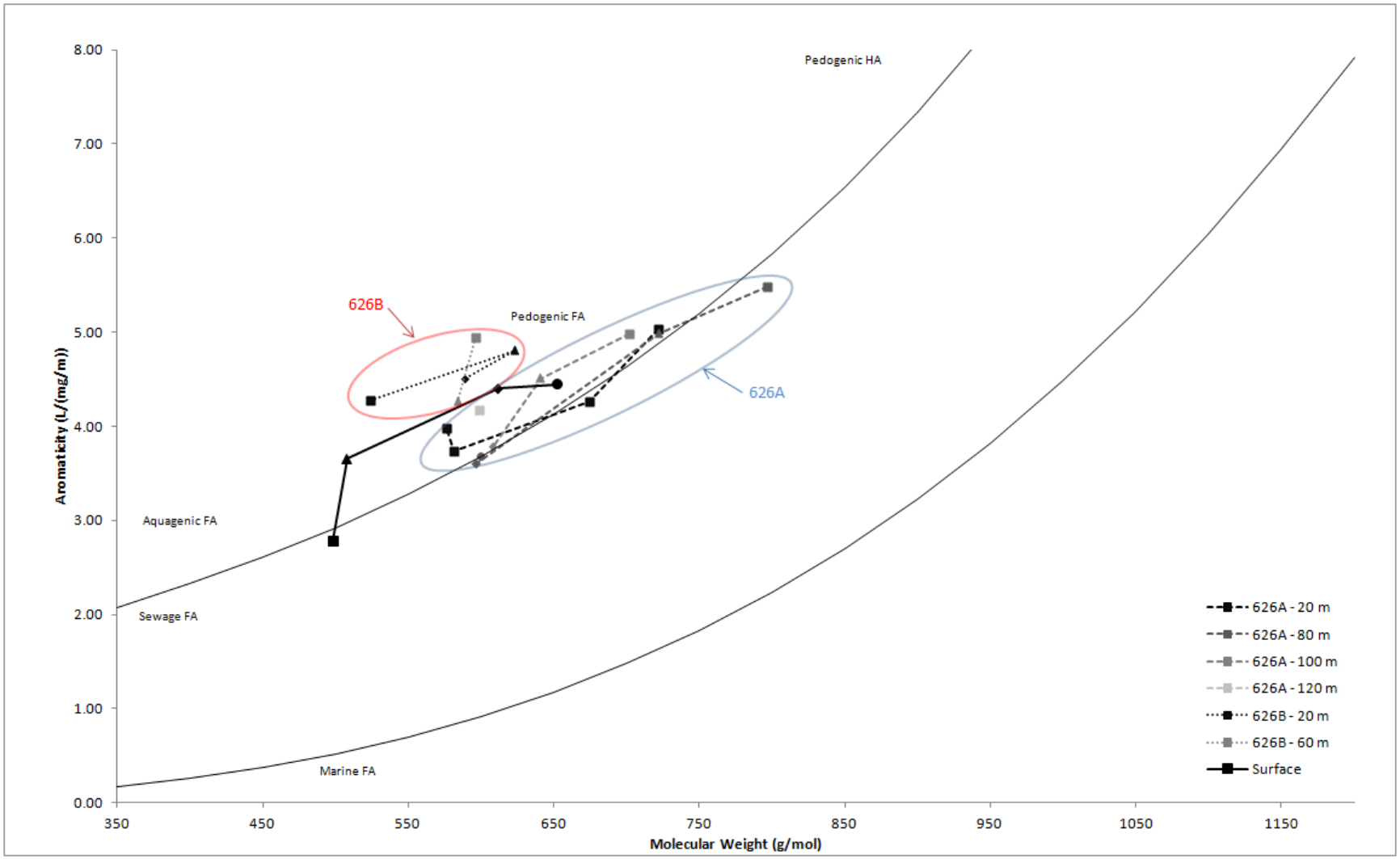
Pedogenic HA
626B
Pedogenic FA
626A
Aquagenic FA
Sewage FA
Marine FA
Aromaticity (L/(mg/m))
Molecular Weight (g/mol)
8.00
7.00
6.00
5.00
4.00
3.00
2.00
1.00
0.00
350
450
550
650
750
850
950
1050
1150
626A - 20 m
626A - 80 m
626A - 100 m
626A - 120 m
626B - 20 m
626B - 60 m
Surface

APPENDIX

Site	DIC (mg C/L)	CH_4 (umol/L)	DOC (mg C/L)
A20 - 70	57.6	100.3	82.55
A20 - 170	64.3	524.3	44.46
A20 - 270	56.0	526.5	33.69
A20 - 370	62.4	690.2	20.31
A80 - 50			85.40
A80 - 150	44.1	466.8	55.80
A80 - 250	53.4	582.3	28.81
A80 - 385	48.1	457.3	33.72
A100 - 50	26.7	75.8	86.14
A100 - 150	49.7	403.7	59.23
A100 - 250	46.1	433.3	33.31
A120 - 90	47.6	86.2	24.28
B20 - 60	33.9	90.4	37.13
B20 - 120	64.3	160.3	65.04
B20 - 241	59.3	489.1	17.98
B60 - 70	57.8	282.9	55.63
B60 - 137	69.8	363.0	48.30
A inflow	2.1	0.6	5.70
A outflow / B inflow	2.8	3.2	7.27
B outflow	2.8	3.5	7.33
625 Inflow from B	2.3	0.2	7.23
Diversion Inflow	1.7	0.3	6.29
625 Inflow from Diversion	5.6	0.1	22.07

Sample Name	δ^{13}C-DIC (permil)	δ^{13}C-CH_4 (permil)
626A Inflow	- 12.04	N.D.
626A Outflow/626B Inflow	- 14.48	- 57.73
626B Ouflow	- 13.49	- 59.30
625 Inflow from 626B	- 15.83	N.D.
Diversion Inflow	- 15.04	N.D.
625 Inflow from Diversion	- 23.66	N.D.
626B T20m-60cm	- 6.20	- 57.15
626B T20m-120cm	- 4.08	- 68.88
626B T20m-241cm	- 4.33	- 73.27
626B T60m-70cm	- 4.23	- 69.88
626B T60m-137cm	- 0.90	- 63.46
626A T20m-170cm	- 4.76	- 66.38
626A T20m-270cm	- 3.68	- 67.40
626A T20m-370cm	- 2.30	- 67.38
626A T80m-150cm	+ 3.74	- 67.44
626A T80m-250cm	+ 2.91	- 62.87
626A T80m-385cm	+ 2.13	- 68.47
626A T100m-50cm	- 4.69	- 66.74
626A T100m-150cm	+ 1.07	- 62.53
626A T100m-250cm	+ 3.41	- 68.47
626A T120m-90cm	- 5.22	- 64.34

#	Sample	Lab#	Result	Repeat	3H	Result	± 1σ	Result	± 1σ	AZD	
			VSMOW								
1	626A T80 - 50	264638			X	7.4	8.0			AZD	*50ml container
2	626A T80 - 150	264639			X	7.1	8.0				500ml bottle
3	626A T80 - 250	264640			X	<6.0	8.0				500ml bottle
4	626A T80 - 385	264641			X	<6.0	8.0				500ml bottle
5	626B T20 - 60	264642			X	<6.0	8.0			AZD	*50ml container
6	626B T20 - 120	264643			X	<6.0	8.0				500ml bottle
7	626B T20 - 241	264644			X	<6.0	8.0				500ml bottle

*Acidified w HCl

DIRECT ANALYSIS RESULTS

2 AZD (Azeotropic Distillations)

Tritium is reported in Tritium Units.

1TU = 3.221 Picocurries/L per IAEA, 2000 Report.

1TU = 0.11919 Becquerels/L per IAEA, 2000 Report.

ENRICHED ANALYSIS RESULTS

#	Sample	Lab#	Result	Repeat	E3H	Result	± 1σ	Repeat	± 2σ
			VSMOW						
1	626A T80 - 150	275798			X	8.9	0.8		1.6
2	626A T80 - 250	275799			X	4.7	0.5		1
3	626A T80 - 385	275800			X	1.9	0.4		0.8
4	626B T20 - 120	275801			X	10.0	0.9		1.8
5	626B T20 - 241	275802			X	8.1	0.8		1.6

#	Sample	Lab#	Result	Repeat	E3H	Result	± 1σ	
			VSMOW					
1	626A T80 - 150	275798			X	28.7	2.6	Pq/L
2	626A T80 - 250	275799			X	15.1	1.6	
3	626A T80 - 385	275800			X	6.1	1.3	
4	626B T20 - 120	275801			X	32.2	2.9	
5	626B T20 - 241	275802			X	26.1	2.6	

#	Sample	Lab#	Result	Repeat	E3H	Result	± 1σ	
			VSMOW					
1	626A T80 - 150	275798			X	1.1	0.10	Bq/L
2	626A T80 - 250	275799			X	0.6	0.06	
3	626A T80 - 385	275800			X	0.2	0.05	
4	626B T20 - 120	275801			X	1.2	0.11	
5	626B T20 - 241	275802			X	1.0	0.10	

		Sample ID	DOC		Hydrophobic		Hydrophilic		Biopolymers	
			ppb-C	%	ppb-C	%	ppb-C	%	ppb-C	%
1552	A20 - 70	ELA MA - 1	82547	100%	7513	9.10%	75034	90.90%	5066	6.14%
1553	A20 - 170	ELA MA - 2	44460	100%	4329	9.74%	40131	90.26%	2633	5.92%
1554	A20 - 270	ELA MA - 3	33687	100%	3023	8.97%	30664	91.03%	4066	12.07%
1555	A20 - 370	ELA MA - 4	20308	100%	2051	10.10%	18257	89.90%	1537	7.57%
1556	A80 - 50	ELA MA - 5	85400	100%	7209	8.44%	78191	91.56%	3779	4.43%
1557	A80 - 150	ELA MA - 6	55800	100%	4895	8.77%	50905	91.23%	2077	3.72%
1558	A80 - 250	ELA MA - 7	28812	100%	2603	9.04%	26209	90.96%	3328	11.55%
1559	A80 - 385	ELA MA - 8	33720	100%	3944	11.70%	29776	88.30%	2523	7.48%
1560	A100 - 50	ELA MA - 9	86135	100%	9735	11.30%	76400	88.70%	4124	4.79%
1561	A100 - 150	ELA MA - 10	59228	100%	5124	8.65%	54104	91.35%	2726	4.60%
1562	A100 - 250	ELA MA - 11	33309	100%	3663	11.00%	29646	89.00%	2601	7.81%
1563	A120 - 90	ELA MA - 12	24282	100%	3314	13.65%	20968	86.35%	1886	7.77%
1564	B20 - 60	ELA MA - 13	37130	100%	3958	10.66%	33172	89.34%	1618	4.36%
1565	B20 - 120	ELA MA - 14	65040	100%	10142	15.59%	54898	84.41%	2878	4.42%
1566	B20 - 241	ELA MA - 15	17980	100%	2377	13.22%	15603	86.78%	605	3.37%
1567	B60 - 70	ELA MA - 16	55627	100%	7856	14.12%	47771	85.88%	3245	5.83%
1568	B60 - 137	ELA MA - 17	48300	100%	6126	12.68%	42174	87.32%	3588	7.43%
1569	A inflow	ELA MA - 18	5700	100%	803	14.09%	4897	85.91%	722	12.66%
1570	A outflow / B inflow	ELA MA - 19	7270	100%	614	8.45%	6656	91.55%	977	13.44%
1571	B outflow	ELA MA - 20	7332	100%	834	11.38%	6498	88.62%	796	10.85%
1572	625 Inflow from B	ELA MA - 21	7232	100%	527	7.29%	6705	92.71%	674	9.32%
1573	Diversion Inflow	ELA MA - 22	6286	100%	500	7.95%	5786	92.05%	604	9.61%
1574	625 Inflow from Diversion	ELA MA - 23	22065	100%	809	3.67%	21256	96.33%	909	4.12%
1551=blank										

Humic Substances		Aromaticity	Molecular Weight	Building Blocks		LMW Neutrals		LMW Acids		Inorg. Colloids	SUVA
ppb-C	%	L/(mg*m)	g/mol	ppb-C	%	ppb-C	%	ppb-C	%		
33586	40.69%	5.03	722	6851	8.30%	25121	30.43%	4410	5.34%	3.82	2.93
23304	52.42%	4.26	674	3451	7.76%	10743	24.16%	n.q.	--	22.76	3.73
11981	35.56%	3.74	581	3114	9.24%	10464	31.06%	1040	3.09%	47.04	3.65
6017	29.63%	3.98	576	2269	11.17%	8335	41.04%	100	0.49%	45.01	4.12
34579	40.49%	5.48	797	3975	4.65%	35857	41.99%	n.q.	--	4.35	2.92
31420	56.31%	4.98	722	4295	7.70%	13088	23.45%	25	0.04%	2.82	3.80
13932	48.36%	3.60	597	2675	9.29%	6272	21.77%	n.q.	--	46.44	4.62
8724	25.87%	3.68	600	2945	8.74%	15582	46.21%	n.q.	--	53.37	3.25
27736	32.20%	4.98	702	3686	4.28%	40858	47.43%	n.q.	--	2.00	2.24
23259	39.27%	4.51	641	3387	5.72%	24735	41.76%	n.q.	--	8.18	2.81
13716	41.18%	3.78	608	2497	7.50%	10833	32.52%	n.q.	--	4.59	2.65
3576	14.73%	4.18	599	1752	7.22%	13406	55.21%	347	1.43%	28.95	2.40
10975	29.56%	4.28	524	1128	3.04%	19441	52.36%	11	0.03%	7.56	2.13
7727	11.88%	4.81	623	2521	3.88%	41771	64.22%	n.q.	--	25.20	1.23
3822	21.26%	4.50	589	1808	10.06%	9294	51.69%	73	0.41%	13.38	2.19
16219	29.16%	4.94	596	2416	4.34%	25889	46.54%	1	0.00%	27.76	2.67
9137	18.92%	4.27	584	2772	5.74%	25964	53.76%	713	1.48%	47.43	2.34
2561	44.92%	2.79	498	1120	19.65%	464	8.15%	30	0.53%	0.15	2.36
3662	50.37%	3.66	508	1123	15.45%	864	11.88%	30	0.41%	1.18	2.94
3507	47.83%	4.40	612	1461	19.93%	672	9.16%	62	0.85%	0.74	3.29
3729	51.56%	4.45	652	1536	21.23%	708	9.79%	58	0.80%	1.18	3.49
2728	43.40%	3.76	592	1667	26.52%	729	11.59%	58	0.93%	0.21	2.80
16982	76.96%	5.71	756	1850	8.38%	1466	6.64%	49	0.22%	1.21	5.87

UNIVERSITÉ LAVAL
Laboratoire de Radiochronologie
Radiochronology Laboratory
Centre d'études nordiques
Québec, QC Canada

KECK CARBON CYCLE AMS FACILITY
Earth System Science Dept.
UNIVERSITY OF CALIFORNIA, IRVINE, CA, USA

^{14}C Results

Barry Warner, University Of Waterloo February 6, 2012

University of California #	Université Laval #	Customer ID (sample type)	Pre-Treatments	Fraction modern	±	D^{14}C (‰)	±	^{14}C age (BP)	±
UCIAMS-103970	**ULA-3031**	B20-125MA (peat)	HCl-NaOH-HCl	0.3719	0.0009	-628.1	0.9	**7945**	**20**
UCIAMS-103971	**ULA-3032**	B20-225MA (peat)	HCl-NaOH-HCl	0.3011	0.0009	-698.9	0.9	**9640**	**25**
UCIAMS-103972	**ULA-3033**	A80-110MA (peat)	HCl-NaOH-HCl	0.5419	0.0010	-458.1	1.0	**4920**	**15**
UCIAMS-103973	**ULA-3034**	A80-260MA (peat)	HCl-NaOH-HCl	0.4056	0.0010	-594.4	1.0	**7250**	**20**
UCIAMS-103974	**ULA-3035**	A80-370MA (peat)	HCl-NaOH-HCl	0.2971	0.0009	-702.9	0.9	**9750**	**25**
UCIAMS-108357	**ULA-3231**	A80-45MA (peat)	HCl-NaOH-HCl	0.9928	0.0020	-7.3	2.0	**60**	**20**

Radiocarbon concentrations are given as fractions of the modern standard, D^{14}C, and conventional radiocarbon age, following the conventions of Stuiver and Polach (Radiocarbon, v. 19, p.355, 1977).

Sample preparation backgrounds have been subtracted, based on measurements of ^{14}C-free wood.

All results have been corrected for isotopic fractionation according to the conventions of Stuiver and Polach (1977), with d^{13}C values measured on prepared graphite using the AMS spectrometer. These can differ from d^{13}C of the original material, if fractionation ocurred during sample graphitization or the AMS measurement, and are not shown.

Wetland A	N 49˚ +	W -93˚ +				**Wetland B**	N 49˚ +	W -93˚ +			
Transect				45.324	48.068	Transect			Vegetation Plots		
0 m	45.365	48.099		45.323	48.056	0 m	45.469	48.049	1	45.467	48.030
20 m	45.364	48.085		45.306	48.054	20 m	45.467	48.032	3	45.469	48.048
40 m	45.363	48.072		45.296	48.055	40 m	45.465	48.020	5	45.486	48.040
60 m	45.361	48.056		45.279	48.046	60 m	45.463	47.996	7	45.498	48.022
80 m	45.359	48.039		45.273	48.037	80 m	45.460	47.987	9	45.506	48.023
100 m	45.357	48.019				100 m	45.460	47.970	11	45.519	48.002
120 m	45.358	47.997	Vegetation Plots			120 m	45.461	47.955	13	45.518	48.002
140 m	45.358	47.985	51	45.406	47.994	127 m	45.462	47.949	15	45.510	47.997
150 m	45.356	47.981	53	45.374	48.010				17	45.516	47.995
			55	45.384	48.031	Perimeter			19	45.494	47.999
Perimeter			57	45.385	48.074	Inlet	45.419	48.002	21	45.489	48.003
	45.388	48.037	59	45.394	47.989		45.425	48.009	23	45.472	48.014
outflow	45.412	48.008	61	45.385	47.990		45.454	48.030	25	45.465	48.020
pond edge	45.402	48.005	63	45.376	47.976		45.456	48.049	27	45.454	48.027
	45.347	47.985	65	45.357	47.987		45.506	48.023	29	45.447	48.005
	45.335	47.979	67	45.359	48.005	Outflow	45.527	47.994	31	45.472	47.989
	45.334	48.015	69	45.362	48.020	Pond	45.519	48.002	33	45.491	47.988
	45.323	48.025	71	45.365	48.047	Pond	45.510	47.997	35	45.476	47.964
	45.308	48.016	73	45.387	48.077	Pond	45.516	47.995	37	45.437	47.996
	45.294	48.013	75	45.383	48.097		45.486	47.987	39	45.432	48.004
	45.283	48.018	77	45.336	48.074		45.481	47.970	41	45.419	48.002
inflow	45.275	48.013	79	45.337	48.054		45.474	47.944	43	45.453	47.962
	45.277	48.021	81	45.315	48.049		45.441	47.990	45	45.464	47.964
	45.402	47.995	83	45.291	48.031		45.430	47.989	47	45.459	48.001
	45.394	47.977	85	45.332	48.032		45.452	47.961	49	45.433	48.024
	45.385	47.976	87	45.344	48.023		45.428	48.028			
	45.376	47.976	89	45.348	47.995						
	45.388	48.049	91	45.352	48.036						
	45.391	48.067	93	45.346	48.052						
	45.393	48.105	95	45.356	48.074						
	45.376	48.106	97	45.320	48.040						
	45.340	48.093	99	45.275	48.022						

Sample #	Wgt. Empty Crucible	Wgt. Crucible + Fresh Sample	Wgt. After 105°C	Wgt. After 550°C	Wgt. After 1000°C	Bulk Density (g/cm^3)	Dry Weight (Dry/Fresh)	Organic Carbon LOI	Inorganic Carbon LOI	% Moisture	Fresh Weight	Dry Weight	Ash Weight 550°C	Ash Weight 1000°C
A80 - 400	17.421	18.756	18.488	18.484	18.473	1.067	0.799250936	0.37%	1.03%	20.075	1.335	1.067	1.063	1.052
A80 - 395	16.320	17.274	16.972	16.966	16.957	0.652	0.683438155	0.92%	1.38%	31.656	0.954	0.652	0.646	0.637
A80 - 390	16.426	17.655	17.187	17.175	17.166	0.761	0.619202604	1.58%	1.18%	38.080	1.229	0.761	0.749	0.740
A80 - 385	16.804	17.906	17.473	17.463	17.456	0.669	0.60707804	1.49%	1.05%	39.292	1.102	0.669	0.659	0.652
A80 - 380	17.170	18.194	17.643	17.622	17.614	0.473	0.461914063	4.44%	1.69%	53.809	1.024	0.473	0.452	0.444
A80 - 375	14.705	15.583	14.950	14.924	14.917	0.245	0.27904328	10.61%	2.86%	72.096	0.878	0.245	0.219	0.212
A80 - 370	15.669	16.504	15.870	15.839	15.833	0.201	0.240718563	15.42%	2.99%	75.928	0.835	0.201	0.170	0.164
A80 - 365	18.838	19.640	18.949	18.916	18.912	0.111	0.13840399	29.73%	3.60%	86.160	0.802	0.111	0.078	0.074
A80 - 360	16.762	17.616	16.921	16.885	16.880	0.159	0.18618267	22.64%	3.14%	81.382	0.854	0.159	0.123	0.118
A80 - 355	17.658	18.453	17.769	17.737	17.729	0.111	0.139622642	28.83%	7.21%	86.038	0.795	0.111	0.079	0.071
A80 - 350	16.873	17.662	16.976	16.936	16.933	0.103	0.130544994	38.83%	2.91%	86.946	0.789	0.103	0.063	0.060
A80 - 345	16.413	17.135	16.502	16.469	16.465	0.089	0.123268698	37.08%	4.49%	87.673	0.722	0.089	0.056	0.052
A80 - 340	16.482	17.240	16.589	16.554	16.548	0.107	0.14116095	32.71%	5.61%	85.884	0.758	0.107	0.072	0.066
A80 - 335	15.500	16.231	15.596	15.561	15.557	0.096	0.131326949	36.46%	4.17%	86.867	0.731	0.096	0.061	0.057
A80 - 330	15.260	15.995	15.341	15.306	15.301	0.081	0.110204082	43.21%	6.17%	88.980	0.735	0.081	0.046	0.041
A80 - 325	15.794	16.564	15.882	15.843	15.838	0.088	0.114285714	44.32%	5.68%	88.571	0.770	0.088	0.049	0.044
A80 - 320	15.762	16.495	15.845	15.806	15.803	0.083	0.113233288	46.99%	3.61%	88.677	0.733	0.083	0.044	0.041
A80 - 315	15.109	15.819	15.177	15.139	15.136	0.068	0.095774648	55.88%	4.41%	90.423	0.710	0.068	0.030	0.027
A80 - 310	16.543	17.252	16.610	16.570	16.564	0.067	0.094499295	59.70%	8.96%	90.550	0.709	0.067	0.027	0.021
A80 - 305	16.340	17.022	16.404	16.366	16.364	0.064	0.093841642	59.38%	3.12%	90.616	0.682	0.064	0.026	0.024
A80 - 300	18.518	19.222	18.589	18.548	18.544	0.071	0.100852273	57.75%	5.63%	89.915	0.704	0.071	0.030	0.026
A80 - 295	17.676	18.325	17.738	17.706	17.702	0.062	0.095531587	51.61%	6.45%	90.447	0.649	0.062	0.030	0.026
A80 - 290	17.004	17.659	17.054	17.020	17.013	0.050	0.076335878	68.00%	14.00%	92.366	0.655	0.050	0.016	0.009
A80 - 285	12.406	13.110	12.473	12.428	12.427	0.067	0.095170455	67.16%	1.49%	90.483	0.704	0.067	0.022	0.021
A80 - 280	11.665	12.336	11.728	11.685	11.684	0.063	0.093889717	68.25%	1.59%	90.611	0.671	0.063	0.020	0.019
A80 - 275	12.276	12.949	12.341	12.299	12.296	0.065	0.096582467	64.62%	4.62%	90.342	0.673	0.065	0.023	0.020
A80 - 270	11.205	11.920	11.272	11.225	11.221	0.067	0.093706294	70.15%	5.97%	90.629	0.715	0.067	0.020	0.016
A80 - 265	12.106	12.763	12.166	12.119	12.118	0.060	0.091324201	78.33%	1.67%	90.868	0.657	0.060	0.013	0.012
A80 - 260	12.697	13.423	12.789	12.721	12.718	0.092	0.126721763	73.91%	3.26%	87.328	0.726	0.092	0.024	0.021
A80 - 255	10.948	11.682	11.040	10.970	10.969	0.092	0.125340599	76.09%	1.09%	87.466	0.734	0.092	0.022	0.021
A80 - 250	12.272	12.904	12.345	12.283	12.280	0.073	0.115506329	84.93%	4.11%	88.449	0.632	0.073	0.011	0.008

A80 - 245	11.164	11.938	11.239	11.175	11.174	0.075	0.096899225	85.33%	1.33%	90.310	0.774	0.075	0.011	0.010
A80 - 240	11.727	12.537	11.815	11.741	11.738	0.088	0.108641975	84.09%	3.41%	89.136	0.810	0.088	0.014	0.011
A80 - 235	10.527	11.173	10.602	10.536	10.535	0.075	0.116099071	88.00%	1.33%	88.390	0.646	0.075	0.009	0.008
A80 - 230	11.577	12.343	11.665	11.584	11.583	0.088	0.114882507	92.05%	1.14%	88.512	0.766	0.088	0.007	0.006
A80 - 225	11.653	12.308	11.736	11.663	11.662	0.083	0.126717557	87.95%	1.20%	87.328	0.655	0.083	0.010	0.009
A80 - 220	11.831	12.464	11.902	11.836	11.834	0.071	0.112164297	92.96%	2.82%	88.784	0.633	0.071	0.005	0.003
A80 - 215	10.808	11.454	10.881	10.812	10.811	0.073	0.113003096	94.52%	1.37%	88.700	0.646	0.073	0.004	0.003
A80 - 210	12.693	13.598	12.832	12.700	12.698	0.139	0.15359116	94.96%	1.44%	84.641	0.905	0.139	0.007	0.005
A80 - 205	11.777	12.580	11.874	11.783	11.782	0.097	0.120797011	93.81%	1.03%	87.920	0.803	0.097	0.006	0.005
A80 - 200	12.407	13.034	12.482	12.410	12.409	0.075	0.119617225	96.00%	1.33%	88.038	0.627	0.075	0.003	0.002
A80 - 195	12.347	13.055	12.427	12.349	12.348	0.080	0.11299435	97.50%	1.25%	88.701	0.708	0.080	0.002	0.001
A80 - 190	12.923	13.619	13.013	12.930	12.929	0.090	0.129310345	92.22%	1.11%	87.069	0.696	0.090	0.007	0.006
A80 - 185	11.538	12.040	11.602	11.540	11.539	0.064	0.12749004	96.88%	1.56%	87.251	0.502	0.064	0.002	0.001
A80 - 180	13.463	14.314	13.580	13.471	13.470	0.117	0.137485311	93.16%	0.85%	86.251	0.851	0.117	0.008	0.007
A80 - 175	12.470	13.194	12.564	12.475	12.474	0.094	0.129834254	94.68%	1.06%	87.017	0.724	0.094	0.005	0.004
A80 - 170	17.415	17.891	17.477	17.423	17.418	0.062	0.130252101	87.10%	8.06%	86.975	0.476	0.062	0.008	0.003
A80 - 165	16.313	16.880	16.394	16.323	16.318	0.081	0.142857143	87.65%	6.17%	85.714	0.567	0.081	0.010	0.005
A80 - 160	16.424	17.403	16.569	16.434	16.431	0.145	0.148110317	93.10%	2.07%	85.189	0.979	0.145	0.010	0.007
A80 - 155	16.800	17.663	16.939	16.811	16.810	0.139	0.161066049	92.09%	0.72%	83.893	0.863	0.139	0.011	0.010
A80 - 150	17.165	18.009	17.298	17.179	17.174	0.133	0.157582938	89.47%	3.76%	84.242	0.844	0.133	0.014	0.009
A80 - 145	14.702	15.180	14.775	14.709	14.706	0.073	0.152719665	90.41%	4.11%	84.728	0.478	0.073	0.007	0.004
A80 - 140	15.665	16.259	15.756	15.674	15.670	0.091	0.153198653	90.11%	4.40%	84.680	0.594	0.091	0.009	0.005
A80 - 135	18.834	19.467	18.915	18.842	18.840	0.081	0.127962085	90.12%	2.47%	87.204	0.633	0.081	0.008	0.006
A80 - 130	16.755	17.306	16.818	16.762	16.759	0.063	0.114337568	88.89%	4.76%	88.566	0.551	0.063	0.007	0.004
A80 - 125	17.651	18.281	17.749	17.663	17.661	0.098	0.155555556	87.76%	2.04%	84.444	0.630	0.098	0.012	0.010
A80 - 120	16.867	17.397	16.948	16.873	16.872	0.081	0.152830189	92.59%	1.23%	84.717	0.530	0.081	0.006	0.005
A80 - 115	16.406	16.983	16.498	16.424	16.422	0.092	0.159445407	80.43%	2.17%	84.055	0.577	0.092	0.018	0.016
A80 - 110	16.474	17.056	16.569	16.489	16.488	0.095	0.163230241	84.21%	1.05%	83.677	0.582	0.095	0.015	0.014
A80 - 105	15.492	16.195	15.609	15.505	15.503	0.117	0.166429587	88.89%	1.71%	83.357	0.703	0.117	0.013	0.011
A80 - 100	15.250	16.121	15.399	15.265	15.263	0.149	0.171067738	89.93%	1.34%	82.893	0.871	0.149	0.015	0.013
A80 - 95	15.787	16.421	15.893	15.798	15.796	0.106	0.167192429	89.62%	1.89%	83.281	0.634	0.106	0.011	0.009
A80 - 90	15.759	16.466	15.867	15.770	15.769	0.108	0.152758133	89.81%	0.93%	84.724	0.707	0.108	0.011	0.010
A80 - 85	15.105	15.780	15.209	15.113	15.112	0.104	0.154074074	92.31%	0.96%	84.593	0.675	0.104	0.008	0.007
A80 - 80	16.534	17.213	16.658	16.544	16.542	0.124	0.182621502	91.94%	1.61%	81.738	0.679	0.124	0.010	0.008

A80 - 75	16.336	17.026	16.458	16.353	16.352	0.122	0.176811594	86.07%	0.82%	82.319	0.690	0.122	0.017	0.016
A80 - 70	18.510	19.128	18.626	18.530	18.529	0.116	0.187702265	82.76%	0.86%	81.230	0.618	0.116	0.020	0.019
A80 - 65	17.673	18.328	17.776	17.681	17.680	0.103	0.157251908	92.23%	0.97%	84.275	0.655	0.103	0.008	0.007
A80 - 60	16.995	17.734	17.117	17.006	17.005	0.122	0.165087957	90.98%	0.82%	83.491	0.739	0.122	0.011	0.010
A80 - 55	12.403	12.952	12.506	12.409	12.408	0.103	0.187613843	94.17%	0.97%	81.239	0.549	0.103	0.006	0.005
A80 - 50	11.663	12.352	11.786	11.673	11.672	0.123	0.178519594	91.87%	0.81%	82.148	0.689	0.123	0.010	0.009
A80 - 45	17.650	18.127	17.702	17.656	17.656	0.052	0.109014675	88.46%	0.00%	89.099	0.477	0.052	0.006	0.006
A80 - 40	16.754	17.201	16.806	16.761	16.761	0.052	0.116331096	86.54%	0.00%	88.367	0.447	0.052	0.007	0.007
A80 - 35	18.834	19.453	18.899	18.839	18.839	0.065	0.105008078	92.31%	0.00%	89.499	0.619	0.065	0.005	0.005
A80 - 30	15.664	16.408	15.729	15.670	15.669	0.065	0.087365591	90.77%	1.54%	91.263	0.744	0.065	0.006	0.005
A80 - 25	14.704	15.187	14.759	14.704	14.704	0.055	0.113871636	100.00%	0.00%	88.613	0.483	0.055	0.000	0.000
A80 - 20	17.167	17.656	17.212	17.167	17.167	0.045	0.09202454	100.00%	0.00%	90.798	0.489	0.045	0.000	0.000
A80 - 15	16.804	17.456	16.844	16.804	16.804	0.040	0.061349693	100.00%	0.00%	93.865	0.652	0.040	0.000	0.000
A80 - 10	16.424	17.162	16.495	16.425	16.425	0.071	0.096205962	98.59%	0.00%	90.379	0.738	0.071	0.001	0.001
A80 - 5	16.314	16.822	16.357	16.315	16.315	0.043	0.084645669	97.67%	0.00%	91.535	0.508	0.043	0.001	0.001
A80 - 0	17.416	18.246	17.491	17.419	17.418	0.075	0.090361446	96.00%	1.33%	90.964	0.830	0.075	0.003	0.002
A120 - 95	12.275	12.955	12.390	12.321	12.320	0.115	0.169117647	60.00%	0.87%	83.088	0.680	0.115	0.046	0.045
A120 - 90	11.203	11.914	11.324	11.240	11.239	0.121	0.170182841	69.42%	0.83%	82.982	0.711	0.121	0.037	0.036
A120 - 85	12.103	12.803	12.182	12.125	12.124	0.079	0.112857143	72.15%	1.27%	88.714	0.700	0.079	0.022	0.021
A120 - 80	12.694	13.405	12.782	12.712	12.711	0.088	0.123769339	79.55%	1.14%	87.623	0.711	0.088	0.018	0.017
A120 - 75	10.946	11.747	11.102	11.007	11.006	0.156	0.194756554	60.90%	0.64%	80.524	0.801	0.156	0.061	0.060
A120 - 70	12.268	12.823	12.360	12.294	12.293	0.092	0.165765766	71.74%	1.09%	83.423	0.555	0.092	0.026	0.025
A120 - 65	11.161	11.823	11.263	11.186	11.185	0.102	0.15407855	75.49%	0.98%	84.592	0.662	0.102	0.025	0.024
A120 - 60	11.725	12.318	11.832	11.756	11.755	0.107	0.180438449	71.03%	0.93%	81.956	0.593	0.107	0.031	0.030
A120 - 55	10.526	11.215	10.657	10.563	10.562	0.131	0.190130624	71.76%	0.76%	80.987	0.689	0.131	0.037	0.036
A120 - 50	11.575	12.381	11.727	11.619	11.618	0.152	0.188585608	71.05%	0.66%	81.141	0.806	0.152	0.044	0.043
A120 - 45	16.332	17.014	16.422	16.365	16.359	0.090	0.131964809	63.33%	6.67%	86.804	0.682	0.090	0.033	0.027
A120 - 40	16.531	17.093	16.616	16.559	16.556	0.085	0.151245552	67.06%	3.53%	84.875	0.562	0.085	0.028	0.025
A120 - 35	15.102	15.546	15.156	15.120	15.117	0.054	0.121621622	66.67%	5.56%	87.838	0.444	0.054	0.018	0.015
A120 - 30	15.758	16.275	15.853	15.792	15.790	0.095	0.183752418	64.21%	2.11%	81.625	0.517	0.095	0.034	0.032
A120 - 25	15.787	16.355	15.855	15.815	15.813	0.068	0.11971831	58.82%	2.94%	88.028	0.568	0.068	0.028	0.026
A120 - 20	15.250	15.782	15.328	15.283	15.279	0.078	0.146616541	57.69%	5.13%	85.338	0.532	0.078	0.033	0.029

A20 - 400	11.653	12.717	12.466	12.458	12.454	0.813	0.764097744	0.98%	0.49%	23.590	1.064	0.813	0.805	0.801
A20 - 395	11.829	12.868	12.585	12.575	12.573	0.756	0.727622714	1.32%	0.26%	27.238	1.039	0.756	0.746	0.744
A20 - 390	10.807	11.924	11.570	11.558	11.555	0.763	0.683079678	1.57%	0.39%	31.692	1.117	0.763	0.751	0.748
A20 - 385	12.691	13.603	13.305	13.294	13.293	0.614	0.673245614	1.79%	0.16%	32.675	0.912	0.614	0.603	0.602
A20 - 380	11.774	13.057	12.729	12.720	12.717	0.955	0.744349182	0.94%	0.31%	25.565	1.283	0.955	0.946	0.943
A20 - 375	12.404	13.737	13.386	13.375	13.373	0.982	0.736684171	1.12%	0.20%	26.332	1.333	0.982	0.971	0.969
A20 - 370	12.344	13.063	12.685	12.671	12.669	0.341	0.474269819	4.11%	0.59%	52.573	0.719	0.341	0.327	0.325
A20 - 365	12.919	13.764	13.261	13.238	13.236	0.342	0.404733728	6.73%	0.58%	59.527	0.845	0.342	0.319	0.317
A20 - 360	11.536	12.275	11.812	11.790	11.789	0.276	0.373477673	7.97%	0.36%	62.652	0.739	0.276	0.254	0.253
A20 - 355	13.461	14.205	13.669	13.640	13.639	0.208	0.279569892	13.94%	0.48%	72.043	0.744	0.208	0.179	0.178
A20 - 350	12.468	13.214	12.681	12.651	12.649	0.213	0.285522788	14.08%	0.94%	71.448	0.746	0.213	0.183	0.181
A100 - 50	11.202	11.833	11.317	11.222	11.220	0.115	0.182250396	82.61%	1.74%	81.775	0.631	0.115	0.020	0.018
A100 - 55	12.102	12.651	12.206	12.117	12.116	0.104	0.189435337	85.58%	0.96%	81.056	0.549	0.104	0.015	0.014
A100 - 60	12.694	13.240	12.788	12.706	12.704	0.094	0.172161172	87.23%	2.13%	82.784	0.546	0.094	0.012	0.010
A100 - 65	10.945	11.334	11.009	10.952	10.951	0.064	0.164524422	89.06%	1.56%	83.548	0.389	0.064	0.007	0.006
A100 - 70	12.268	12.891	12.371	12.279	12.276	0.103	0.165329053	89.32%	2.91%	83.467	0.623	0.103	0.011	0.008
A100 - 75	11.161	11.749	11.259	11.174	11.173	0.098	0.166666667	86.73%	1.02%	83.333	0.588	0.098	0.013	0.012
A100 - 80	11.726	12.269	11.815	11.734	11.733	0.089	0.163904236	91.01%	1.12%	83.610	0.543	0.089	0.008	0.007
A100 - 85	10.526	11.111	10.610	10.530	10.529	0.084	0.143589744	95.24%	1.19%	85.641	0.585	0.084	0.004	0.003
A100 - 90	11.575	12.051	11.652	11.579	11.578	0.077	0.161764706	94.81%	1.30%	83.824	0.476	0.077	0.004	0.003
A100 - 95	11.652	12.109	11.723	11.658	11.657	0.071	0.15536105	91.55%	1.41%	84.464	0.457	0.071	0.006	0.005
A100 - 100	11.831	12.531	11.925	11.841	11.839	0.094	0.134285714	89.36%	2.13%	86.571	0.700	0.094	0.010	0.008
A100 - 105	10.807	11.517	10.910	10.817	10.815	0.103	0.145070423	90.29%	1.94%	85.493	0.710	0.103	0.010	0.008
A100 - 110	12.691	13.376	12.794	12.703	12.699	0.103	0.150364964	88.35%	3.88%	84.964	0.685	0.103	0.012	0.008
A100 - 115	11.775	12.357	11.855	11.784	11.782	0.080	0.137457045	88.75%	2.50%	86.254	0.582	0.080	0.009	0.007
A100 - 120	12.406	12.927	12.480	12.417	12.414	0.074	0.142034549	85.14%	4.05%	85.797	0.521	0.074	0.011	0.008
A100 - 125	12.345	13.008	12.447	12.354	12.353	0.102	0.153846154	91.18%	0.98%	84.615	0.663	0.102	0.009	0.008
A100 - 130	12.921	13.706	13.039	12.931	12.929	0.118	0.150318471	91.53%	1.69%	84.968	0.785	0.118	0.010	0.008
A100 - 135	11.535	12.023	11.606	11.544	11.542	0.071	0.145491803	87.32%	2.82%	85.451	0.488	0.071	0.009	0.007
A100 - 140	12.466	12.860	12.513	12.471	12.469	0.047	0.11928934	89.36%	4.26%	88.071	0.394	0.047	0.005	0.003
A100 - 145	13.462	14.117	13.543	13.466	13.464	0.081	0.123664122	95.06%	2.47%	87.634	0.655	0.081	0.004	0.002
A100 - 150	16.995	17.562	17.056	17.000	16.998	0.061	0.107583774	91.80%	3.28%	89.242	0.567	0.061	0.005	0.003

A100 - 155	17.673	18.312	17.746	17.689	17.688	0.073	0.114241002	78.08%	1.37%	88.576	0.639	0.073	0.016	0.015
A100 - 160	18.511	19.116	18.574	18.527	18.526	0.063	0.104132231	74.60%	1.59%	89.587	0.605	0.063	0.016	0.015
A100 - 165	16.336	16.966	16.414	16.366	16.357	0.078	0.123809524	61.54%	11.54%	87.619	0.630	0.078	0.030	0.021
A100 - 170	16.534	17.134	16.602	16.561	16.552	0.068	0.113333333	60.29%	13.24%	88.667	0.600	0.068	0.027	0.018
A100 - 175	15.104	15.729	15.165	15.133	15.126	0.061	0.0976	52.46%	11.48%	90.240	0.625	0.061	0.029	0.022
A100 - 180	15.759	16.378	15.871	15.824	15.819	0.112	0.180936995	41.96%	4.46%	81.906	0.619	0.112	0.065	0.060
A100 - 185	15.788	16.396	15.875	15.831	15.826	0.087	0.143092105	50.57%	5.75%	85.691	0.608	0.087	0.043	0.038
A100 - 190	15.250	15.829	15.313	15.286	15.281	0.063	0.10880829	42.86%	7.94%	89.119	0.579	0.063	0.036	0.031
A100 - 195	15.493	16.100	15.557	15.530	15.526	0.064	0.105436573	42.19%	6.25%	89.456	0.607	0.064	0.037	0.033
A100 - 200	16.477	17.023	16.537	16.515	16.513	0.060	0.10989011	36.67%	3.33%	89.011	0.546	0.060	0.038	0.036
A100 - 205	16.407	17.010	16.483	16.460	16.457	0.076	0.126036484	30.26%	3.95%	87.396	0.603	0.076	0.053	0.050
A100 - 210	16.867	17.440	16.951	16.931	16.930	0.084	0.146596859	23.81%	1.19%	85.340	0.573	0.084	0.064	0.063
A100 - 215	17.651	18.234	17.722	17.702	17.700	0.071	0.121783877	28.17%	2.82%	87.822	0.583	0.071	0.051	0.049
A100 - 220	16.755	17.345	16.854	16.834	16.831	0.099	0.16779661	20.20%	3.03%	83.220	0.590	0.099	0.079	0.076
A100 - 225	18.835	19.438	18.947	18.925	18.924	0.112	0.185737977	19.64%	0.89%	81.426	0.603	0.112	0.090	0.089
A100 - 230	15.665	16.301	15.750	15.727	15.727	0.085	0.133647799	27.06%	0.00%	86.635	0.636	0.085	0.062	0.062
A100 - 235	14.701	15.429	14.829	14.801	14.798	0.128	0.175824176	21.88%	2.34%	82.418	0.728	0.128	0.100	0.097
A100 - 240	17.165	17.886	17.340	17.316	17.314	0.175	0.242718447	13.71%	1.14%	75.728	0.721	0.175	0.151	0.149
A100 - 245	16.802	17.518	16.995	16.976	16.973	0.193	0.269553073	9.84%	1.55%	73.045	0.716	0.193	0.174	0.171
A100 - 250	16.424	17.158	16.691	16.672	16.670	0.267	0.363760218	7.12%	0.75%	63.624	0.734	0.267	0.248	0.246
A100 - 255	16.314	17.303	16.943	16.935	16.931	0.629	0.635995956	1.27%	0.64%	36.400	0.989	0.629	0.621	0.617
A100 - 260	17.417	18.673	18.289	18.280	18.274	0.872	0.694267516	1.03%	0.69%	30.573	1.256	0.872	0.863	0.857
A100 - 265	12.467	13.339	13.103	13.101	13.094	0.636	0.729357798	0.31%	1.10%	27.064	0.872	0.636	0.634	0.627
A100 - 270	13.461	14.496	14.331	14.329	14.321	0.870	0.84057971	0.23%	0.92%	15.942	1.035	0.870	0.868	0.860
B60 - 50	17.416	18.063	17.598	17.504	17.502	0.182	0.2812983	51.65%	1.10%	71.870	0.647	0.182	0.088	0.086
B60 - 55	16.315	16.947	16.495	16.405	16.402	0.180	0.284810127	50.00%	1.67%	71.519	0.632	0.180	0.090	0.087
B60 - 60	16.424	17.042	16.583	16.487	16.485	0.159	0.257281553	60.38%	1.26%	74.272	0.618	0.159	0.063	0.061
B60 - 65	16.806	17.402	16.963	16.855	16.853	0.157	0.263422819	68.79%	1.27%	73.658	0.596	0.157	0.049	0.047
B60 - 70	17.169	17.743	17.279	17.197	17.192	0.110	0.191637631	74.55%	4.55%	80.836	0.574	0.110	0.028	0.023
B60 - 75	14.705	15.321	14.856	14.758	14.753	0.151	0.24512987	64.90%	3.31%	75.487	0.616	0.151	0.053	0.048
B60 - 80	15.666	16.286	15.823	15.719	15.714	0.157	0.253225806	66.24%	3.18%	74.677	0.620	0.157	0.053	0.048
B60 - 85	18.837	19.367	18.963	18.877	18.872	0.126	0.237735849	68.25%	3.97%	76.226	0.530	0.126	0.040	0.035
B60 - 90	16.756	17.270	16.876	16.791	16.788	0.120	0.233463035	70.83%	2.50%	76.654	0.514	0.120	0.035	0.032

B60 - 95	17.654	18.186	17.765	17.685	17.683	0.111	0.208646617	72.07%	1.80%	79.135	0.532	0.111	0.031	0.029
B60 - 100	16.869	17.374	16.954	16.879	16.875	0.085	0.168316832	88.24%	4.71%	83.168	0.505	0.085	0.010	0.006
B60 - 105	16.407	16.922	16.489	16.420	16.415	0.082	0.159223301	84.15%	6.10%	84.078	0.515	0.082	0.013	0.008
B60 - 110	16.475	16.948	16.549	16.489	16.486	0.074	0.156448203	81.08%	4.05%	84.355	0.473	0.074	0.014	0.011
B60 - 115	15.492	16.016	15.563	15.503	15.499	0.071	0.135496183	84.51%	5.63%	86.450	0.524	0.071	0.011	0.007
B60 - 120	15.250	15.775	15.318	15.259	15.254	0.068	0.12952381	86.76%	7.35%	87.048	0.525	0.068	0.009	0.004
B60 - 125	15.788	16.417	15.854	15.810	15.805	0.066	0.104928458	66.67%	7.58%	89.507	0.629	0.066	0.022	0.017
B60 - 130	15.765	16.324	15.838	15.807	15.801	0.073	0.13059034	42.47%	8.22%	86.941	0.559	0.073	0.042	0.036
B60 - 135	15.108	15.638	15.190	15.157	15.150	0.082	0.154716981	40.24%	8.54%	84.528	0.530	0.082	0.049	0.042
B60 - 140	16.536	17.107	16.629	16.598	16.591	0.093	0.162872154	33.33%	7.53%	83.713	0.571	0.093	0.062	0.055
B60 - 145	16.337	16.904	16.445	16.415	16.413	0.108	0.19047619	27.78%	1.85%	80.952	0.567	0.108	0.078	0.076
B60 - 150	18.514	19.096	18.621	18.592	18.589	0.107	0.183848797	27.10%	2.80%	81.615	0.582	0.107	0.078	0.075
B80 - 40	17.675	18.312	17.806	17.730	17.726	0.131	0.205651491	58.02%	3.05%	79.435	0.637	0.131	0.055	0.051
B80 - 45	16.996	17.728	17.157	17.074	17.068	0.161	0.219945355	51.55%	3.73%	78.005	0.732	0.161	0.078	0.072
B80 - 50	12.401	13.104	12.556	12.472	12.469	0.155	0.220483642	54.19%	1.94%	77.952	0.703	0.155	0.071	0.068
B80 - 55	11.662	12.273	11.787	11.712	11.710	0.125	0.204582651	60.00%	1.60%	79.542	0.611	0.125	0.050	0.048
B80 - 60	12.273	12.962	12.429	12.347	12.342	0.156	0.226415094	52.56%	3.21%	77.358	0.689	0.156	0.074	0.069
B80 - 65	11.203	11.915	11.395	11.300	11.296	0.192	0.269662921	49.48%	2.08%	73.034	0.712	0.192	0.097	0.093
B80 - 70	12.104	12.814	12.338	12.236	12.231	0.234	0.329577465	43.59%	2.14%	67.042	0.710	0.234	0.132	0.127
B80 - 75	12.695	13.329	12.880	12.778	12.772	0.185	0.291798107	55.14%	3.24%	70.820	0.634	0.185	0.083	0.077
B80 - 80	10.947	11.642	11.256	11.169	11.161	0.309	0.444604317	28.16%	2.59%	55.540	0.695	0.309	0.222	0.214
B80 - 85	12.271	13.210	12.957	12.904	12.895	0.686	0.73056443	7.73%	1.31%	26.944	0.939	0.686	0.633	0.624
B20 - 0	11.535	11.971	11.596	11.542	11.537	0.061	0.139908257	88.52%	8.20%	86.009	0.436	0.061	0.007	0.002
B20 - 5	12.919	13.721	13.039	12.930	12.927	0.120	0.149625935	90.83%	2.50%	85.037	0.802	0.120	0.011	0.008
B20 - 10	12.344	12.958	12.422	12.358	12.353	0.078	0.127035831	82.05%	6.41%	87.296	0.614	0.078	0.014	0.009
B20 - 15	12.405	12.683	12.436	12.411	12.409	0.031	0.111510791	80.65%	6.45%	88.849	0.278	0.031	0.006	0.004
B20 - 20	11.775	12.325	11.838	11.781	11.781	0.063	0.114545455	90.48%	0.00%	88.545	0.550	0.063	0.006	0.006
B20 - 25	12.691	13.253	12.781	12.707	12.702	0.090	0.160142349	82.22%	5.56%	83.986	0.562	0.090	0.016	0.011
B20 - 30	10.807	11.452	10.887	10.817	10.814	0.080	0.124031008	87.50%	3.75%	87.597	0.645	0.080	0.010	0.007
B20 - 35	11.830	12.082	11.854	11.831	11.831	0.024	0.095238095	95.83%	0.00%	90.476	0.252	0.024	0.001	0.001
B20 - 40	11.652	12.003	11.693	11.660	11.657	0.041	0.116809117	80.49%	7.32%	88.319	0.351	0.041	0.008	0.005
B20 - 45	11.574	12.002	11.624	11.583	11.580	0.050	0.11682243	82.00%	6.00%	88.318	0.428	0.050	0.009	0.006

B20 - 50	11.161	11.649	11.251	11.177	11.172	0.090	0.18442623	82.22%	5.56%	81.557	0.488	0.090	0.016	0.011
B20 - 55	11.728	12.281	11.833	11.742	11.740	0.105	0.189873418	86.67%	1.90%	81.013	0.553	0.105	0.014	0.012
B20 - 60	10.527	11.054	10.619	10.542	10.541	0.092	0.174573055	83.70%	1.09%	82.543	0.527	0.092	0.015	0.014
B20 - 65	11.577	12.214	11.696	11.606	11.604	0.119	0.186813187	75.63%	1.68%	81.319	0.637	0.119	0.029	0.027
B20 - 70	11.655	12.193	11.777	11.701	11.699	0.122	0.226765799	62.30%	1.64%	77.323	0.538	0.122	0.046	0.044
B20 - 75	11.831	12.415	11.952	11.868	11.865	0.121	0.207191781	69.42%	2.48%	79.281	0.584	0.121	0.037	0.034
B20 - 80	10.809	11.413	10.959	10.868	10.865	0.150	0.248344371	60.67%	2.00%	75.166	0.604	0.150	0.059	0.056
B20 - 85	12.693	13.191	12.808	12.735	12.733	0.115	0.230923695	63.48%	1.74%	76.908	0.498	0.115	0.042	0.040
B20 - 90	11.776	12.255	11.880	11.813	11.809	0.104	0.217118998	64.42%	3.85%	78.288	0.479	0.104	0.037	0.033
B20 - 95	12.405	12.926	12.529	12.445	12.441	0.124	0.238003839	67.74%	3.23%	76.200	0.521	0.124	0.040	0.036
B20 - 100	12.344	12.877	12.443	12.369	12.366	0.099	0.185741088	74.75%	3.03%	81.426	0.533	0.099	0.025	0.022
B20 - 105	12.920	13.412	13.015	12.942	12.939	0.095	0.193089431	76.84%	3.16%	80.691	0.492	0.095	0.022	0.019
B20 - 110	11.535	12.161	11.647	11.564	11.561	0.112	0.178913738	74.11%	2.68%	82.109	0.626	0.112	0.029	0.026
B20 - 115	13.461	14.035	13.544	13.470	13.467	0.083	0.144599303	89.16%	3.61%	85.540	0.574	0.083	0.009	0.006
B20 - 120	12.468	13.054	12.548	12.476	12.473	0.080	0.136518771	90.00%	3.75%	86.348	0.586	0.080	0.008	0.005
B20 - 125	17.417	17.954	17.492	17.424	17.423	0.075	0.139664804	90.67%	1.33%	86.034	0.537	0.075	0.007	0.006
B20 - 130	16.315	16.778	16.382	16.323	16.322	0.067	0.144708423	88.06%	1.49%	85.529	0.463	0.067	0.008	0.007
B20 - 135	16.426	16.959	16.490	16.430	16.428	0.064	0.120075047	93.75%	3.12%	87.992	0.533	0.064	0.004	0.002
B20 - 140	16.805	17.360	16.871	16.809	16.808	0.066	0.118918919	93.94%	1.52%	88.108	0.555	0.066	0.004	0.003
B20 - 145	17.168	17.452	17.208	17.168	17.168	0.040	0.14084507	100.00%	0.00%	85.915	0.284	0.040	0.000	0.000
B20 - 150	14.705	15.401	14.796	14.709	14.708	0.091	0.130747126	95.60%	1.10%	86.925	0.696	0.091	0.004	0.003
B20 - 155	15.669	16.141	15.752	15.673	15.672	0.083	0.175847458	95.18%	1.20%	82.415	0.472	0.083	0.004	0.003
B20 - 160	18.839	19.372	18.903	18.839	18.839	0.064	0.120075047	100.00%	0.00%	87.992	0.533	0.064	0.000	0.000
B20 - 165	16.761	17.319	16.831	16.761	16.761	0.070	0.125448029	100.00%	0.00%	87.455	0.558	0.070	0.000	0.000
B20 - 170	17.657	18.138	17.710	17.667	17.665	0.053	0.11018711	81.13%	3.77%	88.981	0.481	0.053	0.010	0.008
B20 - 175	16.867	17.272	16.914	16.887	16.886	0.047	0.116049383	57.45%	2.13%	88.395	0.405	0.047	0.020	0.019
B20 - 180	16.407	17.124	16.529	16.465	16.464	0.122	0.170153417	52.46%	0.82%	82.985	0.717	0.122	0.058	0.057
B20 - 185	16.476	17.039	16.549	16.514	16.513	0.073	0.129662522	47.95%	1.37%	87.034	0.563	0.073	0.038	0.037
B20 - 190	15.494	16.122	15.602	15.545	15.544	0.108	0.171974522	52.78%	0.93%	82.803	0.628	0.108	0.051	0.050
B20 - 195	15.253	15.843	15.326	15.286	15.285	0.073	0.123728814	54.79%	1.37%	87.627	0.590	0.073	0.033	0.032
B20 - 200	15.788	16.380	15.873	15.838	15.836	0.085	0.143581081	41.18%	2.35%	85.642	0.592	0.085	0.050	0.048
B20 - 205	15.761	16.454	15.858	15.828	15.827	0.097	0.13997114	30.93%	1.03%	86.003	0.693	0.097	0.067	0.066
B20 - 210	15.106	15.784	15.214	15.184	15.181	0.108	0.159292035	27.78%	2.78%	84.071	0.678	0.108	0.078	0.075
B20 - 215	16.536	17.235	16.649	16.623	16.618	0.113	0.161659514	23.01%	4.42%	83.834	0.699	0.113	0.087	0.082
B20 - 220	16.338	17.021	16.439	16.411	16.410	0.101	0.147877013	27.72%	0.99%	85.212	0.683	0.101	0.073	0.072
B20 - 225	18.512	19.204	18.661	18.631	18.629	0.149	0.215317919	20.13%	1.34%	78.468	0.692	0.149	0.119	0.117
B20 - 230	17.675	18.457	17.866	17.837	17.835	0.191	0.244245524	15.18%	1.05%	75.575	0.782	0.191	0.162	0.160
B20 - 235	16.997	17.745	17.407	17.388	17.386	0.410	0.548128342	4.63%	0.49%	45.187	0.748	0.410	0.391	0.389
B20 - 240	12.402	13.545	13.155	13.142	13.135	0.753	0.658792651	1.73%	0.93%	34.121	1.143	0.753	0.740	0.733
B20 - 245	11.665	12.506	12.179	12.166	12.161	0.514	0.61117717	2.53%	0.97%	38.882	0.841	0.514	0.501	0.496
B20 - 250	12.275	13.149	12.872	12.864	12.858	0.597	0.683066362	1.34%	1.01%	31.693	0.874	0.597	0.589	0.583